THE UNIVERSITY OF CALGARY

THE FERRANTI INERTIAL LAND SURVEYING SYSTEM (FILS) AS PART OF AN INTEGRATED NAVIGATION AND POSITIONING SYSTEM

by

JOHN E. HAGGLUND

A DISSERTATION
SUBMITTED TO THE FACULTY OF GRADUATE STUDIES
IN PARTIAL FULFILLMENT OF THE REQUIREMENTS FOR THE
DEGREE OF
MASTER OF ENGINEERING

DEPARTMENT OF SURVEYING ENGINEERING

CALGARY, ALBERTA

APRIL, 1987

ISBN 0-315-35981-1

THE UNIVERSITY OF CALGARY

FACULTY OF GRADUATE STUDIES

The undersigned certify that they have read and recommend to the Faculty of Graduate Studies for acceptance, a thesis entitled The Ferranti Land Surveying System (FILS) as Part of an Integrated Navigation and Positioning System submitted by John Edward Hagglund in partial fulfillment of the requirements for the degree of Master of Engineering.

K.P. Schwarz

Dr. K.P. Schwarz
Department of Surveying Engineering

Dr. E.J. Krakiwsky
Department of Surveying Engineering

Dr. E.G. Anderson
Department of Surveying Engineering

Robert Loov

Dr. R.E. Loov
Department of Civil Engineering

May 7, 1987

ABSTRACT

The Ferranti Inertial Land Surveying system is a local level inertial unit which has been used in surveying applications for about the last eight years. It has generally been operated in a manner which required it to be brought to a complete stop relative to the earth's surface every three to five minutes to control error growth in the system. As more and more applications are demanding a continuous dynamic environment or the cost of stopping every three to five minutes is very high, an alternate solution was looked for. The method selected, and described in this dissertation, was to use the strong interfacing capabilities of the FILS unit so as to avoid very expensive and time consuming modifications at the factory.

The characteristics of the FILS hardware and software are discussed with the objective of showing how feedback control can be implemented. The models were set up and an actual feedback control of a FILS MK_II unit was successfully carried out. The results of these tests as well areas for further work are discussed.

Limitations of the FILS system are discussed to assure that the unit is properly used and will not produce unexpected data outputs.

The most promising area for system integration at the present time is with the NAVSTAR GPS system and the NNSS Transit system.

ACKNOWLEDGMENTS

As this dissertation deals with the integration of a specific inertial navigation system, the FERRANTI LAND SURVEYING SYSTEM (FILS) MK II, it would have been difficult to accomplish without support from the manufacturer. I would especially like to thank Dr. R. Tait, Mr. A. Stanley, Mr. R. Carson, Mr. B. Emery, Mr. M. Marshall, and Mr. T. Spoors for the help they provided me in understanding the operation of the FILS system as well as the hospitality they extended during my many visits to Edinburgh.

The equipment used, as well as all of the actual FILS data analyzed, was provided courtesy of NORTECH SURVEYS CANADA (LTD). My thanks to Dr. G. Lachapelle for his encouragement and for providing time off from work when required.

Many thanks to my advisor, Dr. K.P. Schwarz, for the comments and suggestions he provided as the work progressed.

Table of Contents

Appendices

List of Tables

List of Figures

PREFACE

This is an unaltered version of the author's Master of Engineering Dissertation of the same title. This dissertation was accepted by the Faculty of Graduate Studies in May, 1987.

The faculty supervisor for this work was Dr.K.P.Schwarz and the remaining members of the examining committee were Dr.E.J.Krakiwsky, Dr.E.G.Anderson, and Dr.R.E,Loov.

1. Introduction

The Ferranti Inertial Land Surveying System (FILS) is a local level inertial system which has been in use as a surveying tool for about eight years. In this time, although many surveys have been conducted, a readily available description of the system and how it functions has been lacking. While this information was previously available, it tended to be contained in various papers and reports in a somewhat patchwork fashion. As the emphasis of this dissertation is on system integration, a detailed discussion of a number of hardware and software features, usually not found in a general system description, was required. Actual observations are presented which show how the FILS MK_II unit behaves and how it can be integrated with other systems to both improve the accuracy of its own real time solution as well as to widen the areas to which it can be applied. Problems encountered in such an integration are addressed. Emphasis was placed on the MK_II system, with a brief discussion of the MK_I and MK_III version, as most of the data and information presented comes directly from the MK_II unit. The MK_I unit is no longer made and the MK_III unit has many identical features to the MK_II.

1.1. OBJECTIVES

The objectives of this dissertation are as follows:

- To establish a means of controling the Ferranti Inertial Land Surveying MK_II System (FILS MK_II) without the neccessity of requiring hardware or software modifications to the unit;

- To discuss system integration and the consequences of providing feedback to the FILS MK_II unit.

In order to meet these objectives, it was necessary to:

- Consolidate the main information relating to the FILS MK_II system;

- Provide a good general understanding of how the FILS MK_II unit operates both in hardware and software;

- Discuss the type of data available and how it is transferred and stored;

- Discuss limitations of the system.

2. Physical Description of the FILS System

2.1. History

The Ferranti Inertial Land Surveyor is based on a digital navigation system developed for the U.K. Ministry of Defense (Army) which was known as PADS (Position and Azimuth Determining System). The initial development of the PADS system was started in 1970 with the specifications that it must meet a "survey accuracy of 10 m P.E. in Easting and Northing, with an orientation accuracy of 0.3 mil. in azimuth to be achieved in a mission distance of 10 km (or duration of 1 h)" [Hamilton & Ameen Sept. 1977]. In this quotation, the initials P.E. refer to Probable Error, the exact type not being stated, and the term mil is an angular unit used by the military where 6400 mils = 360°. This system was designed to meet the stringent requirements of the military as well as modularity to permit field maintainability by sub-assembly replacement. The PADS system in its turn was based on the Ferranti systems " which had been successfully used in space and aircraft projects" [Hamilton & Ameen Sept. 1977].

The development of the first FILS units was the result of a request by Shell Canada Ltd. in 1976 for a proposal from FERRANTI to produce an inertial system for surveying applications. This resulted in the production of two FERRANTI MK_I FILS units. Following testing of the MK_I units in an actual production field environment, several problem areas appeared, the most troublesome being the instability in the height channel (it should be noted that the PADS units did not contain vertical accelerometers). When these problems were discovered, FERRANTI redesigned their height channel card to the stage that the height is now generally the best channel in the system. Only two MK_I systems were made. The MK_II systems had a different casting and a rapid heat unit different from the previous MK_I systems. This meant that although the system software and output were identical, hardware was not completely interchangeable.

A system very closely related to the FILS MK_II system is the HASINS system (High Accuracy Submersible Inertial Navigation System) which is described in Napier [1985].

Currently, the MK_III system is being marketed by FERRANTI. This system is similar to the MK_II unit in most of its hardware components and real time navigation software. The differences between the MK_III and the MK_II units that are listed below are based on the FERRANTI brochure (LIST: ES/NSD/FILS-3/4-84) and the author's personal knowledge of the MK_II unit. This list may not be complete.

The MK_III unit:

- has a new Control and Display Unit (CDU);
- has an optional EDM unit which mounts on the Inertial Measuring Unit (IMU) box allowing measurements of up to 100 meters to be made without leveling the instrument. These measurements are automatically transferred to the IMU;
- has the Zero Velocity Update period reduced to 10 seconds from the 20 seconds used in the MK_II system;
- has the IEEE488 interface eliminated. Since this is the key component used in real time integration of the MK_II unit, serious problems may be encountered with the MK_III unit if an alternative is not provided;
- displays information in Geographic or Transverse Mercator grid coordinates. The MK_II unit only displays Geographic coordinates;
- has an enlarged computer which allows parameters for all reference ellipsoids to be preprogrammed;
- coordinates up to 62 known stations, stations fixed during a traverse, or approximate coordinates for navigation which may be stored and recalled on the display. The MK_II unit only has storage for one station;
- has the capability to implement ON BOARD MISSION PROCESSING. This provides adjusted values for previously displayed real time coordinates and

enhances subsequent real time observations. The MK_II unit has no ON BOARD MISSION PROCESSING unless this is done on an external computer linked to the MK_II unit via the IEEE488 interface.

2.2. FILS MK_II Characteristics and Components

As mentioned in the introduction, this dissertation will target on the FILS MK_II system as this is the unit for which system integration is to be considered. All of the system components and data discussed from this point on will refer to the FILS MK_II unit. This unit has the following general characteristics:

Physical Size and Weight:

	Width (cm)	Depth (cm)	Height (cm)	Weight (kg)
Control Display Unit (CDP)	21.5	18.5	25.0	7
Inertial Measuring Unit(IMU)	54.2	45.4	30.4	51
Frame	60.2	46.4	58.6	13

The platform is comprised of three miniature single axis floated rate integrating gyroscopes (Gyro Type 125), three FA2 series single axis force feedback, torque restrained pendulous accelerometers, and a four axis gimbal system sealed within a case which is temperature regulated by heat pipes. The stable platform containing the gyros and accelerometers is connected to the azimuth axis of the gimbal system. The azimuth axis is connected to the inner roll gimbal ring which is driven by the inner roll motor about the inner roll axis. This axis in turn is connected to the pitch gimbal ring which is driven by the pitch motor about the pitch axis. The pitch axis in turn is connected to the outer roll gimbal ring which is driven by the outer roll motor about the outer roll axis. The outer roll axis is connected to the platform casing which is rigidly attached to the main casing of the FILS unit. Each axis also contains a synchro which allows the rotational angle about each axis to be monitored. A diagram of this gimbal system is shown in Figure 1. The coordinate systems involved with the FILS MK_II local level inertial system is discussed in detail in Appendix B.

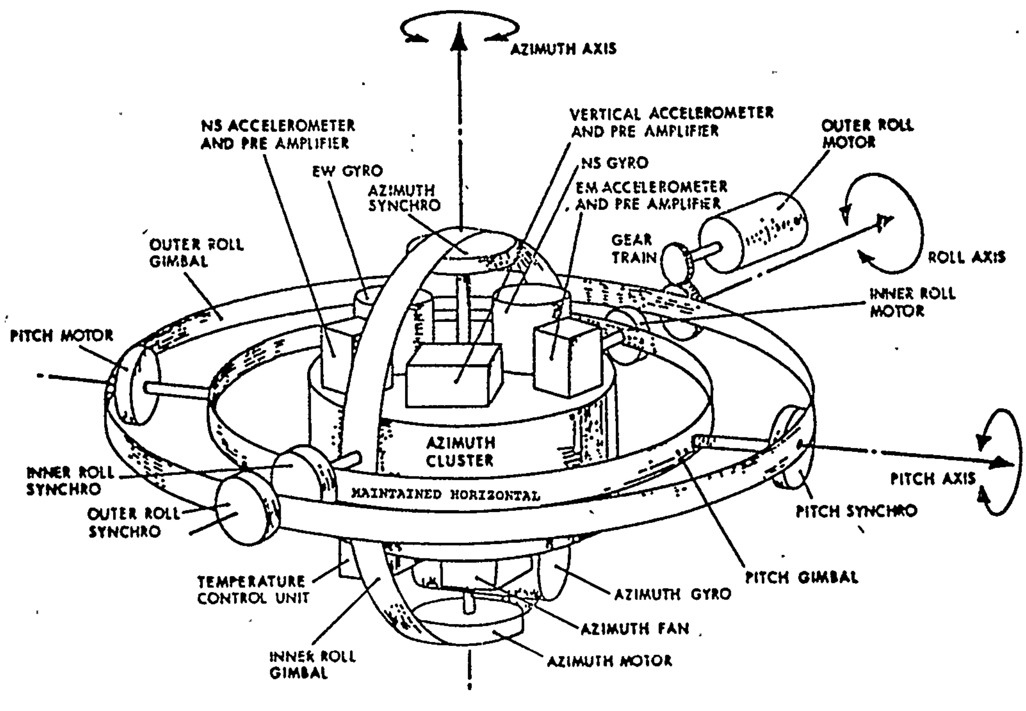

Figure 1. Gimbal System used in FILS MK_II

2.2.1. FA2 Accelerometer

The Ferranti Type FA2F accelerometer was conceived in 1964 when Ferranti Limited commenced a programme to develop a miniature viscous damped accelerometer of high quality suitable for use in inertial navigation equipment. This accelerometer, used in the FILS MK_II system, is a single axis, force feedback, torque restrained pendulous unit with a wide measuring range (±20 g) and good sensitivity over this range. An important feature of the operation of this accelerometer is that its output is an analogue current rather than a quantized digital signal. For this reason, there is no quantization error at this point in the measurement. This also has the advantage that an extremely rapid sampling of the accelerometer output is not required. This does, however, mean that no direct digital reading of the acceleration is available.

A good detailed discussion of accelerometers in general, as well as specific models, is presented in RUEGER [1986]. In section 3.3.1.3.1 of this report, the FA2F accelerometer is mentioned. Here the following statement is made: "In the case of the FILS and PADS 2 systems, an integrating current encoder (22.5 mm/s/pulse) is placed in series with the force coil, which provides a high-resolution digital output of integrated acceleration to the computer". While this statement is correct if properly interpreted, it may give the wrong idea. The "integrated acceleration" is simply the charge on a capacitor (which is external to the IMU platform). The pulses do not go back to the acclerometer to keep it nulled. The nulling of the accelerometer is done by a continuous analogue feedback system. The pulses mention are only used to keep the capacitor from saturating. A discussion of this procedure follows.

The accelerometer works by electrically sensing the relative motion of the pendulous arm with respect to a pick-off bridge which is fastened to the accelerometer casing. The sensed signal is amplified, rectified and fed back to a restoring coil which opposes the pendulous arm displacement. The amount of current which has to pass through the coil to maintain the pendulum at its null position is proportional to the amount of acceleration of the accelerometer casing along this sensitive axis. A diagram of the generalized accelerometer working features is shown in Figure 2. The current required to maintain the pendulum at its null position causes a charging (or discharging) of a capacitor. (There is a separate capacitor unit for each of the three channels, North, East, and Height velocity). The voltage on the capacitor unit, when appropriately scaled, is then a direct measure of the **integral** of the acceleration, ie. the **velocity.** It is this velocity which is digitized in an A/D conversion by the FILS unit once every 20.0704 milliseconds, and integrated numerically to produce linear displacement.

It should be noted that the charge on the capacitor unit has a limited range. For this reason, the voltage level of the capacitor unit is checked each time it is sampled to assure a predefined level (positive or negative) has not been passed. If it has, a fixed current for a fixed time is sent to the capacitor unit. This current can be either positive or negative, and is equivalent to a change in velocity of 2.2860 cm/s. This also causes a digital Channel Reset Store to be either incremented or decremented by one depending on the sign of the current applied. These reset stores are accessible through a stores inspect of 1200, 1201, and 1202 for the East, North, and Height channel respectively and are shown with their scaling and overflow values in the discussion of **FILS MK_II ADDRESSABLE STORES** found in APPENDIX C.

A diagram illustrating the capacitor resetting procedure is shown in Figure 3.

Scaling of each channel's capacitor unit is carried out when the FILS unit is first switched on and is in modes CS0 and CS1. During these modes, the computer measures the voltage on the capacitors before and after a known current pulse has been output by the Precise Interface. As the amount of current sent to the capacitors is a known quantity, the capacitor scale factor can be determined. The value of the X and Y Capacitor Scale Factor can be observed by doing a stores inspect on 1224 and 1225 respectively and should be in the range 7168 to 9216. The Z Capacitor Scale Factor can be observed by doing a stores inspect on 0524 and should be in the range of 4121 to 5300. If the values are not within these ranges, the Fils unit will display a fault 0 on the CDU.

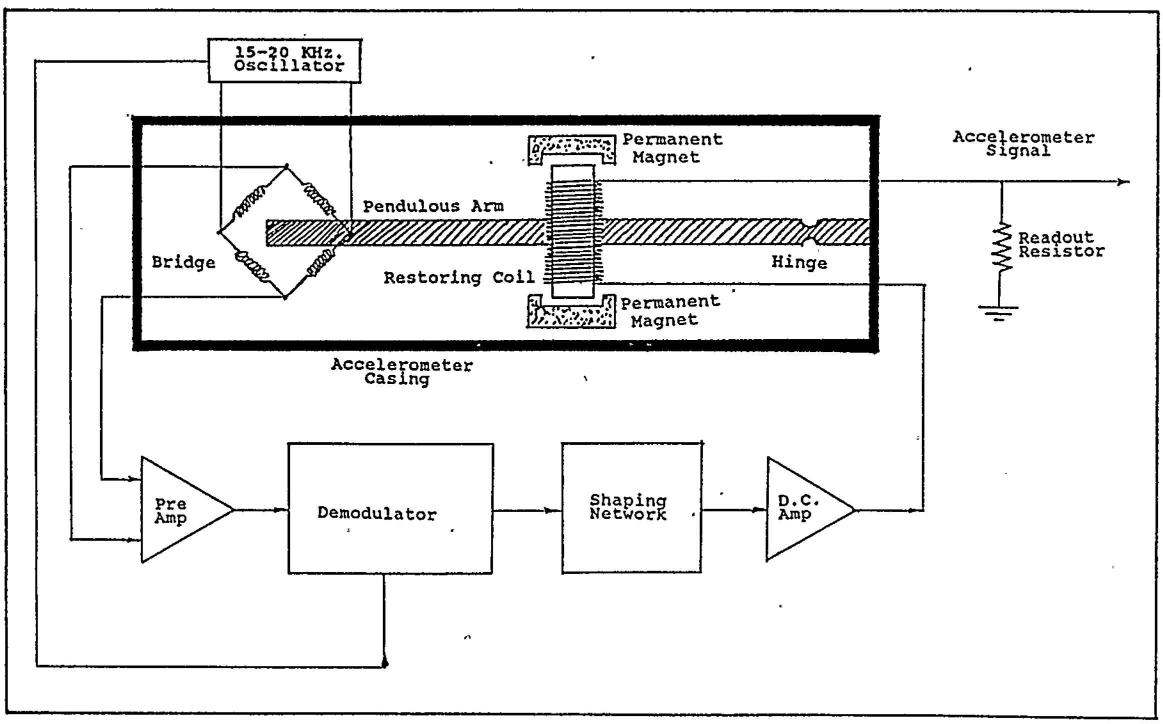

Figure 2. Generalized Diagram of the FILS accelerometer operation

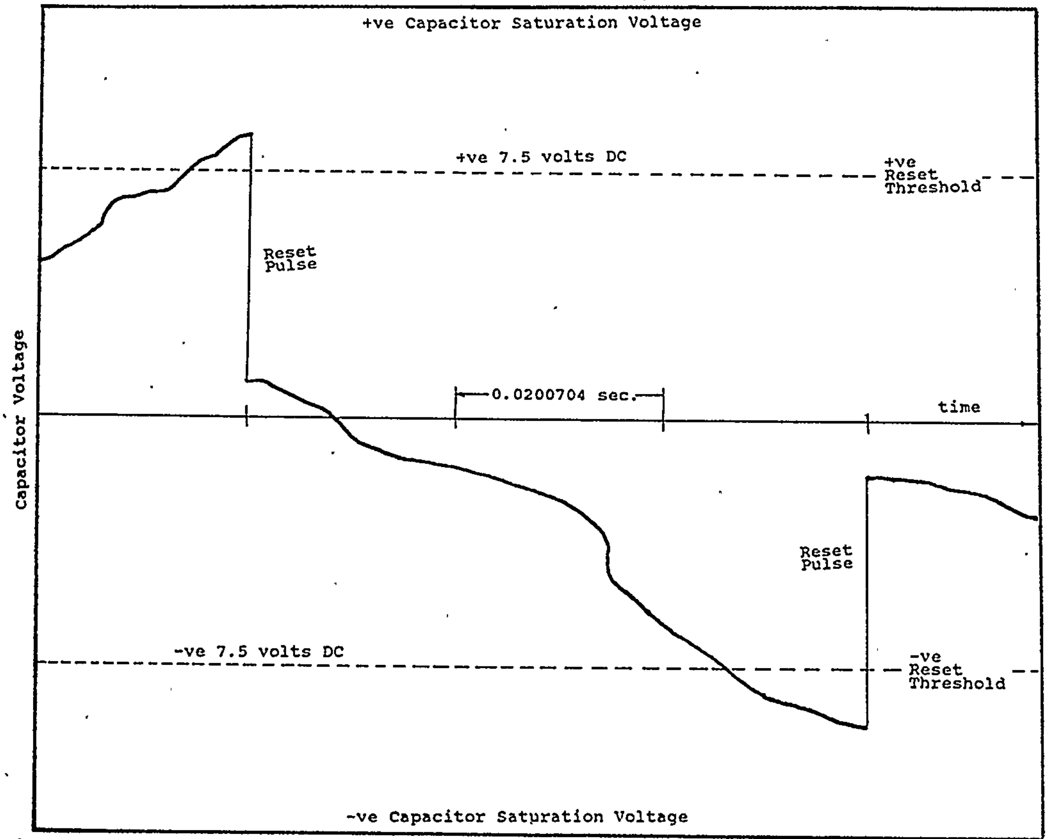

Figure 3. Capacitor Resetting in the FILS MK_II unit

2.2.2. Hardware Backoff of the Vertical Accelerometer

The manner in which the FA2 accelerometers function has already been discussed. This section addresses the special problem which is present in the vertical channel.

While the horizontal accelerometers would sense no accelerations when the platform is at rest with respect to the earth's surface and perpendicular to the gravity vector, this is not the case with the vertical accelerometer. In this situation, the vertical accelerometer would be sensing the complete gravity acceleration (approximately 9.8 m/s). If the vertical acclerometer was to function entirely as the horizontal accelerometers do, this would mean the height capacitors would have to be continually reset and the vertical velocity would soon grow outside the fixed point arithmetic bounds. To avoid this situation, a fixed **backoff** current is continually supplied to the restoring coil of the vertical accelerometer. This current must be extremely stable and is set up at the Ferranti factory to backoff an "average" value of gravity. As the actual gravity vector varies from place to place, a residual amount of acceleration (either positive or negative) is sensed by the accelerometer. This residual acceleration is calibrated during alignment and is backed off in software (not hardware). This software backoff would also account for any error in position or platform alignment as well as accelerometer bias which may be present at the start of a run. Once the system goes into navigate from align, the value of this software vertical acceleration backoff term is frozen in store 0503 having a least significant bit equal to about 1.7 milligals.

2.2.3. Gyro Type 125

The gyroscope Type 125 (formerly M2519) used in the FILS MK_II unit is a high performance single axis floated rate integrating instrument manufactured by Ferranti under license from Singer-Kearfott. It has been subject to development and production improvement by Ferranti since 1960. Its motor shift and float use beryllium to obtain high angular momentum of the flywheel without sacrificing stiffness. Its normal running speed is 350 Hz. The floatation and damping oil used to fill the gyro is chemically inert over a range of -40°C to 90°C. A bellows is fitted to allow for the change in volume of the oil as the temperature varies. A simplified diagram of the gyro is shown in Figure 4.

The gyro was designed to have a well matched coefficient of thermal expansion to minimize problems caused by any thermal gradients which may be present. This problem is also addressed by maintaining the gyro at its nominal operating temperature of 70°C with very little fluctuation.

A sealing of the gyro assembly is done with a positive pressure on the fluid which is maintained down to the lowest storage temperature.

The gyro is provided with magnetic shielding to minimize the affect of varying magnetic fields as the IMU changes position relative to the rest of the FILS unit.

Fine adjustment of the gyro mass unbalance is allowed for on an easily accessible card external to the platform. This makes it relatively easy to fine tune the gyro for this effect.

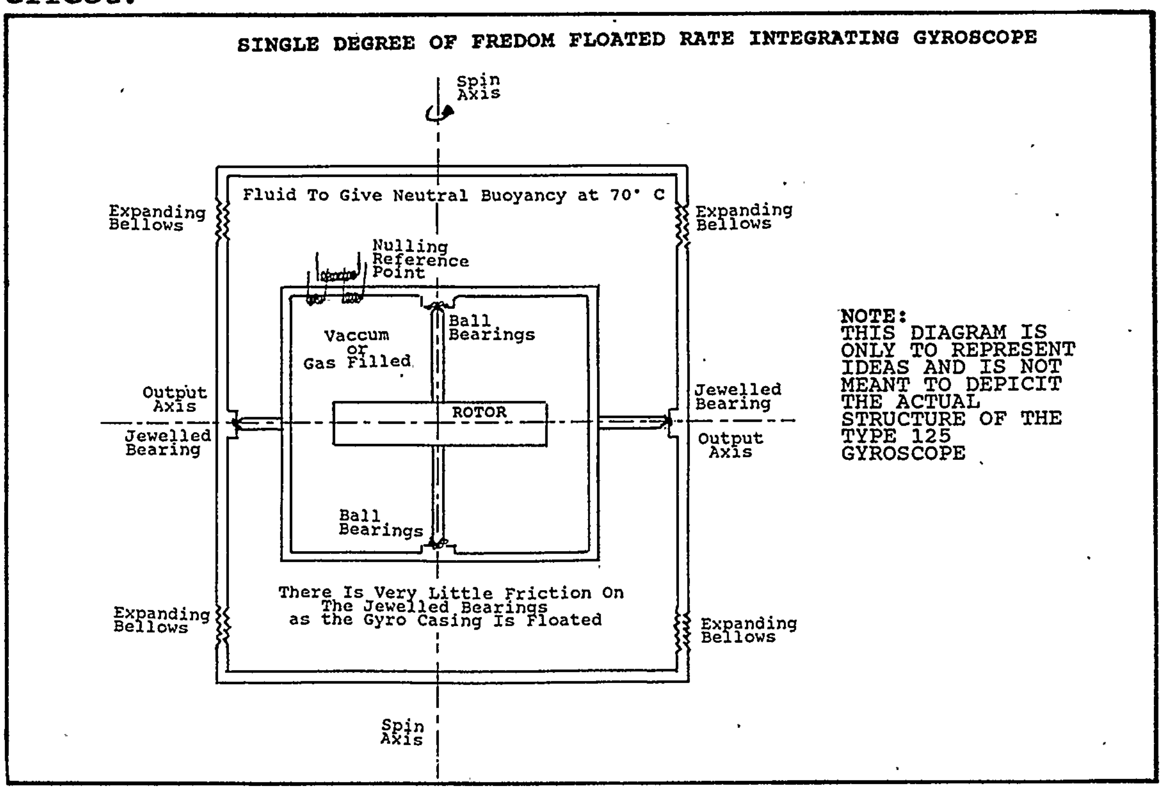

Figure 4. Generalized Diagram of the Type 125 Gyro

The Type 125 gyro is 8.3 cm in length, having a diameter of 5.29mm and a weight of 450 g. Typical performance terms given in Ferranti literature are:

Azimuth short term drift (1σ)	0.008°/h
Vertical short term drift(1σ)	0.0007°/h
Azimuth day to day drift (1σ)	0.040°/h
Vertical day to day drift(1σ)	0.0033°/h
Mass Unbalance	0.3°/h/G max
Anisoelastic drift	0.04°/h/G^2 max

The orientation of a gyroscope is maintained with respect to inertial space unless an external force is applied to it causing it to precess. All mechanical gyroscopes have some amount of drift in them, the amount being a function of the quality and design of the gyroscope. To account for this, allowance is made to input torquing pulses to maintain a particular orientation. In the case of a **space stable** system, the only torques applied are those to offset small instrumental gyro drifts. In the case of **local level** systems, such as the FILS, additional torques are applied to maintain the platform in the local north, east, and up system. Later in this report, when control of the platform orientation is discussed, it will be shown how the fixed gyro drift torquing pulses can be used for this purpose.

The size of the torquing pulses as implemented in the FILS MK_II system are 0.48543 arc seconds for the X and Y gyro, and sixteen times this (7.76368 arc seconds) for the Z gyro. The fixed rate gyro drift stores used by the FILS MK_II unit has a least significant bit of 0.000738°/h. For more information on gyroscopes in general, WRIGLEY [1969] and RUEGER [1982] can be consulted.

2.2.4. Program and Stores Allocation

The FILS MK_II system stores its program in 16K bytes of ROM. This program is coded in machine language code (later versions used a language called CORAL) and is not accessible to the operator. For this reason, the only means of making the system do something, which it is not directly programmed to do, is by understanding what its internal program is presently doing, and modifying the RAM stores it works on. An important point to be remembered when integrating the FILS MK_II with other systems is that it works in a fixed point arithmetic mode (for reasons of speed) and therefore cannot exceed certain boundaries. At present, the FILS MK_II system cannot have a velocity greater than 93.63456 m/s (182 knots) without causing a large positive velocity to suddenly become a large negative velocity or vice versa.

There is 1K byte of RAM in the system where the working data is stored. It can be accessed by the computer, by the operator via the CDU and stores inspect, or by another computer via the IEEE488 interface. It is this interface which is used for system integration of the FILS with other units.

A complete description of the RAM stores is provided in APPENDIX C of this report.

2.2.5. FILS serial data dump

The serial data which the FILS MK_II unit dumps to the recording device consists of four types known by the code they send with their data. These types are 01,44,88, and 32 and correspond to operator keystroke tracking, update data dumps, navigation timed data dumps, and station identification/offset data. A detailed description of each of these is given in APPENDIX D. The important thing to note is that the rate at which the navigation data is dumped, as well as the actual data output, can be altered by fusing the code contained in the two **DUMP CHIPS** located on the Serial Data I/F board in slot number seventeen (17). This is especially usefully for projects such as ground profiling where the main data required is the inertial unit's position between the updates, and not at the updates as is the case with the normal mode of operation. The dump chips should be able to dump from once every 0.64 seconds to any higher multiple. Experience indicates that the fastest rate which should actually be used is 1.28 seconds. The dump rate set at the factory and normally used for outputting navigation data is once every 10.28 seconds.

During updates, the FILS system outputs data once every 0.64 seconds for 20.6 seconds.

2.2.6. Analogue Data Available

Although normally used only for maintenance of equipment, the FILS MK_II unit does have a 155 pin connector which allows access to many signal levels. Great care must be exercised when making use of this output as improper connections may damage the system. There are however uses to which these outputs can be put. One of the most important is direct access to the analogue signal output from the roll, pitch, and azimuth syncros. This allows (with the use of an external A/D converter) a high rate of available attitude readings without interrupting the FILS computer program. This is of particular importance for projects such as LASER profiling where the laser beam must be made to point vertically down no matter what the helicopter attitude is.

A detailed table of what is available from the FILS MK_II pinout is given in APPENDIX E.

2.2.7. FILS System Timing

All timing signals within the Fils unit are derived from a high stability 5MHz crystal oscillator found on the current source and clock printed circuit board. This clock is divided down in many stages for various uses, but the one that is of main importance for the purpose of this discussion has to do with the integration period interval. This period, nominally called a twenty (20) millisecond period is actually 20.0704 milliseconds. This value is obtained from the 5MHz clock by the following sequence of signal divisions in hardware on various boards:

1) ÷ 128
2) ÷ 4
3) ÷ 14
4) ÷ 2
5) ÷ 7

This results in a frequency of 49.82461736 Hz. which has a period of 20.0704 milliseconds. All the capacitor measurements, total velocity assembly, and displacement integration are carried out at this rate. The other signal generated along the way are used for other system functions.

3. FILS Internal Software Implementation

The FILS unit is a **local level navigation system** which utilizes the earth's rotation and gravity to establish a navigational reference system. It measures **changes** in position rather than absolute position by doubly integrating vehicle accelerations in the direction of its accelerometer sensitive axis. This direction is maintained by controlling the attitude of the stable platform by the feedback from spinning gyroscopes. Both the accelerometers and gyroscopes are mounted on the same stable platform. A description of the FILS navigational implementation follows.

3.1. Basic Navigation Equations Used

The basic system equations which the FILS MK_II system mechanizes are given [Emery,1980] as follows:

$$V_N = \int A_N - (2\Omega + \dot{\lambda}) \sin\Phi_P * V_E - \dot{\Phi} * \dot{h} \qquad (3.1.1)$$

$$D_N = \int V_N \qquad (3.1.2)$$

$$V_E = \int A_E + (2\Omega + \dot{\lambda}) \sin\Phi_P * V_N - (2\Omega + \dot{\lambda}) \cos\Phi_P * \dot{h} \qquad (3.1.3)$$

$$D_E = \int V_E \qquad (3.1.4)$$

$$V_H = \int A_H + \dot{\Phi} * V_N + (2\Omega + \dot{\lambda}) \cos\Phi_P * V_E - g_L \qquad (3.1.5)$$

$$D_H = \int V_H \qquad (3.1.6)$$

where: $\dot{\lambda} = V_E / ((R_{PV} + h_P) * \cos \Phi_P)$ (3.1.7)

A_N = instrument sensed north acceleration
A_E = instrument sensed east acceleration
A_H = instrument sensed height acceleration
Ω = Earth Rate = $7.2921151467*10^{-5}$ rad/s
Φ_P = FILS Predicted Latitude

V_N = Uncorrected North Velocity (+ve NORTH)
V_E = Uncorrected East Velocity (+ve EAST)
V_H = Uncorrected Height Velocity (+ve UP)
g_L = Free air correction term + normal gravity + fixed current backoff + gravity residue
$\dot{h}$ = FILS uncorrected height velocity (+ve UP)

TORQUING RATES

$$N/S\ RATE = \{V_E/(R_{PV} + h_P)\} + \Omega * \cos\Phi_P + W_Y \tag{3.1.8}$$

$$E/W\ RATE = \{V_N/(R_M + h_P)\} + W_X \tag{3.1.9}$$

$$AZ.\ RATE = \{V_E/(R_{PV} + h_P)\} * \tan\Phi_P + \Omega * \sin\Phi_P + W_Z \tag{3.1.10}$$

where: W = Fixed Gyro Drift Corrections applied by FILS
R_M = Radius of curvature in the Meridian
R_{PV} = Radius of curvature in the Prime Vertical
h_P = FILS Predicted Height

3.2. Examination of FILS MK_II Basic Equations

The basic equations, shown in section 3.1, are as given in the system documentation from Ferranti [EMERY, 1980]. The FILS coordinate system is defined as **positive** North, East, and Up. The order in which the velocities are calculated is:

1.) Total Height Velocity,
2.) Total North Velocity,
3.) Total East Velocity.

These equations agree with equations 7-3 in BRITTING [1971] which give the earth referenced velocities as

$$\dot{V}^n = \begin{bmatrix} \dot{V}_N \\ \dot{V}_E \\ \dot{V}_D \end{bmatrix} = \begin{bmatrix} \hat{f}_N - \hat{V}_E(\dot{\hat{l}} + 2\omega_{ie})\sin\hat{L} + \dot{\hat{L}}\hat{V}_D \\ \hat{f}_E + \hat{V}_N(\dot{\hat{l}} + 2\omega_{ie})\sin\hat{L} + \hat{V}_D(l + 2\omega_{ie})\cos\hat{L} \\ \hat{f}_D - \hat{V}_E(l + 2\omega_{ie})\cos L - \hat{L}V_N + \hat{g} \end{bmatrix} \quad \dots (3.2.1)$$

$$\hat{v}^n = \int \dot{\hat{v}}^n dt + \hat{v}^n(0) \qquad (3.2.2)$$

with the obvious substitutions

$$A_{E,N,H} = f_{E,N,-D}$$
$$\Omega = \omega_{ie}$$
$$\lambda = l$$
$$\Phi = L$$

Differences in sign are a direct result of the FILS equations having **UP** defined as **positive** while the BRITTING equations have **DOWN** defined as **positive.** An estimated or computed value is denoted by (ˆ). For a concise derivation of these formulas, see FARRELL [1976]. The derivation of these equations can also be found in ADAMS [1979, equ. 3-37] where the Z axis is defined as **positive UP.** It should be noted that these equations relate to the forces sensed and not the corrections applied.

A very important feature of the equations used by the FILS system is that **predicted** values for the latitude (Φ_p) and height (h_p) are used rather than the uncorrected ones which are obtained from the numerical integration of the uncorrected velocities. If this was not done, the sine and cosine values would be incorrect and the error in the normal gravity and free air acceleration terms would cause the height velocity to grow quickly out of bounds.

The manner of calculating the corrections which are applied to the uncorrected positions to yield the predicted positions is covered under the section entitled **FILS internal position correction algorithm.**

In the basic equations of the FILS system, the accelerations denoted by A_N, A_E, and A_D are directly integrated in hardware by the charging (or discharging) of capacitors by the restoring current which is required to maintain the pendulum accelerometer at its null location. These sensed accelerations include the cross product acceleration forces. Since the actual measurements are velocities (ie. the voltage on the capacitors), the corrective terms for the cross product accelerations, which are calculated, must also be integrated before they can be applied to the measured velocities. This should be borne in mind when reading the section on **Assembly of the FILS Total Velocity** where the terms VZ_X, VZRES, VN_X, VNRES, VE_X, and VERES refer to the numerically integrated values of the **cross product velocity correction** terms.

An additional point of importance in understanding how the FILS MK_II system functions is the fact that during alignment it calculates a gravity residue, denoted as **GRES**, and stores this value in the FILS addressable stores at location 0503 (see APPENDIX C). **GRES** is used to backoff in software any acceleration which is not accounted for by the fixed hardware backoff g_o, the normal gravity formula, and the freeair correction used. This means that only the **difference** in gravity anomaly, not the total gravity anomaly, will cause an error in the height velocity. This is of particular importance when considering the operator changeable term known as the **FREE-AIR** correction which determines the change in acceleration due to a change in height as $\mathbf{F}*h_p$ where **F** is an abbreviation for **FREE-AIR**.

The term g_L used in the basic equation is implemented as

$$g_L = 0.051723143 \sin^2\Phi_p - \mathbf{F}*h_p + G_o + \text{GRES} \qquad (3.2.3)$$

where : G_o = hardware backoff = 9.78049 m/s^2
0.051723143 = the 1924 normal gravity coefficient

The 1967 normal gravity coefficient (not used in FILS) is 0.051859158 m/s. The sin(2Φ) term, amounting to -0.00000577*sin(2Φ), is not implemented in the FILS unit.

3.2.1. FREE-AIR Correction Term

The FILS MK_II height corrective term referred to as the **FREE-AIR** correction is a complete Bouguer correction as described in HEISKANEN and MORITZ [1967] for variable density values.

The Normal gravity **on** the reference ellipsoid is given by the formula 2-126 in HEISKANEN and MORITZ:

$$\gamma = 978.0490(1 + 0.0052884 \sin^2\phi - 0.0000059\sin^2 2\phi) \text{ gal} \qquad \ldots (3.2.4)$$

If the point at which the measurement is made is a distance h above the reference ellipsoid, the free-air correction is of the form:

$$(\partial\gamma/\partial h) = -0.3086 - 0.0002 * \cos(2\Phi) \quad \text{mgal/m} \qquad \ldots (3.2.5)$$

Neglecting the small terms with 2ϕ values in them yields:

$$\gamma = (\ 978049.0 + 5172.3143 \sin^2\phi \ -0.3086h\ ) \text{mgal} \qquad \ldots (3.2.6)$$

which corresponds to formula (3.2.3) for

G_o = 978049.0 mgal
F = 0.3086 mgal/m
GRES = 0

It should be noted that this formulation does not consider masses between the ellipsoid and the surface point. If the area around the surface point is considered flat, and the density between the ellipsoid and the surface constant, then the **slab** between this surface and the ellipsoidal surface contributes an effect known as the **Bouguer effect.** The Bouguer effect is conveniently combined with the **Free-air** term and is then called the complete Bouguer correction.

It is usually approximated by:

$$c = k\,h \tag{3.2.7}$$

where: $k = 0.1967$ mgal/h for a density of $2.67 g/cm^3$
h is in metres.

This formula changes (3.2.6) to

$$\gamma = (\ 978049.0 + 5172.3143 \sin^2\phi \ - k\,h\ )\text{mgal} \tag{3.2.8}$$

It is this combined term having both Free-air and Bouguer Correction, which is entered as a fixed value in the **Free-Air** store of the FILS computer. The **terrain** correction term, which determines the effect of topographic variation about the Bouguer plane, is not included as it is not easy to implement, and can be best handled in a post processing environment. This compromise does not appear to have significantly affected the FILS height determination which is generally the best of the three channels.

The manner in which the FILS applies its height correction is easy to reproduce in post-processing modes where the error it introduces can be calculated. This might be much more difficult to do if a real time filter control was used which could not be exactly reproduced in post processing.

3.3. Assembly of the FILS total Velocity

The total velocity, which is calculated every 20.0704 ms in the FILS unit and integrated to give displacement, does not use the previous total velocity for the channel being calculated (except for some non-orthogonality terms), but rather assembles various stores as shown below. It should be noted that the implied multiplications and divisions for the individual terms are not shown here as they would only clutter the presentation.

(0530,31)

$$VZ_{tot} = VZ_{A/D} - VZ_E - VZ_I + VN_{tot}^{MSHL}*ZNORTH + VE_{tot}^{MSHL}*ZEORTH + \{ VZ_X + VZRES \} \qquad (3.3.1)$$

(1400,01)

$$VN_{tot} = (VN_{A/D} - VN_E + VN_I)*(1.0 + YSCALE) + VE_{tot}^{MSHL}*ORTHN + \{ VN_X + VNRES \} \qquad (3.3.2)$$

(1402,03)

$$VE_{tot} = (VE_{A/D} - VE_E + VE_I)*(1.0 + XSCALE) + VN_{tot}^{MSHP}*EORTH + \{ VE_X + VERES \} \qquad (3.3.3)$$

where:

VN_E = initial capacitor voltage (vel.) on Y (store 1332)
VE_E = initial capacitor voltage (vel.) on X (store 1333)
VZ_E = initial capacitor voltage (vel.) on Z (store 0532)
$VN_{A/D}$ = A/D voltage (vel.) on Y for present interrupt (working store, 1006)
$VE_{A/D}$ = A/D voltage (vel.) on X for present interrupt (working store, 1007)
$VZ_{A/D}$ = A/D voltage (vel.) on Z for present interrupt (working store, 1005)
VNRES = Y velocity residue (stores 1014,1015)
VERES = X velocity residue (stores 1032,1033)
VZRES = Z velocity residue (stores 0504,0505)

VN_I = summed resets from north velocity (1201)
VE_I = summed resets from east velocity (1200)
VZ_I = summed resets from height velocity (1202)

VN_X = north cross product acceleration (1330)
VE_X = east cross product acceleration (1331)
VZ_X = height cross product acceleration (0533)

XSCALE = scale factor for the X accelerometer (store 0231, **SF21**)
YSCALE = scale factor for the Y accelerometer (store 0232, **SF22**)
EORTH = non orthogonality of X accel. to north (store 0226, **SF24**)
ORTHN = non orthogonality of Y accel. to east (store 0223, **SF25**)
ZEORTH = non orthogonality of Z accel. to east (store 0230, **SF26**)
ZNORTH = non orthogonality of Z accel. to north (store 0227, **SF27**)
SF = FILS SPECIAL FUNCTION DESIGNATION
MSHL = Most Significant Half from Last 20 ms Cycle
MSHP = Most Significant Half from Present Cycle
{ } = Numerically integrated cross product velocity correction terms which are the accumulation of all the 20 ms periods since going into navigate mode. Note: these values are not applied during the CS0 mode.

3.4. FILS internal position correction algorithm

The FILS MK_II system uses the measured velocities, during stationary periods when updates are made, to calculate a position error. When applied to the uncorrected position it yields the FILS real time corrected or predicted position. The term predicted implies the additional position correction which is made from the last update reference time to the present display time. As the update reference time is in the middle of the update period, all corrected position information has at least 10 seconds of prediction as well.

It is important to understand how the FILS MK_II position correction and prediction algorithms function as this will be one of the key areas in feedback control of the system. The algorithm is based on a summation of the position corrections determined by fitting a quadratic curve fit through the last three update velocity values (a separate curve fit is done for each of the three velocities, North(Y), East(X), and UP(Z)). These update velocities are refered to as ZUPTS (zero velocity updates) as the velocity should measure zero when the vehicle is stopped relative to the earth's surface. The curve fit is then through **error velocities** rather than total (actual + error) velocities. No correction is possible until the first update is done. A linear correction and prediction is done from the first update until the second update is done. At this point, the quadratic velocity curve fitting is started, and the linear correction of the first period is replaced by it's quadratic equivalent.

The quadratic curve fit is based on time intervals and is formulated as follows:

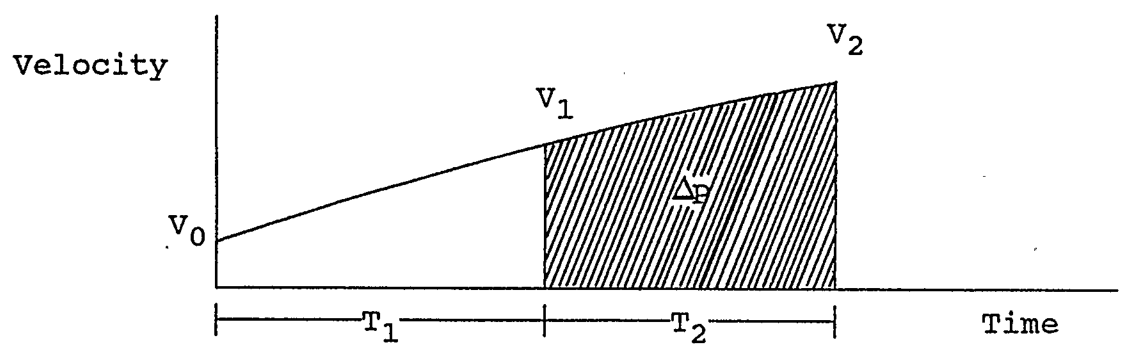

Figure 5. FILS MK_II Internal Position Correction Method

A quadratic curve fit of the form $v = at^2 + bt + c$ is used. The shaded area shown in Figure 4 can then be obtained as follows:

$$DP = \int_{T_1}^{T_1+T_2} v\,dt = \left[(at^3)/3 + (bt^2)/2 + ct \right]_{T_1}^{T_1+T_2} \qquad (3.4.1)$$

$$= (a/3)*(T_2^3 + 3T_1^2T_2 + 3T_1T_2^2) + (b/2)*(T_2^2 + 2T_1T_2) + cT_2$$

Let $A = aT_1T_2$, $B = bT_1T_2 /(T_1 + T_2)$ $C = c$

Then the value for DP can be rewritten in the form:

$$DP = (T_1+T_2)*\{ A + B + A*(T_2/3T_1)*(T_2/(T_1+T_2))$$
$$+ B*(T_2/2T_1) + C*(T_2/(T_1+T_2) \} \qquad (3.4.2)$$

The values for the A,B, and C coefficients can be determined from the measured velocity errors as follows:

$$A = (V_0 - V_1)-(V_0 - V_2) * (T_1 /(T_1 + T_2)) \qquad (3.4.3)$$

$$B = (V_0 - V_2) * (T_1 /(T_1 + T_2))^2 - (V_0 - V_1) \qquad (3.4.4)$$

$$C = V_0 \qquad (3.4.5)$$

At each update, the value of DP calculated is added to a store which holds the summation of all the DP values to date. This gives the total correction up to the middle of the last update performed. To get the additional correction up to the present time, a prediction method based on the previously calculated quadratic coefficients is used. This is illustrated in Figure 6 below.

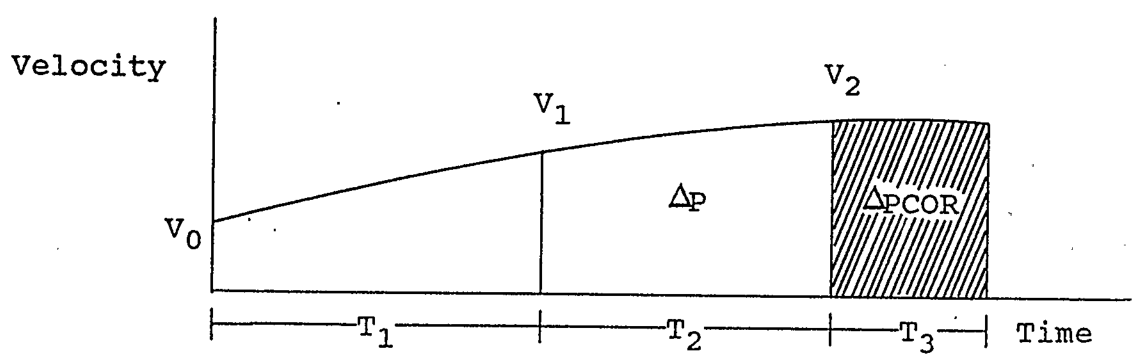

Figure 6. FILS MK_II Internal Position Prediction Method

The same basic equation and form is used as in the correction method, but the integration limits are different.

The basic equation is still $v = at^2 + bt + c$ but now the predicted correction has the following limits:

$$\mathrm{DPCOR} = \int_{T_1+T_2}^{T_1+T_2+T_3} v\,dt = \Big[\,(at^3)/3 + (bt^2)/2 + ct\,\Big]_{T_1+T_2}^{T_1+T_2+T_3} \qquad (3.4.6)$$

In order to make use of the same subroutine which was used in the calculation of DP, the equation for DPCOR is rewritten as:

$$\mathrm{DPCOR} = \Big[\,\ldots\,\Big]_{T_1}^{T_1+T_2+T_3} - \Big[\,\ldots\,\Big]_{T_1}^{T_1+T_2} \qquad (3.4.7)$$

$$= \Big[\,(at^3)/3 + (bt^2)/2 + ct\,\Big]_{T_1}^{T_1+T_2+T_3} - \mathrm{DP} \qquad (3.4.8)$$

where DP is the correction value calculated at the last update (not the summed correction value).

As it is the quadratic coefficients "a" and "b" which do not change with time, and not the values of "A" and "B", it is necessary that these values be modified to "A_p" and "B_p" to correspond to the present time. This is done as follows:

$$A_p = A\ (T_2 + T_3)/T_2 \qquad (3.4.9)$$

$$B_p = B\ [(T_1 + T_2)(T_2 + T_3)]/[T_2(T_1 + T_2 + T_3)] \qquad (3.4.10)$$

This prediction method is shown to indicate it is done in real time being handled within the FILS MK_II computer. It is not necessary nor desirable for these A_p and B_p

coefficients to be modified by an external computer as it would merely duplicate effort creating extra data transfer.

3.5. Approximations Made In The FILS MK_II Software

The normal gravity approximation has already been discussed. In addition to this, there are some other approximations made to speed up the calculation time. These generally have very little significance for short term missions (3 hours or less), and are minimized by the fact that inertial systems measure differences in position rather than absolute positions.

One approximation is that of assuming that the ellipsoid on which the FILS system is operating is geocentric. While the operator can modify the ellipsoid shape, all ellipsoids are implicitly considered to be earth centered.

The equations to calculate the radii of curvature in the Meridian and Prime Vertical are given in Bomford [1971] as:

$$R_M = a * (1-e^2) / (1 - e^2\sin^2\Phi)^{3/2} \qquad (3.5.1)$$

$$R_{PV} = a / (1 - e^2\sin^2\Phi)^{1/2} \qquad (3.5.2)$$

$$e^2 = (a^2 - b^2) / a^2 = 2*f - f^2 \qquad (3.5.3)$$

where:
- a = semi-major axis
- b = semi-minor axis
- e^2 = first eccentricity squared
- f = flattening
- Φ = geodetic latitude

To speed up calculations, the radius of curvature in the meridian and prime vertical are approximated by the following equations:

$$R_M = a*(1-e^2)(1 + 1.5*e^2*\sin^2\Phi_P) \qquad (3.5.4)$$

$$R_{PV} = a + 0.5*a*e^2\sin^2\Phi_P \qquad (3.5.5)$$

These are derived from truncating a series expansion for these two terms for any values e greater than e^2.

Figures 7 and 8 show the error in metres versus latitude which this introduces. The latitude range shown is from -90° to +90° although the FILS system itself is only specified to operate from -75° to +75° in latitude.

As this error is very small in relation to the total radius, and relatively constant over the work area, it has little significance in the conversion of linear distance traveled to angular distance. For example, an error of 100 metres in the radius term would make an error of 100/3276205 or 0.00000031 % . For a survey of 50 kilometres this would be 1.53 metres. Almost all of this error would have been removed by the estimated accelerometer scale factor. Any residual error would be spread linearly along the traverse.

3.6. Limitations of the FILS MK_II system

As with most systems,the FILS MK_II has certain restrictions imposed on it largely as a result of the available hardware and software at the time of its design. In addition, some restrictions were made to improve the overall reliability of the system. This section lists the most important of these limitations with, when required, a brief discussion of why they exist.

The FILS unit performs a large number of calculations every twenty milliseconds to sample and assemble the velocity, integrate this velocity to get position change and required gyro torquing, and service the platform. This takes about 75% of the time leaving 25% (or 5 ms) to do

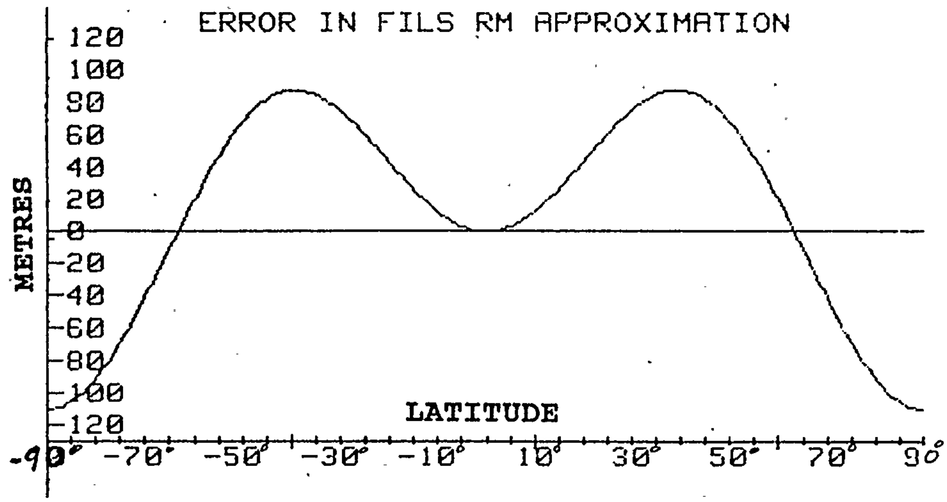

Figure 7. Radius of Curvature in the Meridian Approximation Error

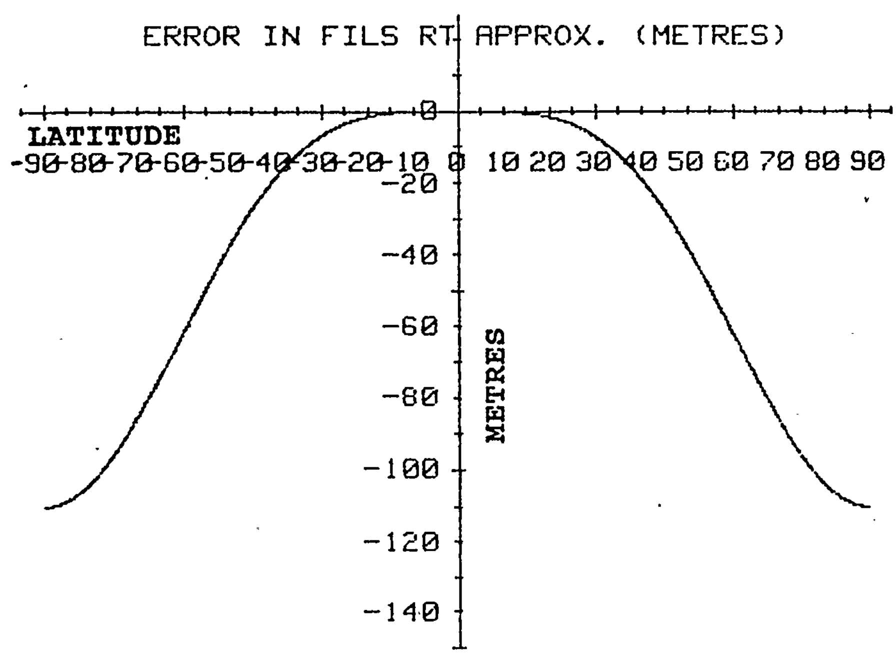

Figure 8. Radius of Curvature in the Prime Vertical Approximation Error

navigation calculations, data output, as well as CDU display and servicing. At the time the FILS systems were being designed, this could only be done by writing machine code language working in fixed point arithmetic. This fixed point arithmetic is the predominant reason for the most restrictive limitation of the FILS MK_II system. It limits the maximum velocity in any axis to **93.63456 m/s**. This includes both the error velocity and the "true" velocity. The maximum **zero velocity** which can be handled at updates is 16 times less than this (i.e. **5.85216 m/s**).

The spacing between zero velocity updates can not be closer than **one minute.** The ratio of adjacent update intervals should not exceed **1:6** and the sum of the two adjacent intervals can not be greater than **21.922 minutes** or the FILS system will revert back to its uncorrected positions (instead of the predicted positions). The first two restrictions are due to numerical reasons while the last is due to the fact that a quadratic curve fit only adequately tracks the error velocity over a short period of time.

The system has no limitation in terms of longitude, but its **latitude operating range** is specified to be **-75°C** to **+75°C.** This limitation is due to the fact that the platform is implemented as a local level system without a wander angle. At high latitude it will not gyrocompass as well and the amount of torquing required to keep the platform pointed to north goes to infinity as the system approaches the pole.

Other physical limitations include such things as temperature, maximum acceleration, gimbal angular freedom, and maximum angular rates and accelerations. These are as follows:

Temperature: IMU and CDU

Operational:	-31°C to +52°C
Storage:	-34°C to +70°C

Acceleration: Maximum continuous acceleration in one channel only is **3.59G**
Maximum continuous acceleration in one plane only (ie. two channels) is **3.11G**
Maximum continuous acceleration vectorially in three dimension is **2.75G**
where **G** = 9.80665 m/s^2

The linear acceleration restrictions are imposed as a result of the maximum rate at which the capacitors (ie. the integrators of the accelerometer signal) can be serviced. If they cannot be serviced fast enough, they will saturate. This has been discussed in the section on accelerometers.

Gimbal Angular Freedom:

Azimuth:	360°
Pitch:	± 95°
Roll(outer):	± 95°
Roll(inner):	± 11°

Although the pitch angular freedom is given as ±95°, it is recommended not to exceed ±80° to avoid **gimbal flip** (an interaction between the inner roll axis and the pitch axis). The limit on the roll and pitch angles is a result of replacing the slip rings which are present in aircraft systems with direct connections via a ribbon wire to improve reliability. This was done on the premise that surveyors would not be doing loop the loops.

The maximum rates at which the stable platform attitude can be controlled are given in terms of angular rates and accelerations. These are as follows:

Angular Rate:

Azimuth:	200°/s
Pitch:	150°/s
Roll:	100°/s

Angular Acceleration:

Azimuth:	$300°/s^2$
Pitch:	$200°/s^2$
Roll:	$200°/s^2$

These specifications refer to the MK_II system and should be confirmed with Ferranti if they are of significance for a specific application. They may not be exactly the same for the MK_III system.

4. Improvement of the FILS Solution by External Processing

The emphasis of this section is on ways to improve the FILS solution in a real time operating environment rather than in post mission processing. Post mission processing of inertial data involves methods and data which most often are simply not available in **real time** applications. A discussion of post mission data processing can be found in [Hannah, 1982], [Wong, 1982], [Vassiliou, 1984], and [Schwarz et al., 1984]. The concept of **external processing**, as used here, is the reworking of FILS data by an external computer (such as the HP200 series computer) as well as the combination of additional data (ie. GPS derived position and velocity information) to form a feedback control mechanization having the objective of extending the useful period over which the systems can be operated. This mechanization will allow the performance of tasks which none of the component units could adequately handle alone. A generalization of the information flow is shown below:

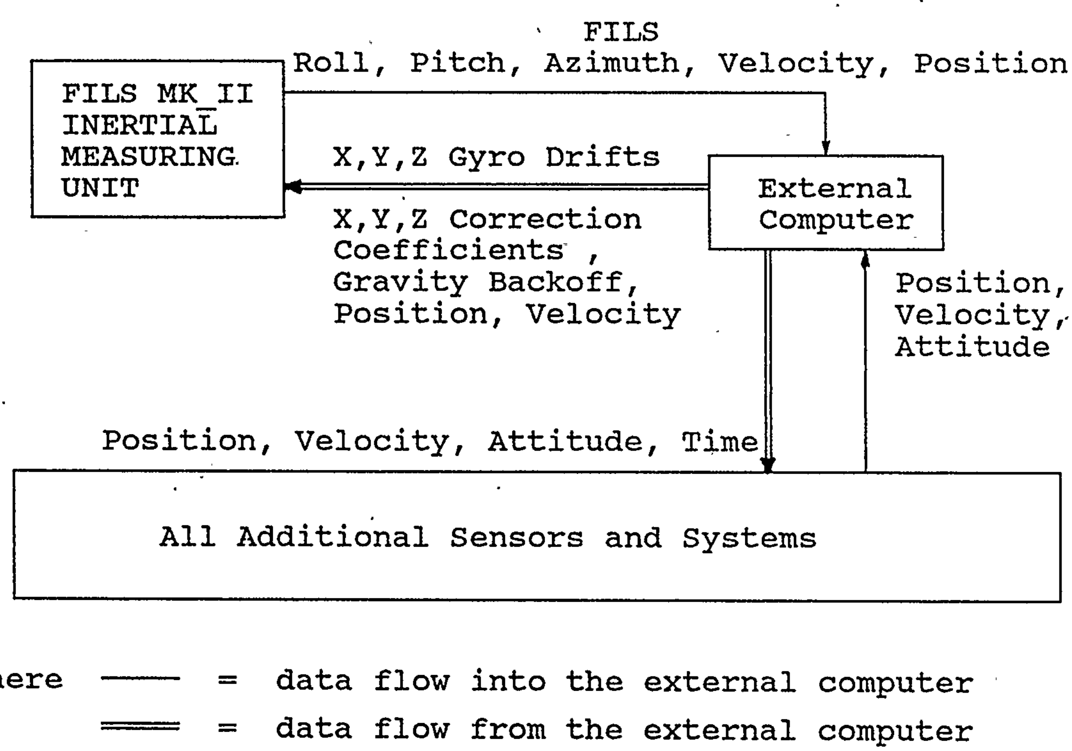

Figure 9. Generalized Real-Time System Data Flow

In Figure 9, it has been assumed that the FILS MK_II unit is a standard unit which expects zero velocity updates every 5 to 10 minutes. Hardware modifications for use at sea will be discussed later.

4.1. Real Time FILS MK_II Data Availability

As has been mentioned in sections 2.2.3, 2.2.4, and 2.2.5, there are three main sources of information available from the FILS unit which can be of use to an external computer. These are:

1.) Serial data controlled by the information fused on a set of dump chips,
2.) Data read from RAM stores via the IEEE488 interface, and
3.) Analogue attitude information which can be digitized by an external A/D device.

A fourth method of obtaining data is operator transfer via the control display unit (CDU). This is not a viable method for rapidly changing data which must be accurately time tagged.

For the purposes of monitoring the FILS to generate feedback control, only the serial data output (RS232C) and the IEEE488 interface are significant. The advantages and disadvantages of these two methods are shown in Table 1.

4.1.1. Time Tagging and Correlation

The concept of accurately time correlating data from integrated systems has often not been given the attention it deserves. This is, at least in part, historical in nature. The uncertainty in position fixes and ranges from earlier types of positioning systems were often noisy enough to allow for several seconds of timing discontinuities between systems to go by unnoticed. These timing differences were often accentuated by heavy loading of the monitoring computer. In addition, each system normally had its own crystal clock and its own measurement time boundaries.

Table 1. FILS IEEE488 & Serial data interfaces

INTERFACE	IEEE488	SERIAL RS232C
IMPLEMENTATION	-not all standards but almost so, has all features needed for most applications	-not complete two way data flow with handshaking -only predefined data flow
ADVANTAGES	-direct access to any of the RAM stores with the ability to read and modify them at any time -data transfer is faster than over a serial line -easiest and most direct means of external computer feedback control of the FILS unit	-data output is controlled by the FILS unit, and problems of data assemble from same 20ms period are not present -no inference with normal FILS operation -the external computer does not have to ask for the data.
DISADVANTAGES	-possible interference with FILS functioning if data is requested at a continuous high data rate -data which must be assembled from more than one store may not refer to the same time boundary ie. MSH and LSH of a double length word -location in FILS program execution not exactly known at instant data is requested	-only a predefined set of data is output -the data output is controlled by the FILS unit not the external computer. The external computer must provide a continuous transfer buffer into which the data can go. -data output is available only at the time and rate set in the dump chips. -uses syncro to digital frequency

With the advent of measuring systems such as high precision inertial systems, and the satellite Global Positioning System (GPS), the need for accurate time correlation became more and more important. Over long duration missions, the drifts between all the various systems clocks must be accounted for.

There are a number of approaches to solving this problem. One solution is to run all of the systems from one common frequency standard. Unless money and time are of no concern, this approach is unlikely to work as few off the shelf systems allow for external frequency input.

Another approach is to have an accurate timing unit which can be used to tie all of the other system's time bases to its own. To be practical, this unit must be computer addressable, allow for various types of time tagging, but should not be slowed down by computer loading. This approach has been used by NORTECH SURVEYS CANADA (INC) with good results.

An additional approach, which is perhaps the least expensive and most widely used, is to use the time from the monitor computer to tie all the data together. This has the drawback that generally speaking, computers do not have very good time systems for various types of interrupts. As well, if they have a heavy computational load, they may not acknowledge an interrupt at the time it occurs. With the rapid changes occurring in computer technology, this situation may change, but great care should be taken if this is the approach chosen for time correlation.

4.1.2. FILS MK_II Internal Time Boundaries

As mentioned in section 2.2.6, the FILS makes all its capacitor measurements, total velocity assembly, displacement integration, and torquing, once every 20.0704 ms. This is the rate at which the stores are updated and theoretically the rate at which an external computer could obtain new information. At this stage however, the position and velocity information is scattered about in many store locations. To get all the information required, the computer would have to be continuously interrogating stores via the IEEE488 interface as well as assuring that the data from all stores refer to the same 20 ms interval. It may not even be possible to do this, and if it could be done, it may produce adverse affects on the FILS unit itself. In addition to all these considerations, the external computer would have to assemble all the split up data properly. For these reasons, the method advocated is to use the **FROZEN** 0.64 second values.

The 0.64 second values are assembled by the FILS unit and put in the 0.64 second stores. In addition, the rate of once every 0.64 seconds should not tax the IEEE488 interface. This frozen value is also the value which is sent out with the UPDATE and TIME DUMP information on the serial line.

A few importance facts about the **FROZEN** data which should be noted are:

- 0.64 s. is actually (32 * 0.0200704)
  = 0.6422528 s.
- the output time tag is for the end of this period.
- the **FROZEN** velocity is the average over this period and therefore refers to the middle time of this period.
- the **FROZEN** position refers to the end of the period.

4.1.3. FROZEN Stores Type and Location

The frozen stores type and location within the FILS system is an important element for system feedback control. They are shown in Table 2:

Table 2. Frozen Stores Type and Location

STORE ADDRESS	DATA IN STORE	SYMBOL	LSB OF MSH
0610	Time since mode change	TOTIM	0.6422528 s
1632,33	VN for 0.64 Average	VNAV	0.0028575 m/s
1634,35	VE for 0.64 Average	VEAV	0.0028575 m/s
0416,17	VZ for 0.64 AVERAGE	VZAV	0.00285757 m/s
1604,05	0.64 S. Latitude	LAT6	$\pi * 2^{-15}$
1606,07	0.64 s. Longitude	LONG6	$\pi * 2^{-15}$
1610	0.64 s. Lat. Residue	LATR6	0.00091761868m
1611	0.64 s. Lng. Residue	LONGR6	0.00091761868m
1612	0.64 s. Height	HT6	0.9396415365 m
1613	0.64 s. Hgt. Residue.	HTR6	$0.939..*2^{-13}$ m

4.2. Modeling of the FILS System Dynamics

The dynamic behavior of a local level inertial navigation system error propagation can be viewed as a transition from an initial set of conditions, to a new set of conditions at a future epoch. This is done by forming an analytical transition matrix by such methods as matrix exponential expansion or inverse Laplace transformation. These methods are covered by Wong and Schwarz [1979] and will not be repeated here. The general velocity error trends produced by error sources such as initial tilt, initial velocity, and gyro drift errors are shown in APPENDIX A. It should be noted that while these plots accurately reflect how a theoretical error would propagate, the actual error curves are a combination of many error sources and seldom follow the predicted curves exactly. The degree to which the actual curve will follow the predicted curve has a direct bearing on the length of time the system can be run between updates for a specific required accuracy. One very important consideration in determining how well the theoretical transition matrix used by the external computer will follow the actual velocity error generated by the FILS system, is the clear understanding of how the FILS system implements its equations in hardware and software. The FILS equations and mechanization has been discussed in sections 2 and 3. The areas which may cause this mechanization to differ from the textbook equations will now be discussed.

4.2.1. Special Function Stores and Values

The major cause of deviation from the normally expected system dynamics is the way in which the FILS MK_II unit makes use of special function values in order to keep its REAL TIME solution within acceptable bounds. All the special function stores available are listed in Table 3:

Of the special functions listed, the ones dealing with scale factors, non-orthogonalities, gyro drifts, gravity residue, and free-air correction are the most important. A discussion on each of these groups is given relating their effect on the velocity error propagation.

The manner in which the X and Y special function scale factors affects the velocity is shown in section 3.3 which deals with the assembly of the FILS total velocity. It is multiplied by only the values obtained from capacitor measurements of velocity. This is as expected, and agrees with the accepted method of scaling accelerometer measurements.

Table 3. FILS MK_II Special Functions

Stores Inspect	Special Function Code	Quantity	Least Significant Value
0233	18	X Gyro Drift	0.0001°/h
0234	19	Y Gyro Drift	0.0001°/h
0235	20	Z Gyro Drift	0.0001°/h
0231	21	X Channel Scale Factor	0.0001%
0232	22	Y Channel Scale Factor	0.0001%
0222	23	Z Channel Scale Factor	(Must be Zero)
0226	24	E/W Accel. Misalignment	0.0001%
0223	25	N/S Accel. Misalignment	0.0001%
0227	26	Z Acc. Misalignment about E/W	0.0001%
0230	27	Z Acc. Misalignment about N/S	0.0001%
0224	28	Mirror Misalignment	1 min
0503	29	Gravity Residue	1 milligal
0225	30	Free-Air Correction	$1.0*10^{-9} m/s^2$
0200	31	Protractor Misalignment	1 min
0201	32	Protractor X Offset	0.01 m
0202	33	Protractor Y offset	0.01 m
0203	34	Protractor Z offset	0.01 m
0210,0211	35	Spheroid Parameter AM	1 metre
0214	36	Spheroid Parameter BM	1 metre
0212,0213	37	Spheroid Parameter AT	1 metre
0215	38	Spheroid Parameter BT	1 metre
0204	39	Rotation about X axis (Rho)	1 min
0205	40	Rotation about Y axis (Sig)	1 min
0206	41	Rotation about Z axis (Nu)	1 min
0207	42	Vertical angle constant (DB8)	1 min

NOTE: The least significant value indicated refers to the display value and not necessarily to the Least Significant Bit of the stores inspect value.

The north and east accelerometer misalignment from "true" north and east respectively, are fixed values multiplied by the most significant half of the east and north velocity respectively. The key point here is that these values are fixed relative to "true" north and east and do not account for the fact that the whole stable platform may rotate, and thus the misalignment of the north and east accelerometers will be continually changing (although the misalignment between the two accelerometers on the stable platform should remain fixed). The FILS mechanization is not normally part of derived transition matrices, but must be included to properly model this system.

The non-orthogonality of the vertical accelerometer to the north and to the east are also entered as fixed values. As the stable platform tilts about the X and Y axis, the actual values of these misalignment change. For this reason, this implementation should also be considered in the transition matrix.

The special function gyro drift values are primarily used to compensate for a continuous instrumental gyro drift. For this reason, the value in the gyro drift store should not normally be considered as a gyro drift error. It will be shown later, however, to be a very useful method of controlling the platform orientation. If it is used in this manner, the **difference** between the normal gyro drift store value and the modified value, must be placed in the transition matrix.

The Bouguer correction term and the frozen gravity residue term are not normally changed once the system has gone into the **navigate** mode from the **align** mode. If either or both of these terms is to be modified during navigation as a means of controlling the system, they should be included as part of the transition matrix. The gravity residue term in this situation can be viewed as being similar to a vertical accelerometer bias correction term.

It can be seen that the implementation of the FILS mechanization is not difficult, but it must be done with great care. This is especially true as the FILS velocities are not zeroed at updates and can grow to several metres per second causing cross-product terms to become more significant.

5. Long Duration FILS runs

The main area in which an integrated feedback system to the FILS will be of immediate value is long duration marine gravity work. This type of surveying requires an accurate determination of the east velocity component of motion to correct for the Eotvos effect which amounts to about 7.49 mgals per knot at the equator. Normally in this type of environment, the ship will be out for several months, and may be far from shore. When the full GPS constellation is deployed, the velocity can be determined from this source. At the present time, something is required to bridge the gap between good satellite coverage and poor or no satellite coverage providing an accuracy which is sufficiently good for the stated requirements in position and velocity.

5.1. FILS 18 Hour Bench Run with Normal Updates

In order to get an idea of how the FILS MK_II system would operate over long periods of time, a bench run was made which lasted eighteen hours. For this test the system was updated every three minutes by a standard zero velocity update. In the actual situation, this would have to be replaced by some other type of velocity update, coming e.g. from sonar or GPS. A graphical presentation of the first fourteen hours of this run is shown in Figures 10 to 20. These will provide a basis for discussing system feedback and the problems to beware of.

Figures 10, 11, and 12 show the north, east, and height velocities in metres per second. As this was a bench run, the velocities shown are in fact a continuous presentation of the velocity error. Although the run was actually of 18 hours duration, the fixed point arithmetic of the FILS caused the system to become unstable at about 11.71 hours. This breakpoint is clearly visible in Figures 13 to 16. The

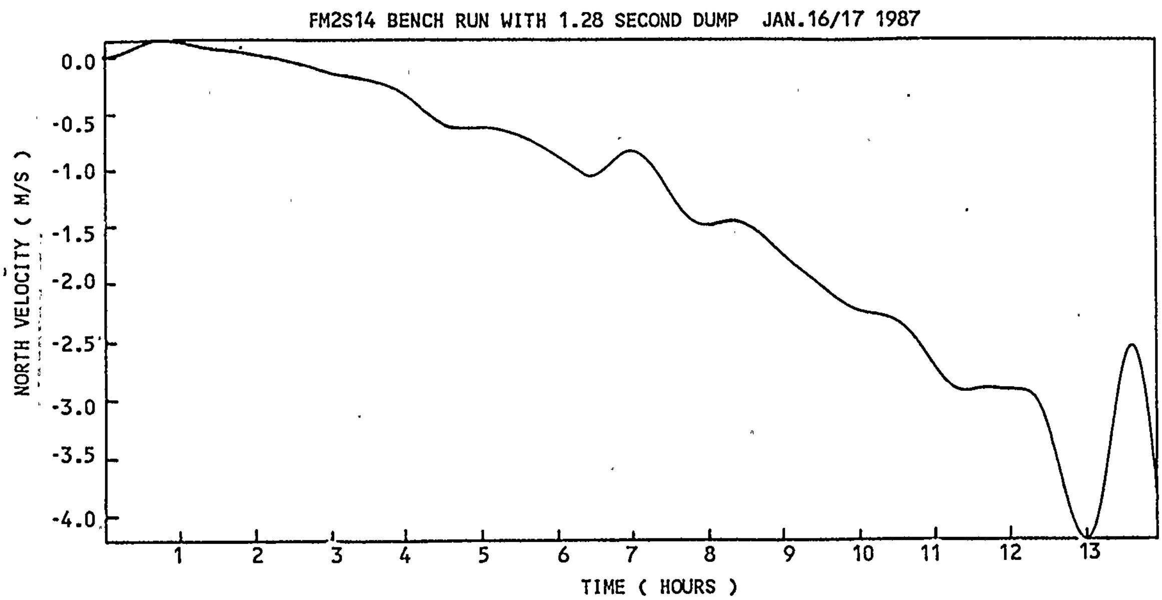

Figure 10. 14 h BENCH RUN NORTH VEL. VS. TIME

problem was caused by the update height velocity exceeding the fixed point arithmetic limit of 5.85216 m/s as discussed in the section on FILS limitations. At this point in time, the correction to the predicted height is calculated improperly causing the predicted height used in the free-air correction term to produce incorrect acceleration values. The affect of this can be seen in Figure 12 where the height velocity error is seen to climb to 45.17 m/s and then go down to -57.40 m/s with some gyrations along the way. The acceleration effect on this velocity can be directly related to the predicted height plot shown in Figure 16. Until 11.71 hours, the predicted height had been maintained within five metres of the true height as illustrated in Figure 17. After this time, it varies between plus and minus 30790 m, which is the range of a 16 bit word having a least significant bit of 0.9396415365 m. This top bit sign fluctuation is the reason for the sudden changes in the slope of the height velocity as shown in Figure 12.

The north velocity curve illustrated in Figure 10, shows a steady downward trend with a few wiggles on it until the time the height prediction breaks down at 11.71 hours. Prior to this, the main cause of the growing north velocity error is the azimuth gyro drift. From Figure 20, it can be seen to be approximately 0.054°/h. Following the breakdown of the height prediction, the erroneous height velocity overflows into the north and east channels as cross product acceleration terms.

The east velocity is not as directly affected by the azimuth gyro drift as the north. This fact is illustrated in Figure 11 which exhibits fairly small velocity errors prior to the breakdown of the height prediction. In this figure, the Schuler period of 84 minutes is also clearly visible. Following the height prediction breakdown, the east velocity can be seen to rapidly change its oscillation pattern.

Figures 14 and 15 show the predicted latitude and longitude position variation in terms of metres. While they are not as much in error as the predicted height position, they still exhibit rapid changes with discontinuities following the breakdown of the predicted height. This is due to the fact that a quadratic curve fit cannot follow the abrupt changes in velocity slope which are caused by the height velocity cross product terms.

Torquing errors can be directly related to the uncorrected delta latitude and longitude plots shown in Figures 18 and 19 which is the integral of the north and east velocities respectively. This relationship is shown in equations 3.1.8 to 3.1.10. The azimuth error in Figure 20 is clearly related to Figure 19.

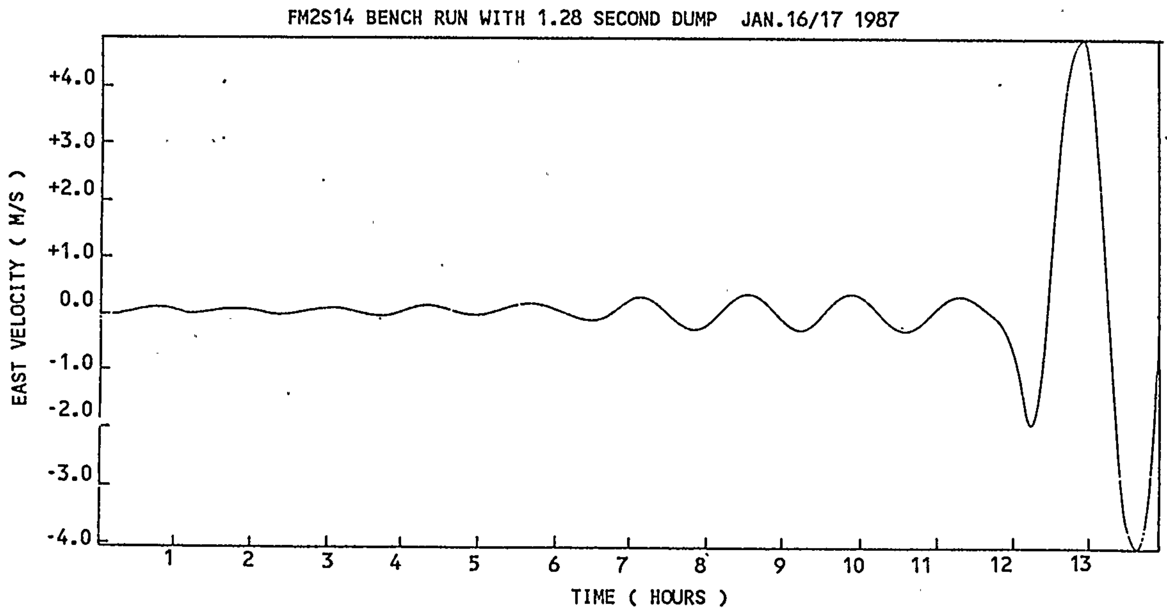

Figure 11. 14 HR. BENCH RUN EAST VEL. VS. TIME

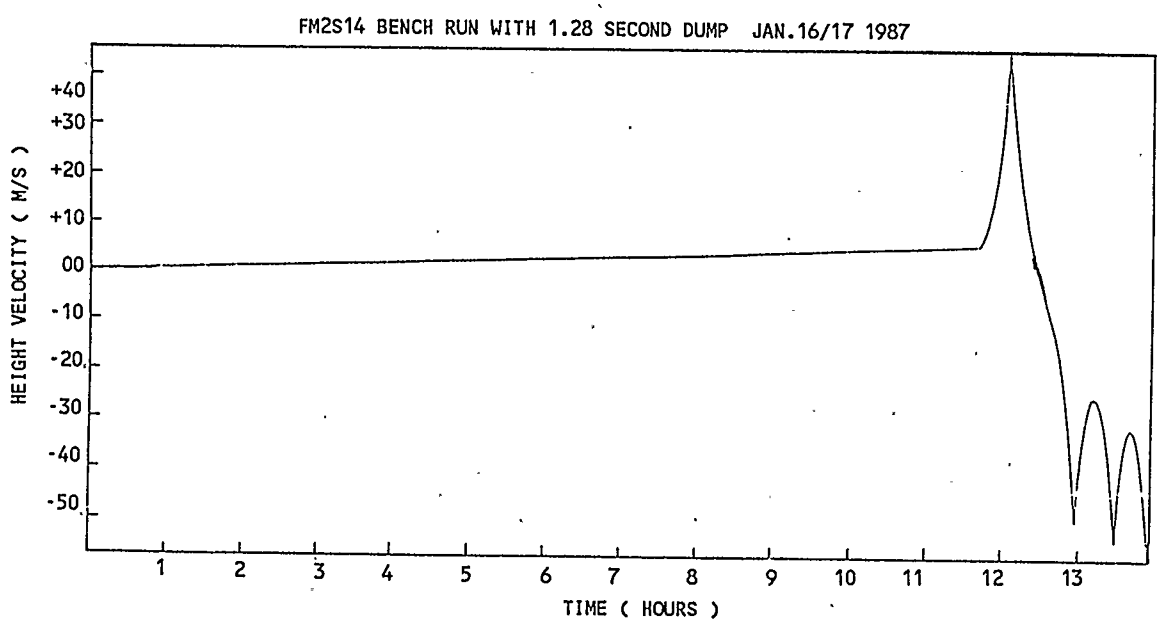

Figure 12. 14 HR. BENCH RUN HEIGHT VEL. VS. TIME

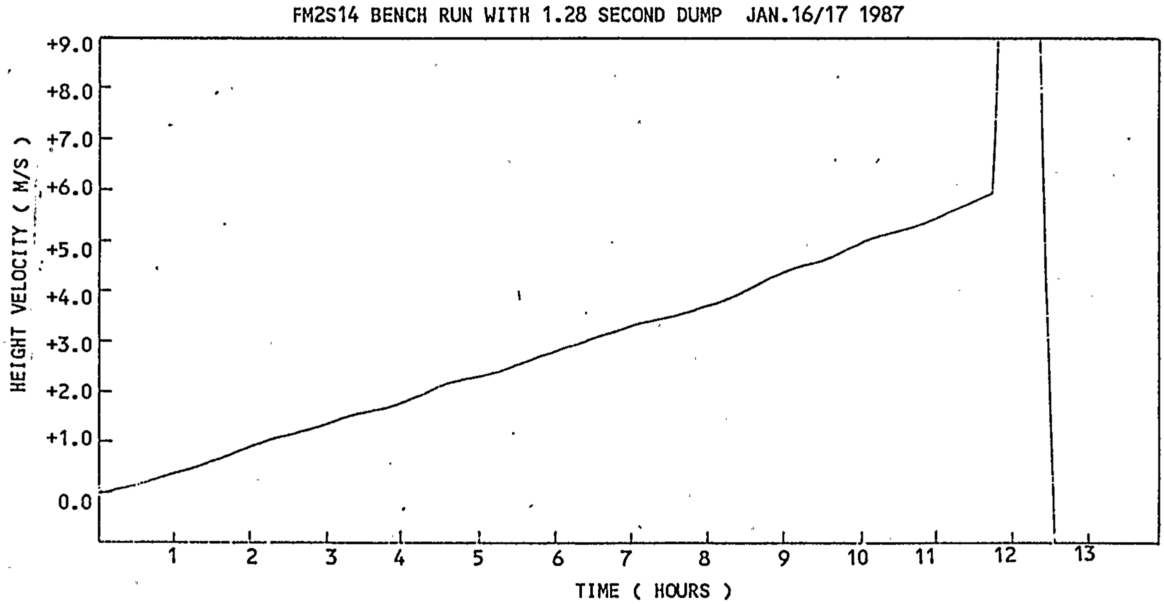

Figure 13. 14 h BENCH RUN EXPANDED HEIGHT VEL. VS. TIME

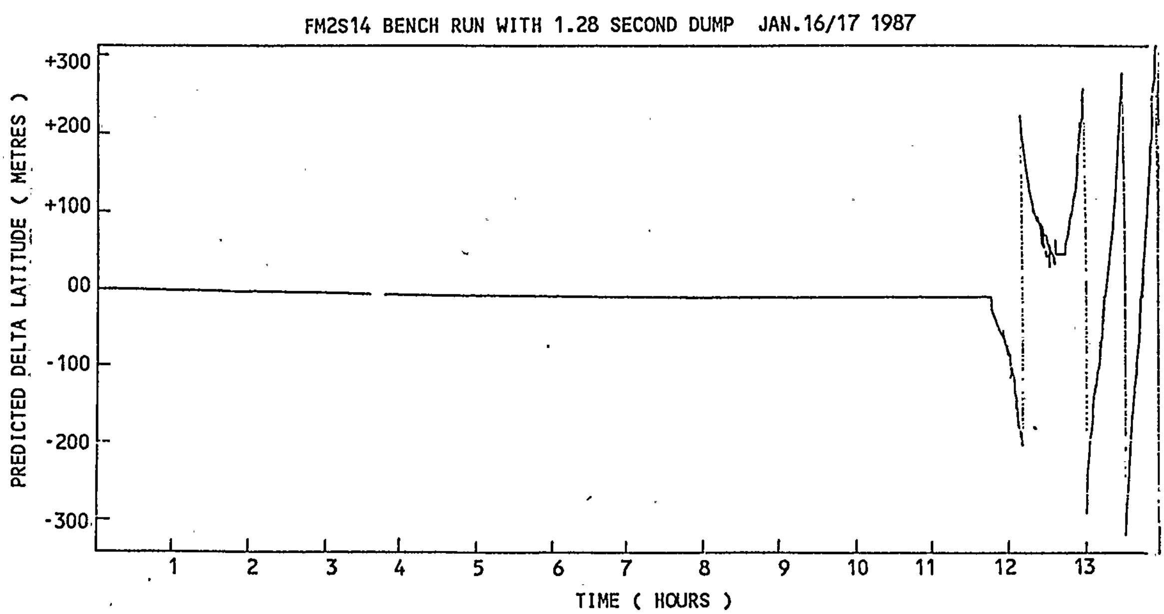

Figure 14. 14 h BENCH RUN
PREDICTED DELTA LATITUDE VS. TIME

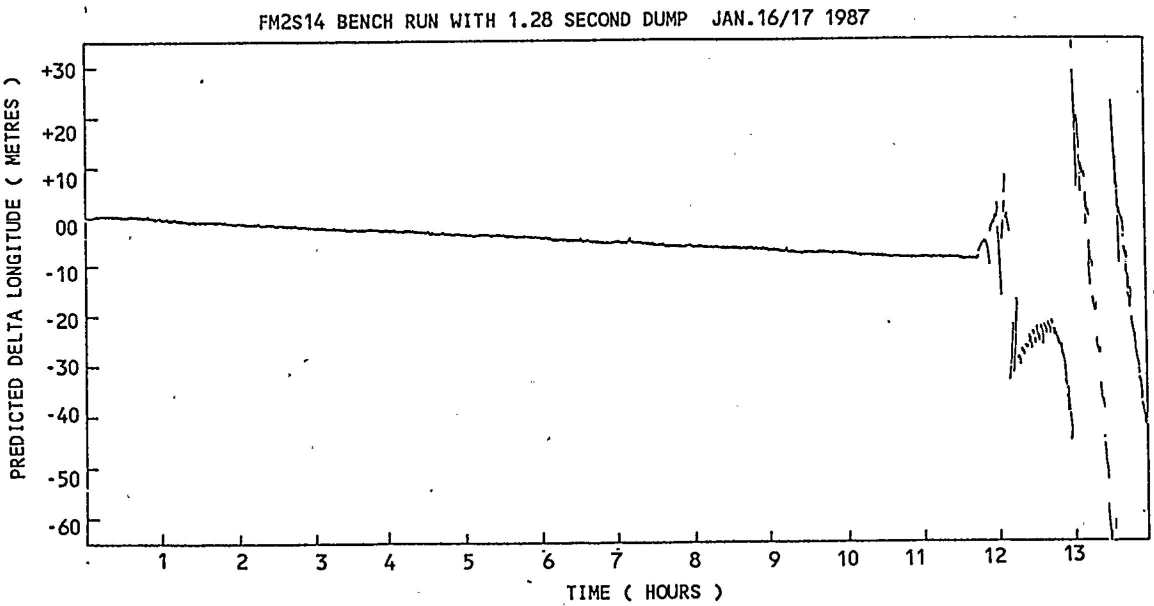

**Figure 15. 14 h BENCH RUN
PREDICTED DELTA LONGITUDE VS. TIME**

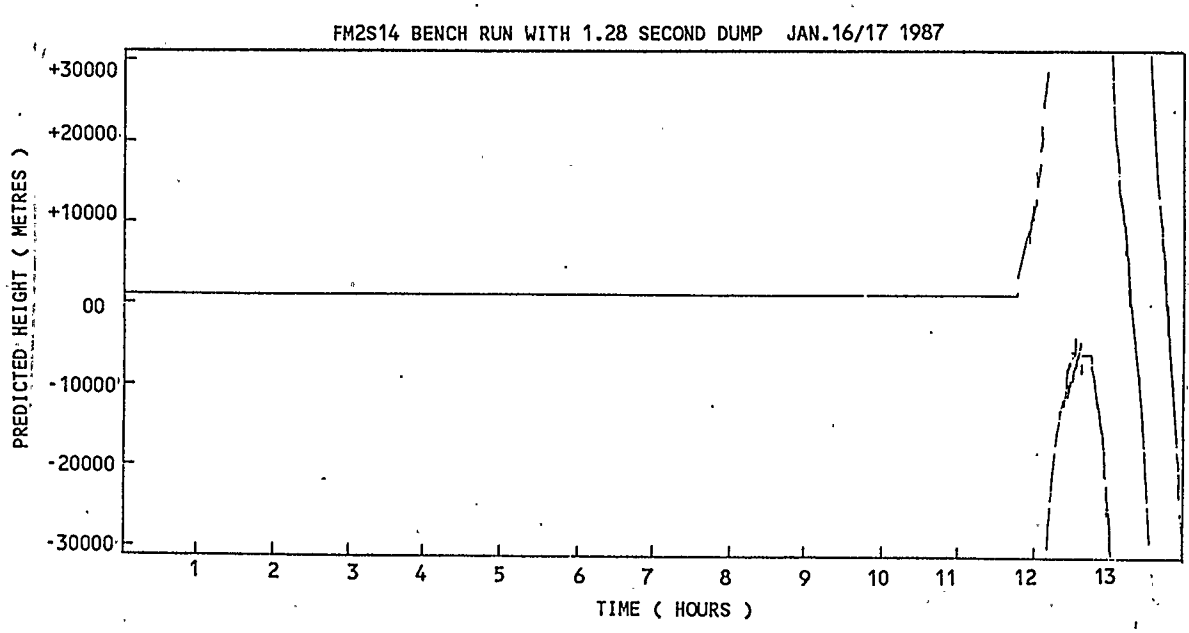

Figure 16. 14 h BENCH RUN PREDICTED HEIGHT VS. TIME

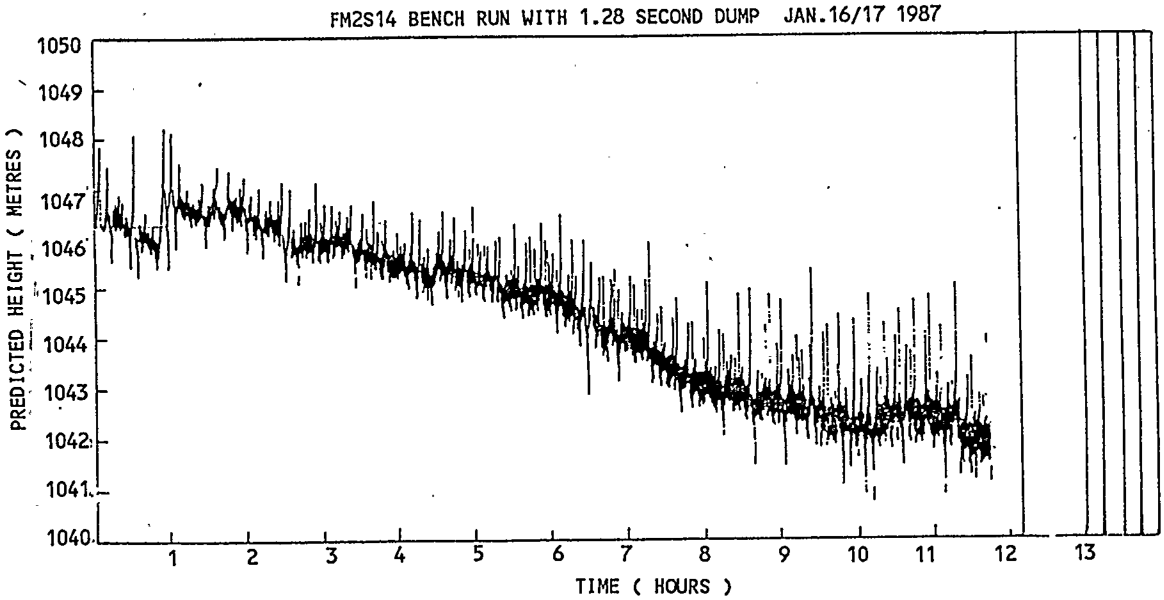

Figure 17. 14 h BENCH RUN
EXPANDED PREDICTED HEIGHT VS. TIME

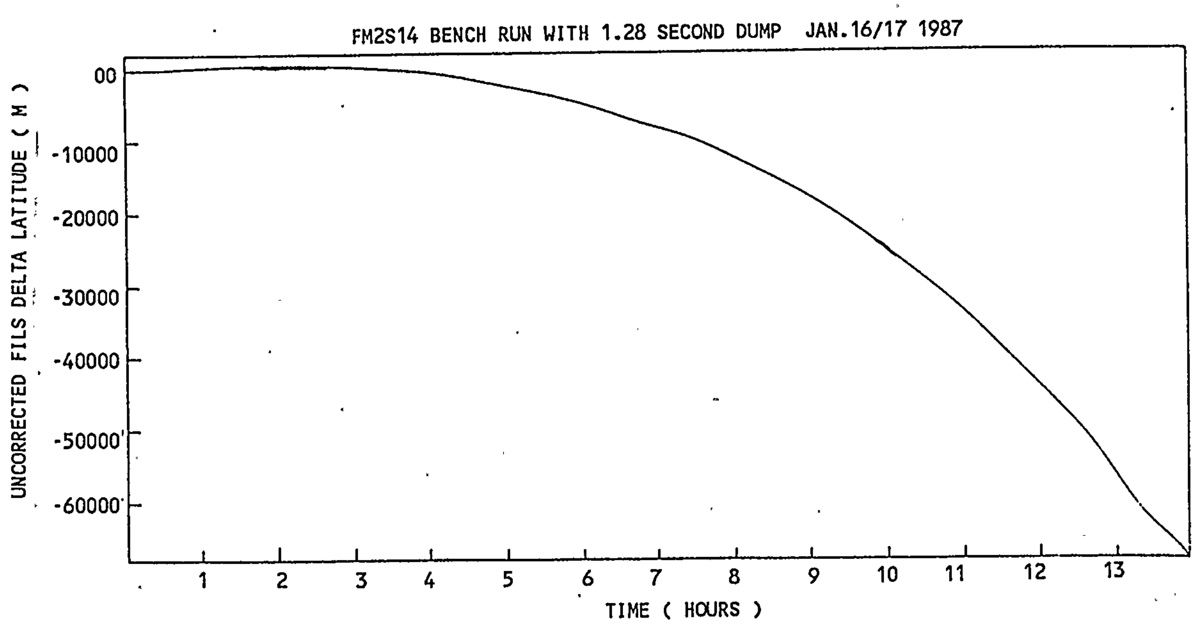

Figure 18. 14 h BENCH RUN
UNCORRECTED DELTA LATITUDE VS. TIME

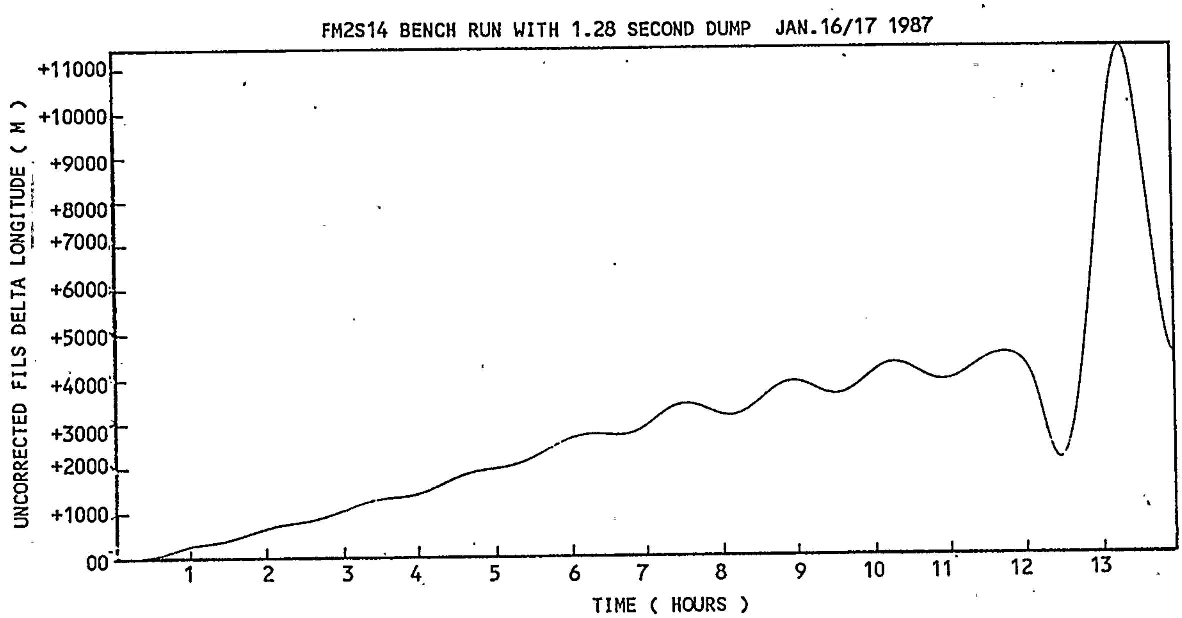

Figure 19. 14 h BENCH RUN
UNCORRECTED DELTA LONGITUDE VS. TIME

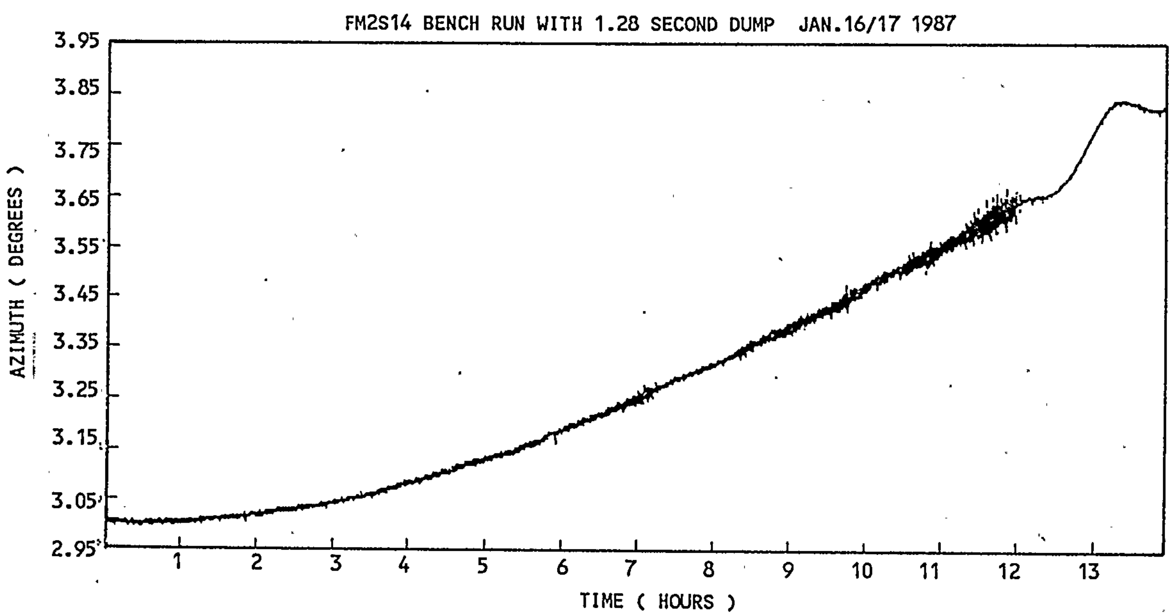

Figure 20. 14 h BENCH RUN FILS AZIMUTH VALUE VS. TIME

5.2. FILS 34.5 Hour Bench Run With Normal Updates

A second bench run lasting a period of 34.5 hours was made with the FILS unit using normal updates. On this run the height velocity did not reach the 5.85216 m/s fixed point arithmetic boundary problem until 26 hours into the run. The velocity profiles, and predicted height for this run were similar the the 18 hour run, and can be found in Appendix G.

5.3. Kalman Filter Mechanization

Use of the Kalman filter and its variations has grown rapidly since it was first introduced by R.E.Kalman in 1960. There are many books available which cover this topic, e.g. Gelb [1974], Brown [1983], and Sinha [1986] to mention but a few. The derivation of Kalman filter equations specifically for a local level inertial system can be found in Britting [1971] or Wong [1982]. Only a very generalized overview of the topic will be presented here as the main thrust of this presentation is on how to implement the solved state vector values as feedback to the FILS unit rather than the testing of the Kalman filter itself. This is a topic which will be pursued outside the context of this dissertation.

An important point to bear in mind is that the following discussion is **not** about a redesign of the FILS unit. The idea is rather to implement an external feedback loop without making hardware or software changes within the standard FILS MK_II unit.

The error behaviour of the inertial system can be described by a system of first order differential equations of the form:

$$\dot{\underline{x}} = \mathbf{A}\,\underline{x} + \mathbf{B}\,\underline{u} \tag{5.3.1}$$

where $\underline{x}$ = the state vector

$\mathbf{A}$ = dynamics matrix which describes unforced or zero input system behaviour

$\underline{u}$ = input

$\mathbf{B}$ = characterizes the effect of input on the system dynamics

Update measurements are of the form:

$$\underline{y} = \mathbf{C}\,\underline{x} \tag{5.3.2}$$

where $\underline{y}$ = the observation vector

$\mathbf{C}$ = design matrix relating the states $\underline{x}$, to the observations $\underline{y}$.

The state vector $\underline{x}$ can be estimated from update measurements $\underline{y}$ if the system is completely observable. In that case, the measurement y can be used to control the system by designing a compensation loop for the differential equation:

$$\dot{\hat{\underline{x}}} = \mathbf{A}\,\hat{\underline{x}} + \mathbf{B}\,\underline{u} + \mathbf{L}\,(\,\underline{y} - \hat{\underline{y}}\,) \tag{5.3.3}$$

$$\hat{\underline{y}} = \mathbf{C}\,\hat{\underline{x}} \tag{5.3.4}$$

where $\hat{}$ = an estimated quantity

$\mathbf{L}$ = a suitably chosen gain matrix having compatible dimensioning with x.

The resulting compensater combining the observer with state feedback is shown in Figure 21. Embedded in this figure is the following equation for control feedback:

$$\underline{u} = K [\underline{r} - \underline{k}^T\underline{x}] \qquad (5.3.5)$$

where:

K = DC gain constant

$\underline{k}^T$ = $[k_1 \;\; k_2 \;\; k_3 \;\; \ldots \;\; k_n]$

k_i = gain on the ith state

$\underline{r}$ = reference input (= 0 for FILS mech.)

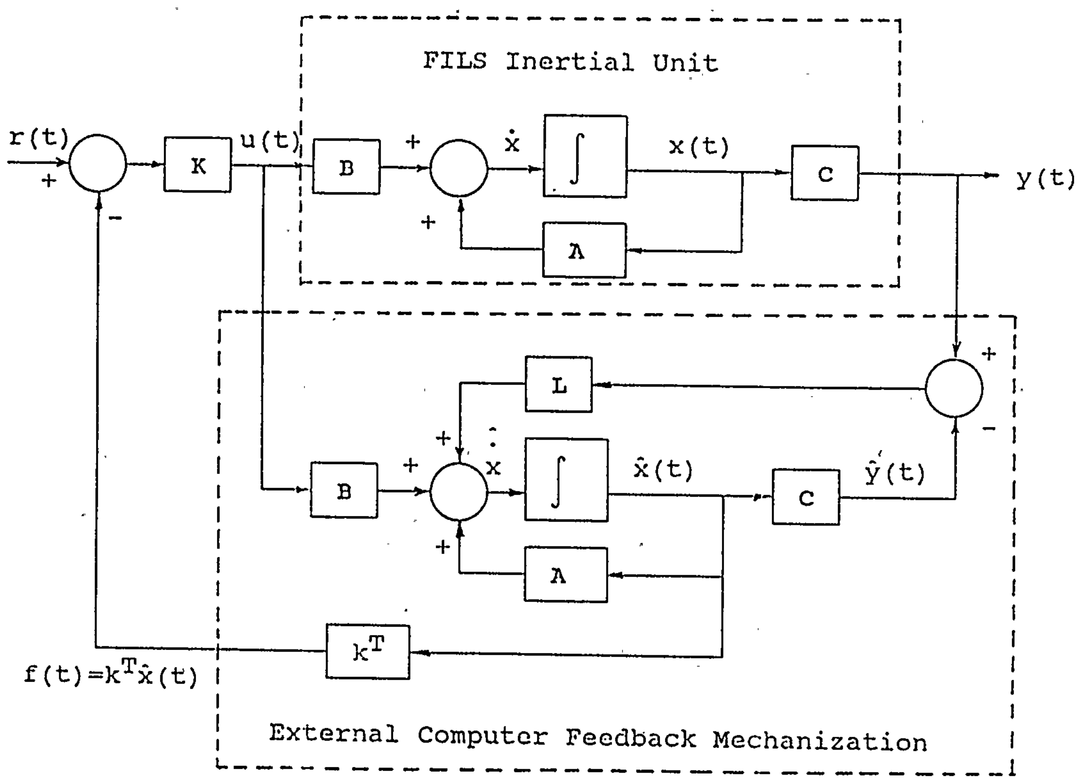

Figure 21. Kalman Filter Feedback Mechanization

The FILS **External Filter** will have 12 states. These are:

1 Latitude Error
2 Longitude Error
3 Height Error
4 North Velocity Error
5 East Velocity Error
6 Height Velocity Error
7 Platform Tilt about the X axis
8 Platform Tilt about the Y axis
9 Platform Tilt about the Z axis (Az.Misalignment)
10 X Gyro Drift Error
11 Y Gyro Drift Error
12 Z Gyro Drift Error

Additional states such as accelerometer biases, are possible, but will only be implemented if it is determined that the 12 state estimation is not adequate to meet the stated requirements.

The actual filter design and implementation will not be discussed here. However, specifics of the FILS unit which relate to its design, both in modeling the output signal as well as in controlling the FILS unit, will be covered.

Testing of the feedback mechanism is done in a static environment, where the position, velocity, and attitude are known and therefore do not have to be estimated.

5.4. Real Time Feedback Control of the FILS MK_II system

The FILS MK_II system can be controlled from an external computer by altering the values held in its RAM stores. This allows manipulation of the system operation without actually having to control the platform directly. In order to do this in a successful manner, the way in which these stores are used by the FILS computer must be understood. While some of this has been discussed previously, this section will specify how particular stores can be used to achieve specific objectives. These objectives will be addressed along with various means of attaining them.

5.4.1. Objective: Control the FILS Predicted Position

The FILS predicted position is normally controlled internally by the use of zero velocity updates at regular intervals. This has traditionally required the FILS unit to be brought to a complete stop (relative to the earth's surface) for a period of twenty seconds every three to five minutes. In some applications (such as navigation at sea) this is physically not possible. If the FILS system has not seen what it considers to be a zero velocity update within twenty-one minutes, it will stop applying any corrections to its positions, and these "uncorrected" positions will then be used in place of predicted positions. To appreciate the effect of this, the navigation equations as given in section 3.1 should be consulted. Any place a predicted latitude or height term appears in these equations will be affected. The height channel will become unstable very quickly and the other channels (although Schuler damped), will also begin to exhibit large changes. These effects can clearly be seen from the figures in Appendix G showing a bench run of 34.5 hours duration. The cause of the predicted height becoming unstable, as previously mentioned, is due to the fixed point arithmetic being done on the zero height velocity update. It can be seen that the problem happens when the height velocity error exceeds the fixed point store limit of **5.85216 m/s** imposed on the zero velocity update coefficient calculations. This also points out a requirement which must be met to successfully use the FILS predicted position algorithm. That is:

The actual system error velocity on all channels MUST be maintained below ±5.85216 metres per second.

Implementation of the FILS predictor, without actually stopping and doing zero velocity updates, can be accomplished by externally calculating the quadratic coefficients, as shown in section 3.4. To do this the true velocity for each channel must be available from some other source, such as GPS. This velocity is then subtracted from the FILS velocity for the same time. The result is used as a zero velocity input for the coefficient equations. These coefficients are then written to the appropriate FILS stores along with an adjustment of the time interval stores. The total position correction stores must also be updated in the FILS. These stores hold the linear correction up to the last update time. They can also be altered to finetune the predicted positions for errors which were not covered by the quadratic curve fit of the velocities. By letting the FILS unit do most of the work in maintaining the correct "predicted position", the external computer is freed to do other tasks.

It should be noted that the total correction stores, are in terms of metres. While the double length store itself allows a value of up to 124,554,051 metres to be accumulated without error, it is advisable to hold this to a smaller value. This is due to the fact that the linear value has to be changed to an angular value before it can be applied to the uncorrected position. This can lead to problems, particularly for the longitude correction where the scaling factor is a function of position.

The total correction can be kept small by changing both the uncorrected position store and the correction store by equivalent amounts and appropriate signs.

5.4.2. Objective: Control the FILS Roll, Pitch, and Azimuth

The most effective way to control the FILS attitude is by altering the gyro drift stores from their nominal value, used to counter actual gyro drift in the instrument, to a new value for a specific amount of time. After this period, the nominal values should be put back into the stores. These stores, XDRIFT(0233), YDRIFT(0234), and ZDRIFT(0235), have a least significant bit of 0.000738°/h (ie. 0.000738 arc seconds per second) with a maximum value of 24.182784°/h. Generally speaking, the store should be changed by only a small value to minimize any error in timing of the insertion of this value. In addition, this will mean the FILS hardware has to service the platform less often. When these drift changes are applied, it is very important that the external computer's dynamic model also accounts for the change. Once the system has been initially aligned and leveled, it should not be necessary to change these drift rates very often. If this is done too frequently, it may be difficult to properly assess the system dynamics for long periods without external fixing updates.

5.4.3. Objective: Control the FILS Error Velocities

As mentioned under the section on control of the FILS predicted positions, the velocity error must be maintained below 5.85216 m/s. In fact, a more appropriate goal would be to maintain the velocity error below 0.5 m/s. Trying to go much lower than this may cause more problems than it cures due to the difficulty in properly extracting the FILS dynamics when comparing it against noisy outside references.

There are different ways in which the velocity can be controlled. The most obvious is to change the value in the velocity stores themselves. Here it is important to know which stores to change. The total velocity is obtained from stores 1400,01 for the north velocity, 1402,03 for the east velocity, and 0530,31 for the height velocity. It will, however, do no good to change these store as they are updated by the FILS every 20 milliseconds. As discussed in section 3.3, there are only two terms per channel which have to be altered to effectively control the velocity. To illustrate this, the north channel will be discussed with the same procedure being applicable to the other channels.

For the north channel, only the terms $\mathbf{VN_I}$(1201) and $\mathbf{VN_X}$(1330) can successfully be used to adjust the velocity. The first term is the number of resets which the Y accelerometer has seen and has a least significant bit value of 0.02286 m/s. This store could be rapidly changing if the vehicle motion is not smooth. The other term relates to the calculated cross product velocity generated by cross product acceleration. This store is updated when the **VNRES** store reaches a certain level. The scaling of the least significant bit of the **VNX** store is 0.0028575m/s. While the **VNI** store will alter as a direct function of platform tilt about the X axis, the **VNX** store will not. The problem with resetting these stores is that it is not possible to simply add a value to the store. It requires the store to be read by the external computer, the correction value to be added to this, and the new value to be written back to the store. The problem with doing this procedure is that the store may have been altered between the time the external computer reads it and the time it is written back. This can happen within any twenty millisecond period.

To avoid this problem, another possibility is available. This other option is to use the X gyro drift rate to tilt the platform into (or out of) the gravity vector. This will result in an increase (or decrease) of the acceleration sensed by the Y accelerometer. This in turn will result in an increase (or decrease) of the **VNI** term, but this time under the FILS control avoiding the possible problem which exists with the other method.

As with all other control options, it is imperative that the external computer dynamics model properly accounts for the actual method used.

Control of the height channel velocity can be done in a way which is not permitted for the horizontal channels. This is the use of the gravity residue backoff term **GRES** located in store 0503 and having a least significant bit of 1.737882653 mgals. This store is used during normal system alignment to backoff any residual vertical acceleration seen. When the system is put into navigate mode, this store is frozen at its last estimated value. By altering this value, the constantly applied vertical acceleration can be altered. This is not a function of height, position, or any other FILS feedback and it is therefore very easy to predict the effect a variation of this term will have on the height velocity. Figure 13, showing the height velocity of a bench run, clearly illustrates a situation in which this feedback control method could have been of value. This figure shows a fairly linear vertical acceleration of $13.57*10^{-5}$ m/s^2 which resulted in the system becoming unstable at 11.7 hours. If the **GRES** store had been altered by 8 bits, this growth in the height velocity error could have been countered. The actual effect of changing this value is shown in the section on examples of FILS feedback control mechanization.

5.5. Real Time Integration of Measurements

Due to the nature of the control feedback, the only practical external control would be a Kalman type filter with a transition matrix defined numerically for short period transitions. Although the analytical approach greatly reduces the computational burden of the control computer, it implies that a well defined system with previously known system dynamics be used. While this is possible for limited applications, the flexibility afforded by the numerical approach makes it a more attractive alternative. With the numerical precision and speed of present day computers, successful implementation of the numerical approach can be accomplished with increasing ease.

The most promising external source for integration with inertial systems is the GPS system. During the period in which only limited coverage is available from this system, the NNSS transit system will help to fill the gaps. Additional sensors such as bottom tracking doppler sonar or Loran-C are also possibilities.

5.6. Hardware Modifications for Alignment At Sea

The phrase **alignment at sea** is used to imply that the FILS system can be started up while out at sea. This is to be distinguished from the case where the system is aligned on a ship at near stationary conditions alongside a wharf. In the latter case, a standard FILS unit could be used with no modifications necessary. In the case of a system which must start up while out at sea, there is one major modifications which should be made to protect the platform from being damaged. This modification enables the platform to be **caged** before the gyros have run up to full speed. The term caged means that the platform orientation is maintained by feedback from the gyroscopes rather than from the accelerometers. The reason this is necessary is to prevent large torques being applied at the gyros bearings due to the platform being coarse leveled by the accelerometer outputs. In a stationary environment this is quickly done and the platform remains relatively quiet while the gyros run up. At sea, the platform is continually adjusting itself due to the accelerometer feedback. This results in the platform being moved even as the gyros are approaching full speed. The inertia of the gyroscopes then must be overcome by the bearings applying a torque on the gyro shaft. To minimize this problem, the FILS unit should be modified so that the platform is **caged** before the gyros have run up to full speed. As this is done before the gyros are at full power, their moment of inertia at the time of platform caging is less than with the normal FILS implementation. The penalty one pays for this is the possibility that the platform may stabilize with a large initial tilt relative to the local gravity vector. In addition to the vertical jostling, an azimuthal jitter is present as the platform attempts to maintain a fixed heading relative to the FILS casing which itself is changing in azimuth.

A second modification which may be made for applications at sea is the elimination of the height channel accelerometer hardware integration of velocity. This is accomplished by shorting out the height channel capacitor resulting in an A/D reading always equal to zero. This does not mean, however, that the FILS unit will show the height velocity to be zero. Due to the cross product accelerations from the north and east channels, height velocity readings will differ from zero. To maintain zero height velocity, the cross product height velocity stores must be zeroed out at a rate which is sufficient to maintain its value below a level which can be considered as zero. Figure 22 shows the height velocity from a bench run which had the height channel shorted out. It should be noted that the height velocity was reset whenever it reached 0.002 m/s. Although the number of resets is not very large, the corresponding horizontal velocities are quite small as shown in Figure 23 and 24.

Although shorting out the height channel may appear to be a good idea, it results in the loss of velocity information caused by actual vessel movement. For integration with systems such as GPS which enable precise velocity determination, it may be advisable to maintain the height channel information. Means of controlling this channel have been discussed in the section on FILS feedback control mechanization.

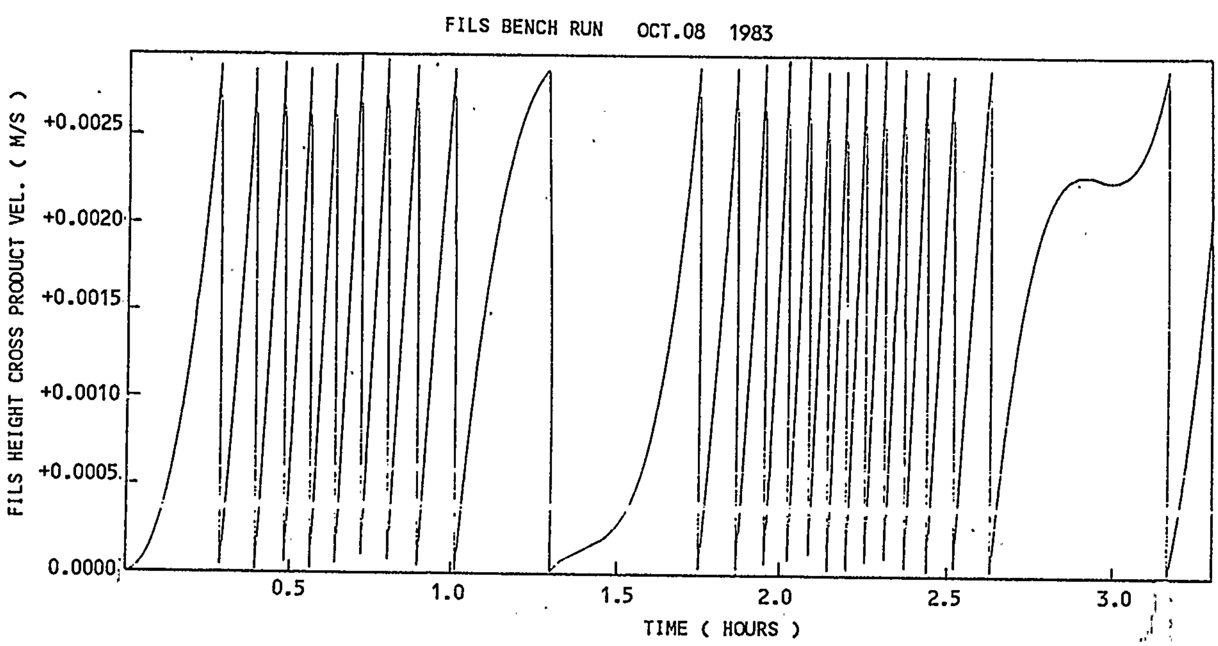

Figure 22. 3.3 h BENCH RUN HEIGHT VEL VS. TIME (VERTICAL CHANNEL SHORTED OUT)

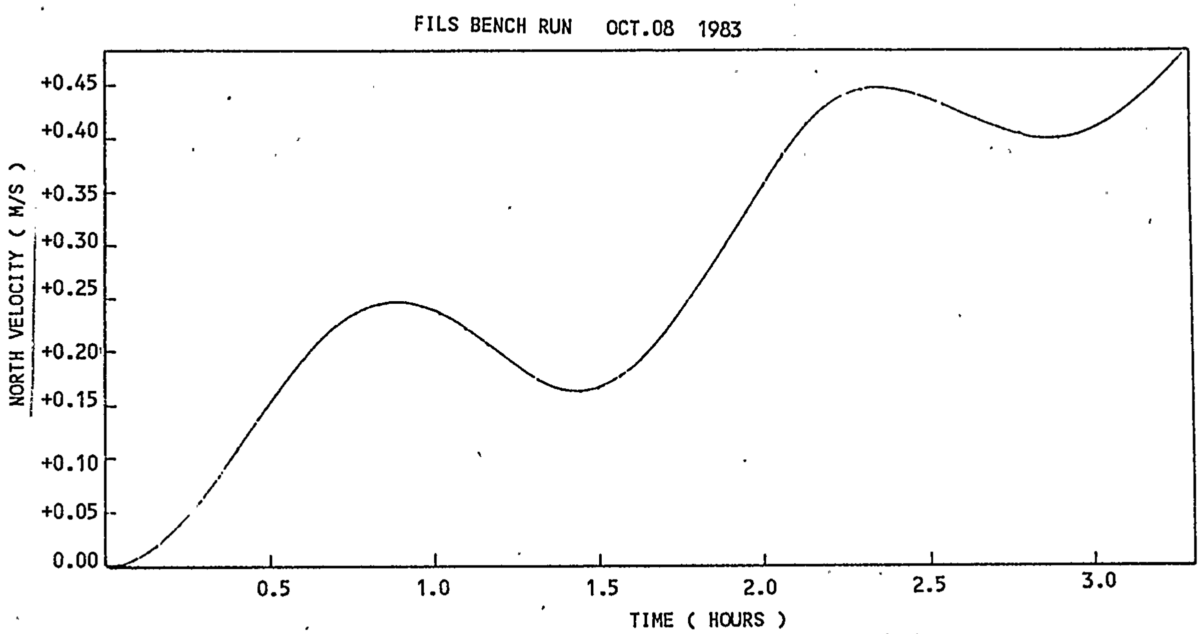

Figure 23. 3.3 h BENCH RUN NORTH VEL. VS. TIME
(VERTICAL CHANNEL SHORTED OUT)

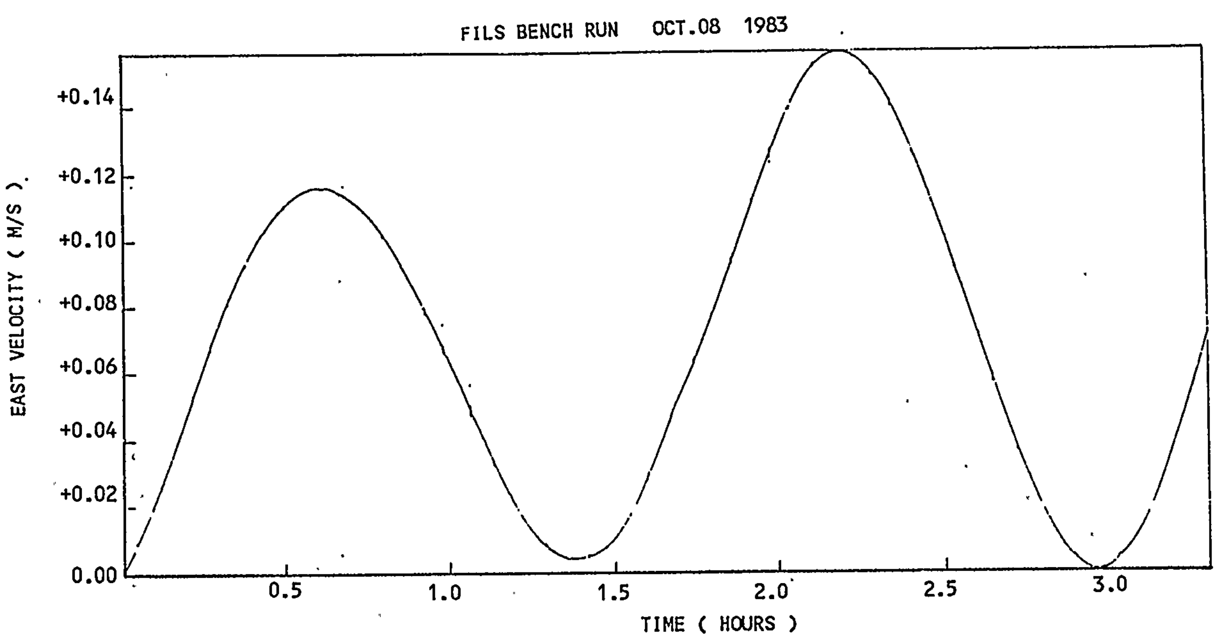

Figure 24. 3.3 h BENCH RUN EAST VEL VS. TIME
(VERTICAL CHANNEL SHORTED OUT)

6. Examples of FILS feedback control mechanization

Implementation of feedback control of the FILS unit, eliminating the need for actual zero velocity updating by the FILS unit itself, is illustrated in Figures 25 to 31. Although this was a bench run of about 20.6 hours duration, the FILS unit was never updated in the standard manner, except for the first two updates. After that, the FILS velocity was monitored by an external computer which every three minutes calculated the update coefficients required by the FILS unit. These coefficients were fed back to the FILS along with required time interval and status stores modification. The only other feedback control used during this run was the adjustment of the gravity backoff term. This was done at various times during the run to keep the height velocity from growing too large. Some of these times and amounts are presented in Table 4.

Table 4. GRES Values for 20.6 Hour run

FILS TIME	Old GRES Value	New GRES Value
07:01:28	- 52 mgal	- 60 mgal
07:18:10	- 62 mgal	- 58 mgal
07:46:20	- 60 mgal	- 70 mgal
09:01:20	- 70 mgal	- 66 mgal
09:16:35	- 66 mgal	- 62 mgal

Figure 25 shows the platform azimuth fluctuation over the run period to be about 2.3 minutes of arc. The discrete steps shown on this figure relate to the least significant bit of the azimuth store which is $\pi * 2^{-15}$ radians (19.775 arc seconds). This drift rate is much lower than that shown in Figure 20.

Figures 26,28, and 30 show the height, north, and east error velocity respectively. These can be seen to have been kept to fairly reasonable values, with the height velocity being the largest of the three. The controlling of the height velocity on this run was done manually through the FILS CPU panel and only at irregular intervals. If this had have been done on the basis of a computer feedback adjustment based on a maximum allowable velocity, the error would have been much smaller. The height velocity ranged between -1.4 and +0.5 m/s. The north and east velocities ranged between -0.19 to +0.10 and -0.55 to +0.12 m/s respectively.

The predicted positions, as shown in Figures 27,29, and 31, were maintained solely by correcting for the area under the velocity curves and held quite well over this 20.6 hour time period. The predicted height remained within 2 metres of the true position for the entire period. The north and east predicted positions changed by about 45 metres and 120 metres respectively. While this is quite a large spread in the horizontal positions, a comparision of the predicted position error with the mirror image of the actual velocity error for the same channel, shows a virtual perfect match. This indicates an error source which is systematic and therefore can be accounted for. A clear understanding of this error source can be obtained from Figure 35 which shows the same error source but over a shorter time period. A discussion of this is given with the comments on the 4.4 h run.

The 20.6 hour run just described had the updates done remotely by an external computer but still had the initial alignment done by the FILS unit in its normal alignment mode which requires the system to be stationary. As this would not be possible with an at sea alignment, the next step

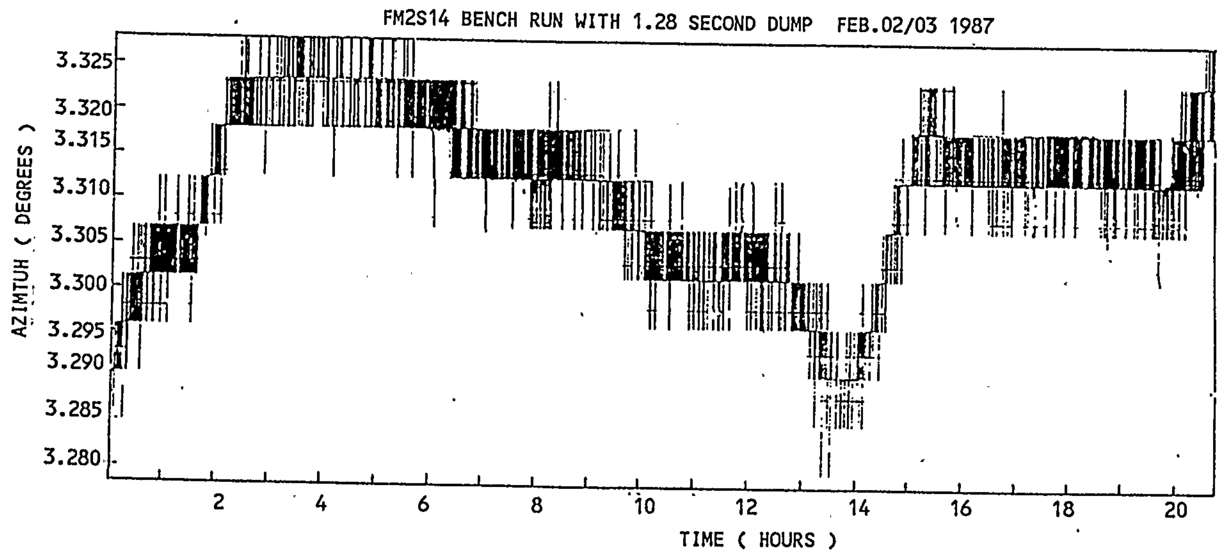

Figure 25. Feedback 20.6 h bench run Azimuth vs. Time

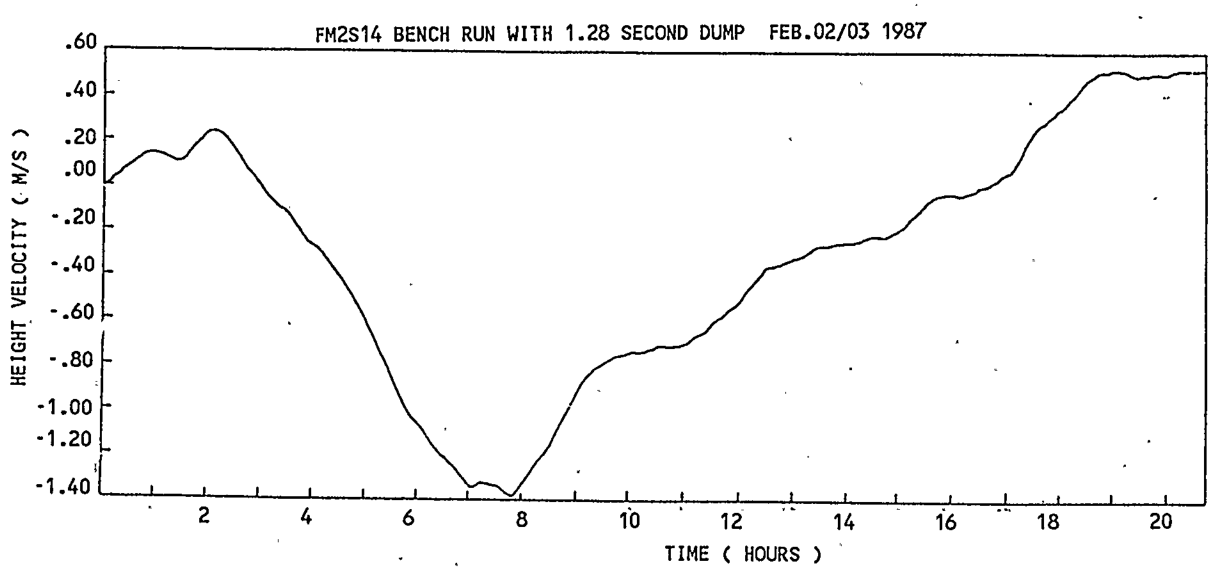

Figure 26. Feedback 20.6 h bench run Height Velocity vs. Time

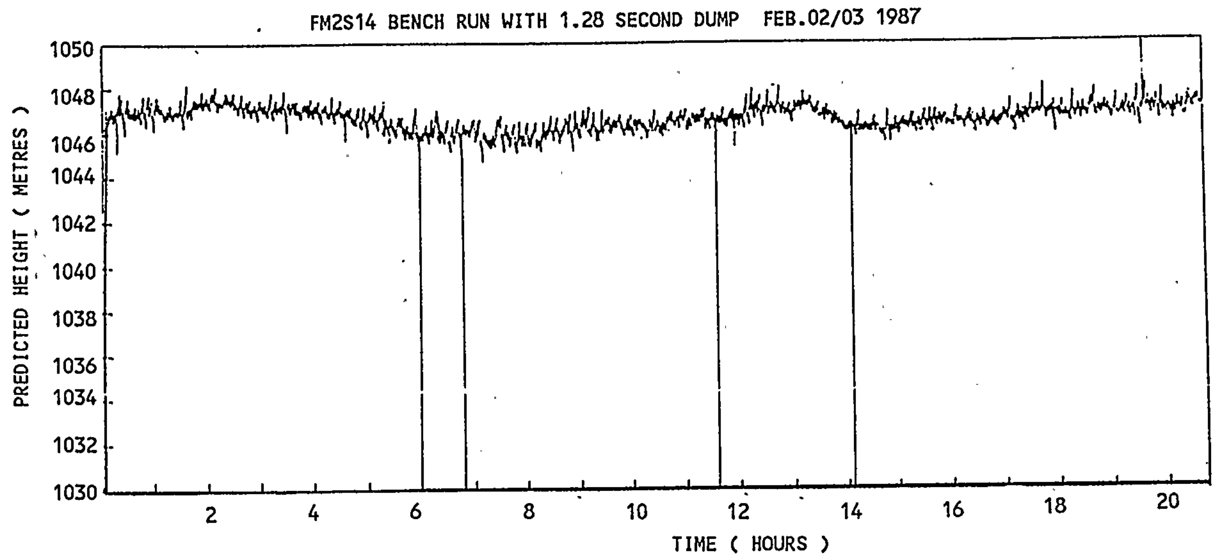

Figure 27. Feedback 20.6 h bench run
Predicted Height vs. Time

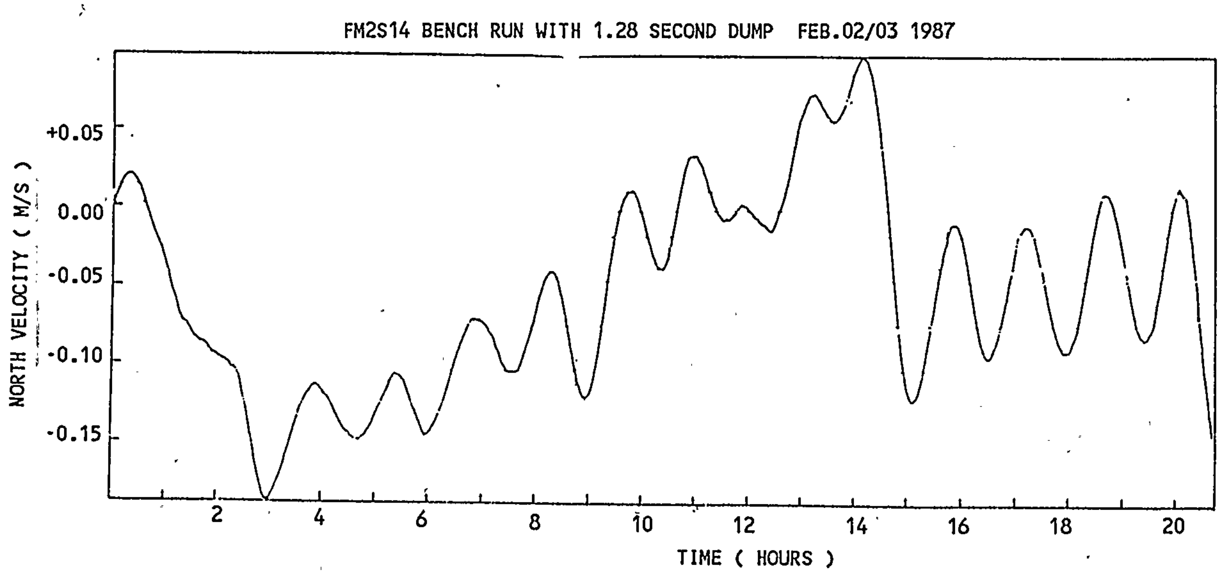

Figure 28. Feedback 20.6 h bench run
North Velocity vs. Time

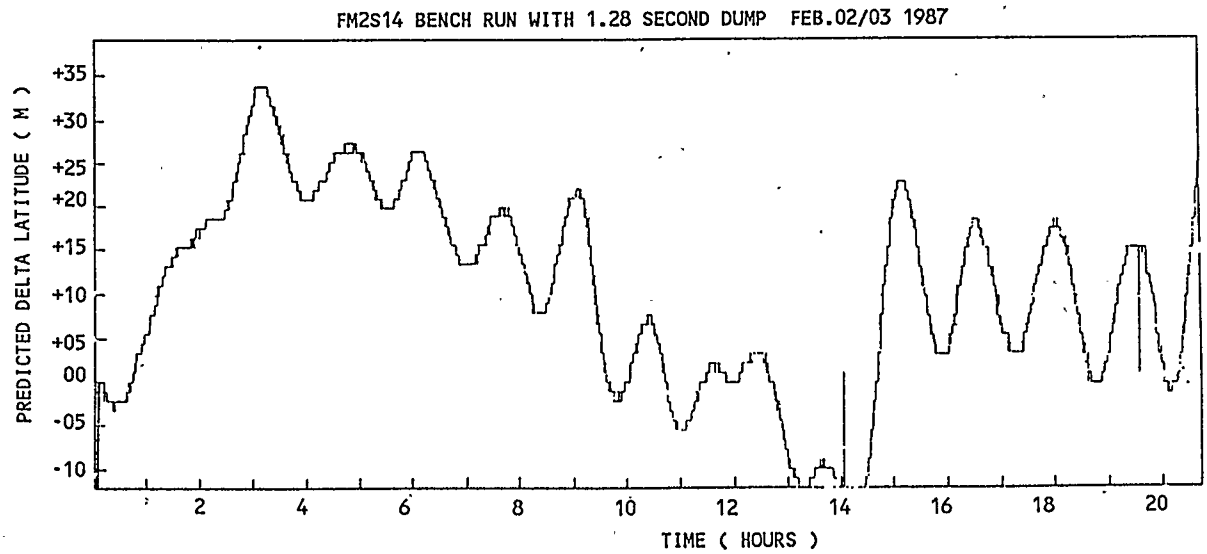

Figure 29. Feedback 20.6 h bench run
Delta Predicted Latitude vs. Time

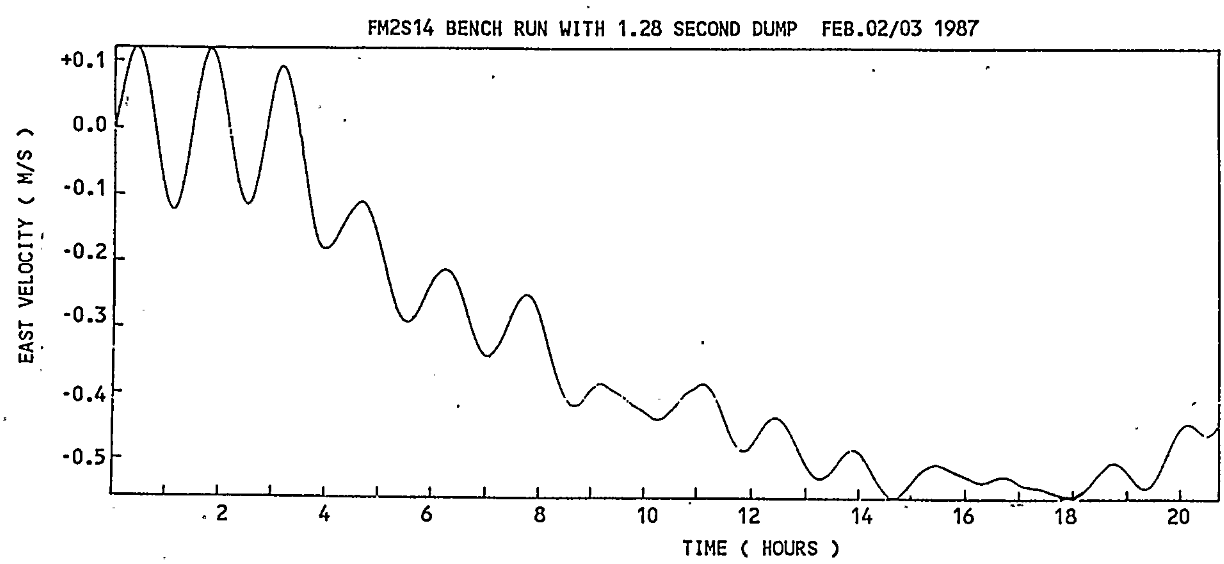

Figure 30. Feedback 20.6 h bench run
East Velocity vs. Time

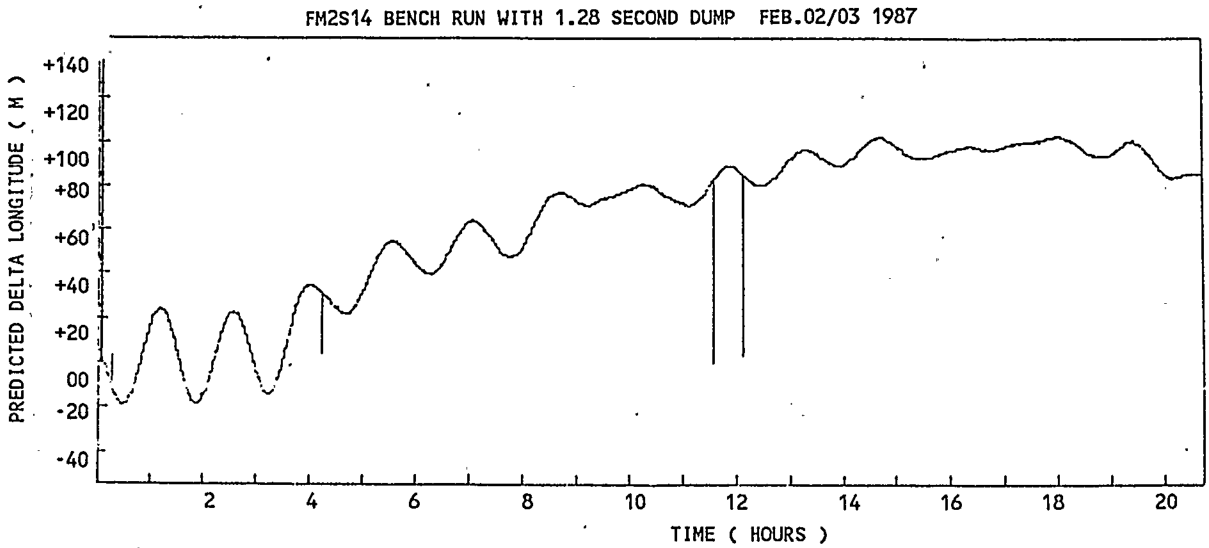

Figure 31. Feedback 20.6 h bench run
Delta Predicted Longitude vs. Time

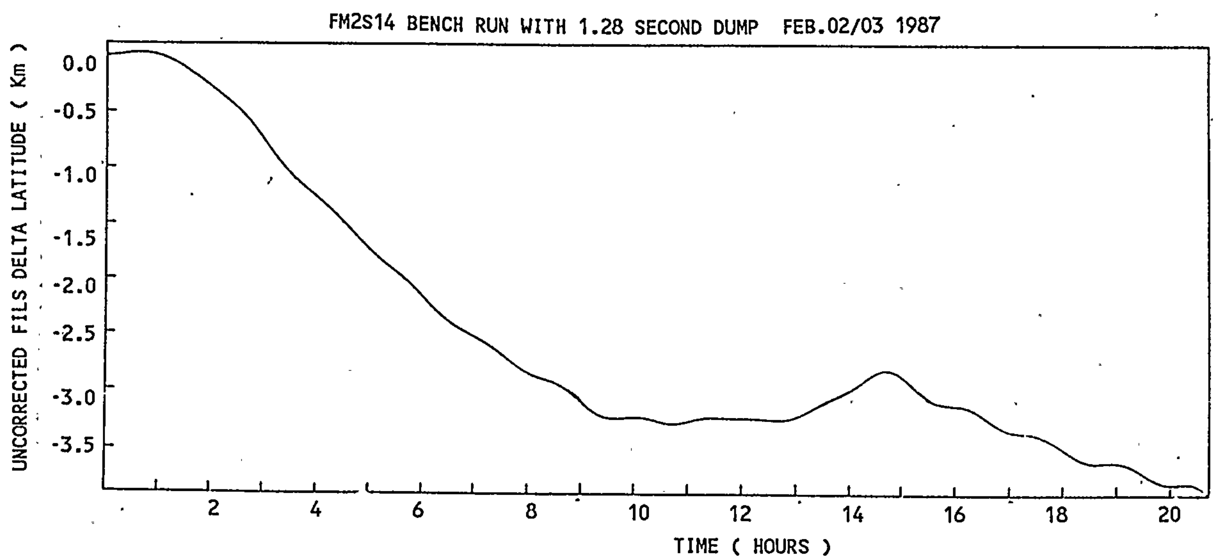

Figure 32. Feedback 20.6 h bench run
Uncorrected Delta Lat. vs. Time

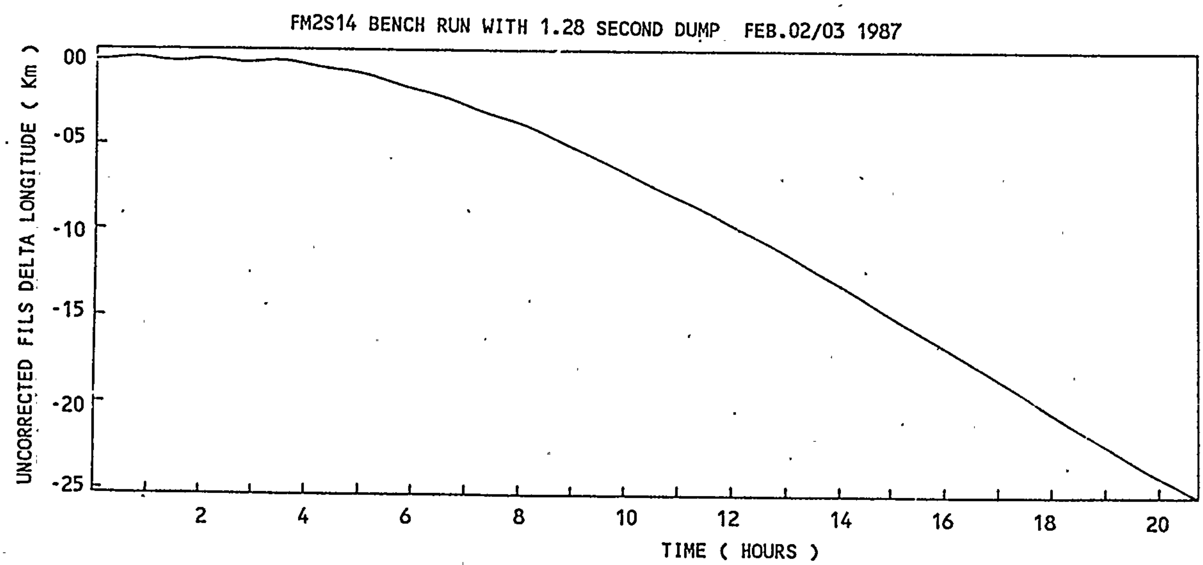

Figure 33. Feedback 20.6 h bench run
Uncorrected Delta Longitude vs. Time

required the alignment as well as the updating to be done by the external computer. To do this, an at sea situation was simulated as follows:

- a normal FILS stationary alignment was done.

- the platform was then purposely misaligned by about 1.42 deg. in azimuth, 0.65 deg. about the X axis, and 0.83 deg. about the Y axis. This was to simulate an attitude in which the platform may have gyro stabilized.

- the platform was then aligned and leveled by the external computer with the following limits specified:
    - Tilt about X to be within 2 seconds of level

- Tilt about Y to be within 2 seconds of level
- Azimuth to be within 45 seconds of reference azimuth
- Only 90% of the calculated change in the gyro drift for platform releveling to be applied. This was to prevent overshooting the level point and oscillation about this point.
- Only a maximum torquing rate of 10°/h for the X, and Y gyros and 15°/h for the Z gyro were permitted.
- The tilt measuring time as well as the releveling time were done in 35 second periods.

- when the alignment criterion were met, the system was put into navigate mode at which time remote updates were done every 180.0 seconds. This would be the normal update period for land surveying applications.

Figures 34 to 38 show the result of this run. It should be noted that the initial part of the graphs shows three overlapping segments as the time was reset to zero for the start of each segment. The first segment shows the tilting of the platform out of alignment. During this phase, the velocities were continually being reset to approximately zero to prevent them from opposing the required torquing. The uncorrected position was also being continually set equal to the reference position. On the velocity graphs, this segment looks like a straight line near the zero line. On the azimuth plot, this section shows the azimuth going from 3.313° to 2.042°.

The next segment is the releveling section. This shows up on the north and east velocity plots as a series of velocities which build up over the 35 second periods of measurement and leveling. As they are produced by the tilt of the platform, their magnitude decreases as the platform gets closer to level.

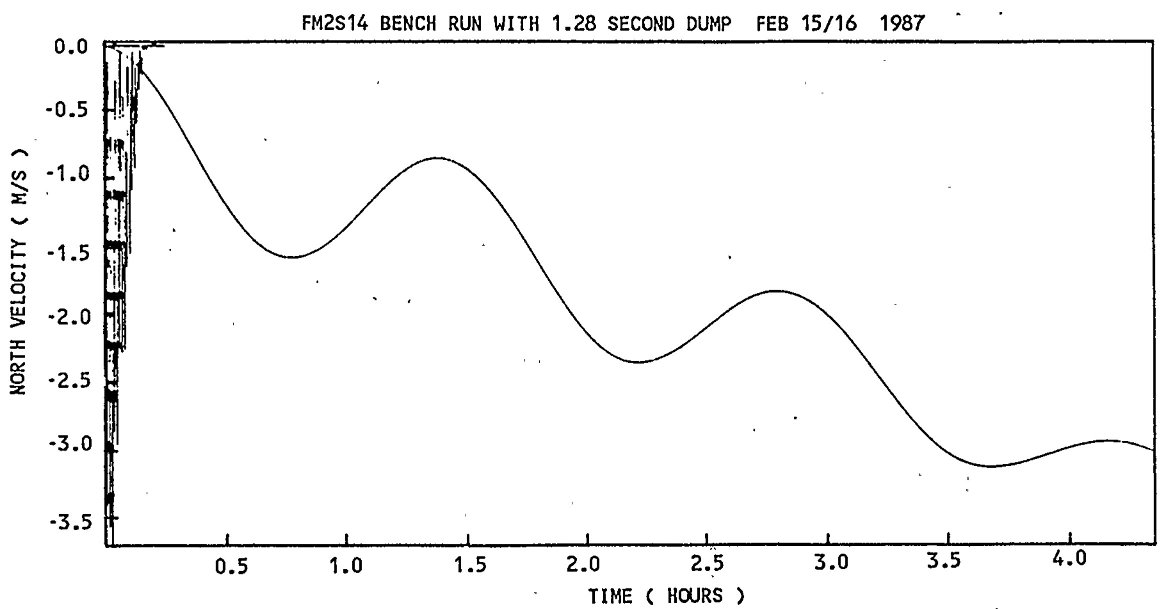

Figure 34. Feedback 4.4 h bench run
North Velocity vs. Time

The last segment is the normal navigation segment which is shown by the smoothly varying velocity curves. In this run, the east and height velocities remain fairly small, while the north velocity can be seen to be ramping of with a Schuler oscillation superimposed on it. The reason for this is an incorrect azimuth gyro drift compensation value. This can be seen in the azimuth plot which has a linear drift of about 0.1226°/h Insertion of this correction to the Z gyro drift torquing store would stop the north velocity ramping effect.

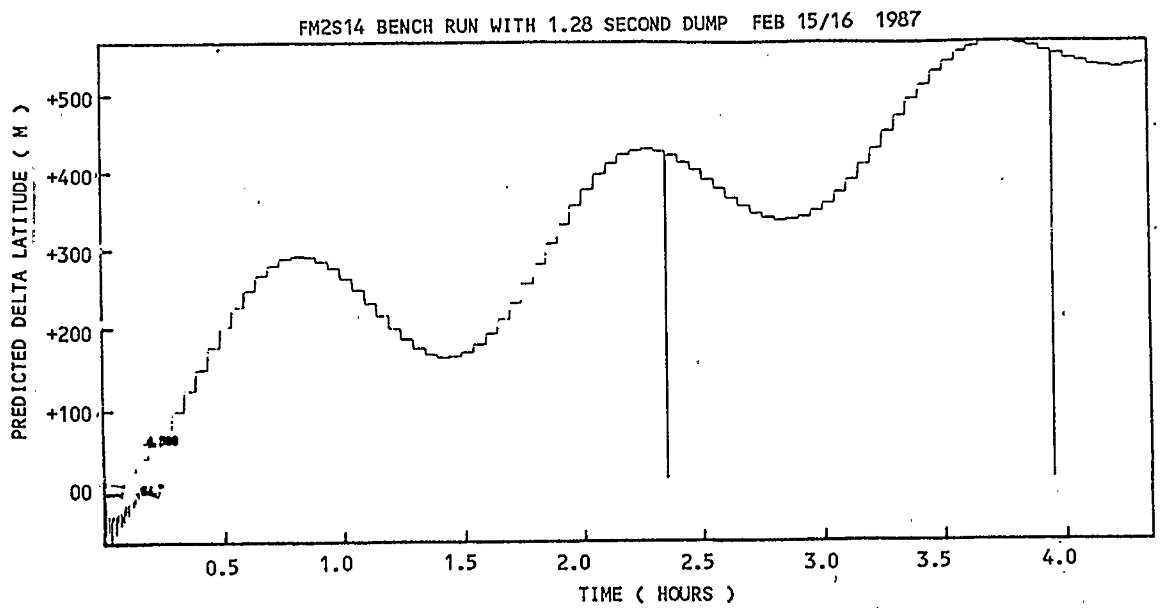

Figure 35. Feedback 4.4 bench run
Delta Predicted Latitude vs. Time

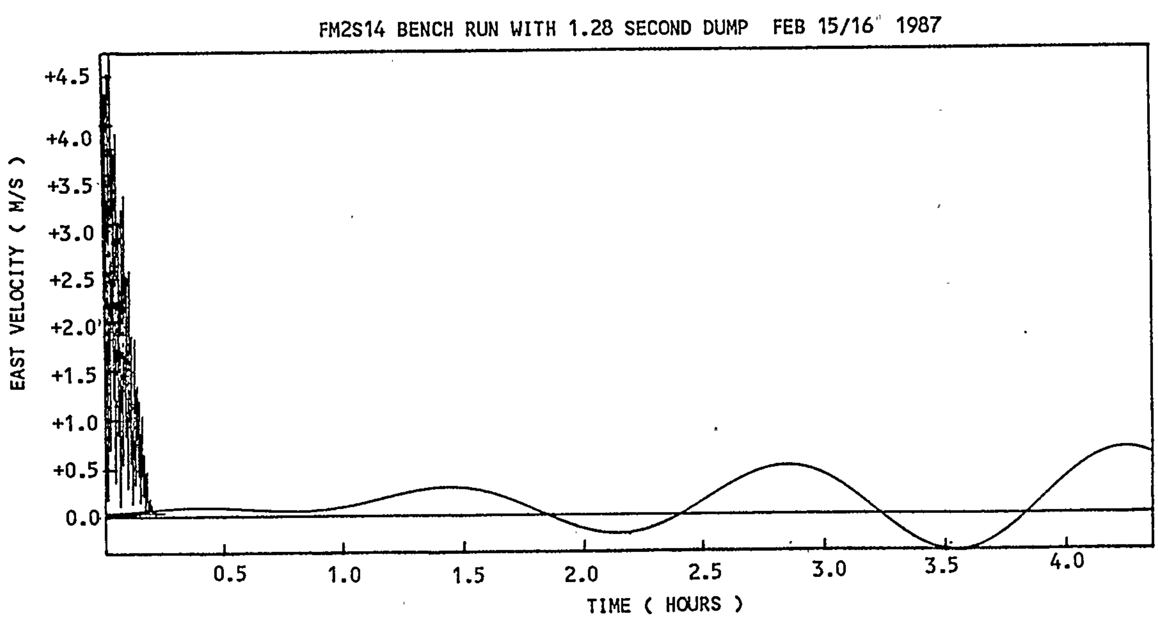

Figure 36. Feedback 4.4 h bench run
East Velocity vs. Time

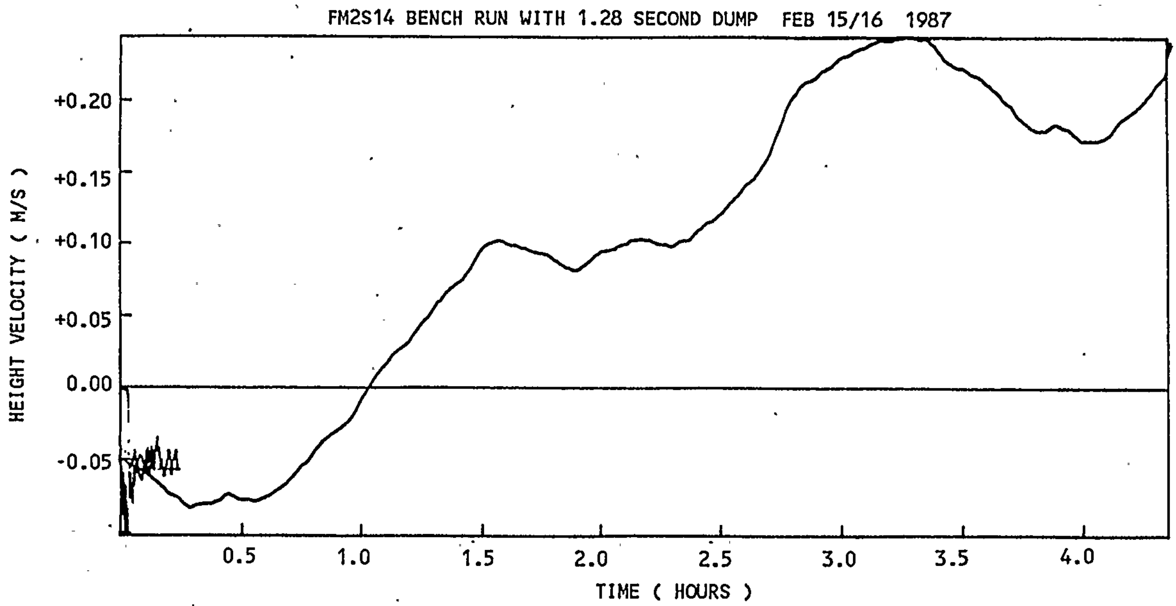

Figure 37. Feedback 4.4 h bench run
Height Velocity vs. Time

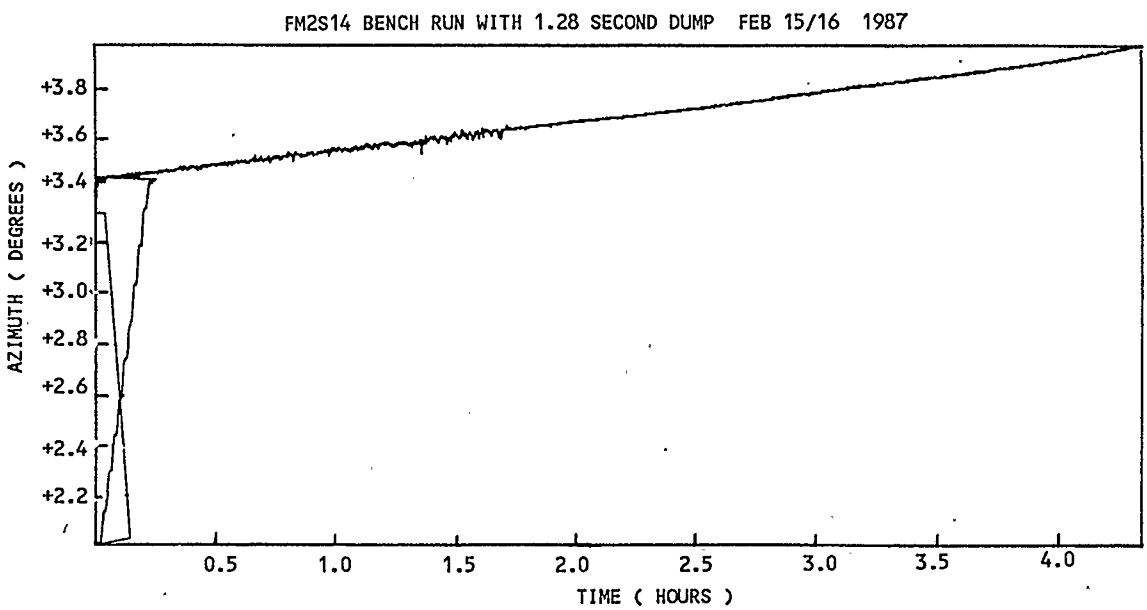

Figure 38. Feedback 4.4 h bench run
FILS Azimuth vs. Time

Table 5. Correction To Figure 35 Predicted Latitude

TIME (h)	N.VEL.ERR. (m/s)	180*N.VEL.ERR. (m)	$D\Phi_p$ (m)	SUM (m)
0.000	-0.0392	-------	-------	-----
0.132	-0.1818	- 32.73	+ 33.59	- 0.86
0.184	-0.2873	- 51.71	+ 49.69	- 2.02
0.235	-0.4141	- 74.54	+ 70.29	- 4.25
0.284	-0.5495	- 98.92	+ 93.75	- 5.17
0.335	-0.7041	-126.75	+120.12	- 6.62
0.384	-0.8542	-153.76	+147.07	- 6.69
0.435	-1.0101	-181.82	+175.07	- 6.75
0.487	-1.1575	-202.80	+201.15	- 1.65
0.535	-1.2839	-231.10	+226.40	- 4.70
0.589	-1.3968	-251.43	+247.45	- 3.98
0.638	-1.4824	-266.84	+266.09	- 0.75
0.686	-1.5433	-277.80	+278.44	+ 0.64
0.738	-1.5746	-283.44	+287.40	+ 3.97
0.786	-1.5814	-284.65	+290.23	+ 5.57
0.838	-1.5587	-280.57	+289.62	+ 9.05
0.886	-1.5189	-273.40	+283.10	+ 9.70
0.938	-1.4556	-262.00	+274.78	+12.78
0.986	-1.3803	-248.46	+261.68	+13.22
1.037	-1.2898	-232.16	+246.99	+14.83
1.089	-1.1941	-214.94	+230.45	+15.51
1.137	-1.1057	-199.03	+214.25	+15.22
1.189	-1.0185	-183.34	+198.12	+14.78
1.500	-0.9318	-167.72	+168.05	+ 0.34
2.000	-2.1410	-385.39	+376.86	- 8.53
2.500	-2.0899	-376.19	+389.70	+13.52
3.000	-2.0058	-361.04	+358.83	- 2.21
3.500	-3.0184	-543.30	+540.97	- 2.34
4.000	-2.9839	-537.10	+550.43	+13.33
4.362	-3.0107	-541.92	+543.22	+ 1.30

As in the 20.6 hour run, the predicted latitude graph is the mirror image of the north velocity curve. As the time scale is somewhat larger on this plot than in the 20.6 hour plot, it is easier to see that the error has steps at the updates while being fairly flat between updates. The reason for this behaviour was found to be an error in the program generating the feedback to the FILS unit. The area fed back was one update out of sequence. This resulted not only in the steps seen, but also in almost all of the total predicted position error. The system was updated every 180 seconds and Table 5 was complied from hard copy output of the predicted latitude and velocity errors for the latitude error shown in figure 35. This table shows that a dramatic reduction in the predicted position error will occur if the error in the feedback program is eliminated.

Appendix F shows the printout of the external computer's measurements used to relevel the platform following its intentional misorientation.

7. Conclusions and Recommendations

CONCLUSIONS

The data presented in this dissertation shows that it is possible to control a standard FILS MK_II inertial surveying system in such a manner as to bypass the normal requirement of having to come to a complete stop every 5 to 10 minutes to do a zero velocity update. This makes the unit a fairly flexible one which can be used as a main component of an integrated system without the requirement and expense of altering the inertial system itself. The approach presented also leaves the responsibility of servicing the actual inertial platform with the Ferranti system itself where it belongs.

Access to all the main system data is readily available by use of a standard IEEE488 interface. This is a feature which few other systems provide so easily if at all. By proper manipulation of the data system stores, it is possible to integrate this system with others via a general purpose external computer. The data flow is bi-directional or unidirectional depending on what interface is used. The FILS unit provides regular data dumps unsolicited by the external computer. They can be collected by the external computer in a buffer without the necessity of being continually requested. For reasons of system control or access to data not included in the time data dump, the computer can access any of the FILS RAM stores.

Means of controlling the FILS unit as well as sample runs are presented and discussed. They show that external control of the FILS unit is indeed possible and fairly easy to implement. With a symbiotic arrangement of various systems, it is possible to exploit the power of each while minimizing their weaknesses. The precise short term position differences available from the inertial system, have a long term error growth in absolute position. They are thus ideally complemented by a system such as GPS which provides good absolute position but with a higher noise level between adjacent positions than those of the inertial system.

In summary, system integration with the FILS inertial surveying system is feasible, and when appropriately used, can provide a powerful integrated position and attitude system.

RECOMMENDATIONS

The time delay problem exhibited by the steps in the FILS predicted position plots must be eliminated. As shown by table 5, its source has been determined and can be easily corrected.

Design of an appropriate Kalman filter for the external computer is required. While many local level Kalman filters have been documented, these filters must be modified to specifically account for the internal FILS equation mechanization.

While the Kalman filter running on the external monitoring computer continually tracks the FILS system behaviour, and can use external information (such as GPS position and velocity) whenever it is available, a direct feedback to the FILS is not done continuously. An optimization of the feedback times must be established such that the error velocity propagation can be clearly established by the external filter without allowing these velocity error to grow to unacceptable size. Abrupt discontinuities in the error velocity curves due to external feedback should be kept as small as possible.

It is essential that proper weighting and prefiltering of the external data used as input to the feedback control filter be done. Poor data or gross errors must not be allowed to adversely affect the inertial systems operation.

8. References

Adams,J.R. (1979), *Description of the Local Level Inertial Survey System and Its Simulation*, University Of New Brunswick, Department Of Surveying Engineering, Research Report # 59.

Bomford,G. (1971), *Geodesy*, 3rd. ed., Oxford University Press.

Britting,K.R. (1971),*Inertial Navigation Systems Analysis*, John Wiley & Sons, Inc. ISBN 0-471-10485-X.

Brown,R.G. (1983), *Introduction To Random Signal Analysis and Kalman Filtering*, John Wiley&Sons,Inc., ISBN 0-471-08732-7.

Cox,D.B. (1980)," Integration of GPS with Inertial Systems", *Global Postioning System Volume I*, papers published in Navigation ISBN 0-936406-00-3.

Emery,B. (1980), *FILS 2 Software Documentation Version B*, Ferranti internal document.

Farrell,J.L. (1976), *Integrated Aircraft Navigation*, Academic Press, Inc. ISBN 0-12-249750-3.

Gelb,A. (1974), *Applied Optimal Estimation*, M.I.T. Press ISBN 0-262-70008-5.

Hamilton,G.B., Y.K.Ameen (1977), *An Accurate Inertial Surveyor For Military Usage with Potential for Higher Order Survey Applications*, DGON Symposium on Gyro Technology,Stuttgart, 28/29 September 1977.

Hannah,J. (1982), *The Development of Comprehensive Error Models and Network Adjustment Techniques For Inertial Surveys*, The Ohio State University, Depart. of Geodetic Science and Surveying, Report No. 330.

Heiskanen,W.A., H.Moritz (1976), *Physical Geodesy*, W.H.Freeman and Company, Library of Congress Cat. Card # 66-24950.

Napier,M.A. (1985), *Application of Inertial Positioning To High Accuracy Underwater Surveys*, University Of Newcastle Upon Tyne, Department Of Surveying

Rueger,J.M. (1982), *Inertial Sensors Part 1:Gyroscopes*, The University of Calgary Publication 30002.

Rueger,J.M. (1986), *Inertial Sensors Part 2:Accelerometers*, The University of Calgary Publication 30008.

Schwarz,K.P. (1983), *Inertial Surveying and Geodesy*, Reviews of Geophysics and Space Physics, Volume 21 No.4 PP. 878-890.

Schwarz,K.P., R.V.C.Wong, J.E.Hagglund, G.Lachapelle (1984), "Marine Positioning with a GPS-Aided Inertial Navigation System", *Proceedings of National Technical Meeting*, San Diego, 1984, Institute of Navigation, Washington, D.C.

Schwarz,K.P., D.A.G.Arden, J.J.H.English (1984), *Comparison of Adjustment and Smoothing Methods For Inertial Networks*, University of Calgary Publication 30006.

Sinha,N.K. (1986), *Control Systems*, CBS College Publishing ISBN 0-03-069357-8.

Vassiliou,A. (1984), *Processing of Unfiltered Inertial Data*, University of Calgary, Publication 20006.

Wong,R.V.C., K.P.Schwarz (1979), *Investigation on the Analytical Form of the Transition Matrix in Inertial Geodesy*, University of New Brunswick, Technical Report No.58.

Wong,R.V.C., K.P.Schwarz (1983), *Dynamic Positioning with an Integrated GPS-INS, Formulae and Baseline Tests*, University of Calgary, Publication 30003.

Wong,R.V.C. (1982), *A Kalman Filter-Smoother For An Inertial System of Loacal Level Type*, University of Calgary, Publication 20001.

Wrigley,W., W.Hollister, W.G.Denhard (1969), *Gyroscopic Theory, Design, and Instrumentation*, M.I.T. Press. SBN 262 23037 2.

Appendix A. Velocity Error Curves From The Fils Mk_II System

Table of Contents

List of Figures

1. Introduction

The theoretical propagation of velocity error profiles are discussed for a local level inertial system which does not relevel or realign its platform during a mission, but does use both predicted latitude and height in a real time mode. The major sources for error propagation are discussed and a graphical representation is given of each. These are later compared with actual velocity error profiles derived from the Ferranti MK_II surveying system. The reason for profile differences is discussed.

The basic navigation equations used by the Ferranti MK_II local level inertial system are given in chapter 3.

The build up of velocity errors can be monitored by bringing the system to a stop relative to the earth's surface and noting the velocity which the system says it has. It is at this point that the philosophy of various local level systems differ. The Ferranti system does not relevel the platform and zero its velocities at "ZUPTS" on the assumption that the platform tilts can be monitored to a higher degree of accuracy than they can be releveled. While this is true, it results in a much higher build up in velocity error than is seen in systems that do relevel and zero their velocity errors. This build up in velocity tends to make the contribution of cross product errors into other channels more significant and also leads to gyro torque errors as the uncorrected north and east velocities are used in the computation of the torquing values. The assumption is these errors are all smoothly propagating and can therefore be removed. Releveling the platform and zeroing the velocities tends to give a better real time data set, but means there is an uncertainty in the assumption of zero tilt on each leg.

2. Theoretical Error Curves From Initial Conditions

The sources of error propagation from initial conditions which will be considered are: initial velocity, initial tilt, horizontal gyro drift errors, azimuth gyro drift error. They are determined by solving the system of differential equations, which describe the system error behavior, for the homogeneous case, see e.g. Wong & Schwarz [1979]. Individual errors are then obtained from the equation:

$$x(t) = \Phi(t,t_o)\, x_o \qquad (2.1)$$

where $x(t)$ is the state vector at time t and $\Phi(t,t_o)$ is the transition matrix between time t_o and t. The initial errors are contained in the vector x_o. Since the initial velocities, tilts, and gyro drifts are elements of the state vector, their time behavior can be obtained by multiplying the respective element of the transition matrix by the initial value. This has been done in the following subsections.

2.1. Initial Velocity Error

An initial velocity error will propagate as follows:

$$V_{Ni} = V_{No} * \cos(\omega t_i) \qquad (2.1.1)$$

where: V_{Ni} = the north velocity error at time t_i
V_{No} = initial north velocity error at t = 0
t_i = time since initial conditions
ω = $(\gamma / a)^{0.5}$
γ = the normal gravity at platform position

a = the radius of curvature in the meridian + hgt

For example: At latitude = 48° 04' 46".449
height = 646.80 m
a = 6371459 metres γ = 9.80696875 m/s^2
therefor: ω = 0.001240646 rad / s
yielding a period of 5064.446 s = 84.4 min.

This period is commonly known as the **Schuler period.** It should be noted that this period is directly proportional to the square root of the radius of curvature used.

Similarly, the east velocity error is given as:

$$V_{Ei} = V_{Eo} * \cos (\omega t_i) \qquad (2.1.2)$$

Note: ω is slightly different as the radius of curvature is in the prime vertical and not the meridian.

The displacement error (area under the velocity error curve) is given by:

$$\text{North Displacement Error}_m = V_{Ni} * \sin(\omega t)/\omega \qquad (2.1.3)$$

$$\text{East Displacement Error}_m = V_{Ei} * \sin(\omega t)/\omega \qquad (2.1.4)$$

2.2. Initial Tilt Error

An initial tilt error will propagate as follows:

$$V_{Ni} = (\gamma T_E/\omega) \sin(\omega t_i) \qquad (2.2.1)$$

where: T_E = tilt about E-W axis in radians at t=0

Similarly the east velocity error is given by:

$$V_{Ei} = (\gamma T_N/\omega) \sin(\omega t_i) \qquad (2.2.2)$$

Again it should be noted that ω is slightly different due to the radius term a.

The displacement error (area under the velocity error curve) is given by:

$$\text{North Displacement Error}_{m} = (\gamma T_E/\omega^2)(1-\cos(\omega t_i)) \qquad (2.2.3)$$

$$\text{East Displacement Error}_{m} = (\gamma T_N/\omega^2)(1-\cos(\omega t_i)) \qquad (2.2.4)$$

2.3. X or Y Gyro Drift Error

An X gyro drift error, where X is defined as +ve towards the east, will propagate as follows:

$$V_{Ni} = a * X_{GDe} * (1-\cos(\omega t_i)) \qquad (2.3.1)$$

where: X_{GDe} = the X gyro drift error in rad / s

It should be noted that an initial azimuth misalignment of the north accelerometer will have the same type of error propagation in the north velocity as an X gyro drift error. This is shown in the equation:

$$\text{Platform drift} = \Omega \cos \Phi \sin \alpha + X_{GDe} \qquad (2.3.2)$$

where: Ω = the earth rate = $7.2921151467*10^{-5}$ rad / s
Φ = platform latitude
α = misalignment of the X axis from east

Similarly the east velocity error is given by:

$$V_{Ei} = a * Y_{GDe} * (1-\cos(\omega t_i)) \tag{2.3.2}$$

where: a = radius of curvature in the prime vertical + hgt.
Y_{GDe} = the Y gyro drift error in rad / s

The displacement (area under the velocity error curve) is given by:

$$\text{North Disp. Error}_m = a\, X_{GDe}\, (t_i-(\sin(\omega t_i))/\omega) \tag{2.3.3}$$

$$\text{East Disp. Error}_m = a\, Y_{GDe}\, (t_i-(\sin(\omega t_i))/\omega) \tag{2.3.4}$$

2.4. Azimuth Gyro Drift Error

An azimuth gyro drift error will propagate as follows:

$$V_{Ni} = - a\, Z_{GDe}\, \Omega \cos \Phi\, (t_i - (\sin(\omega t_i))/\omega) \tag{2.4.1}$$

where: a = radius of curvature in the meridian + hgt
Z_{GDe} = azimuth (Z) gyro drift error (rad / s)

It should be noted that while the azimuth gyro drift error has a significant effect on the north velocity error, its effect on the east velocity error is son small as not to have to be considered in present applications.

2.5. Graphical representation of the Theoretical Velocity Error Curves

A graphical representation of the velocity error propagations discussed in the preceding sections is given for the following conditions:

a. an initial north velocity error of 0.20 m/s (Figure 1);

b. an initial tilt error about the east-west axis of 2 arc seconds (Figure 2);

c. an X gyro drift error of +0.0050 degrees per hour (Figure 3);

d. an azimuth gyro drift error of -0.0050 degrees per hour (Figure 4);

e. a combination of all the above conditions; i.e. a,b,c, and d (Figure 5).

It should be noted that all the curves are very smooth and have no discontinuities. This is also true of the combination of these errors. This implies that if the error curve is tracked long enough to obtain a good estimation of its component parts, then it should be possible to predict the future error propagation with a very high degree of accuracy. This would make it possible to greatly increase the time between required ZUPTS. In the real world however, errors do not propagate entirely as has been described. It is therefore necessary to periodically make velocity error measurements and correct for any defeats in the error propagation model.

3. Actual Velocity Error Profiles

Figures 6,7, and 8 show the error velocity profiles as generated by a bench run of the Ferranti system. The north velocity error seems to be due mainly to an azimuth gyro drift error of -0.0576 degrees per hour. The east velocity error seems to be initially due to a tilt error, but has other components coming into it. The fairly rapid changes in slope along the curve suggest that there may be some numerical problems which still have to be corrected. This is a very important point when considering the use of a filter for prediction as a velocity curve may not always follow what the theory says it should. This may be due to the controlling mechanism used by the manufacturer to handle specific designs in a given system, or due to numerical problems which were not significant in the survey system's military ancestor, but are in the surveying mode.

Other sources of change in the velocity error curves are movement dependent. One obvious source is a deflection of the gravity vertical as a function of position. Its effect is generally compensated by making frequent stops and correcting for any unaccounted for velocity build up.

4. Conclusion

The propagation of a theoretical error velocity curve is relatively easy to define for its main components. This often varies from the actual velocity profile for many different reasons. It is therefore necessary to try and make the model which predicts velocity propagation follow as close as possible to the actual velocity seen. This implies that on top of the broad theoretical velocity error propagation, a model should be included which is specific to the type of system being used and additional information which may be available, such as position dependent errors.

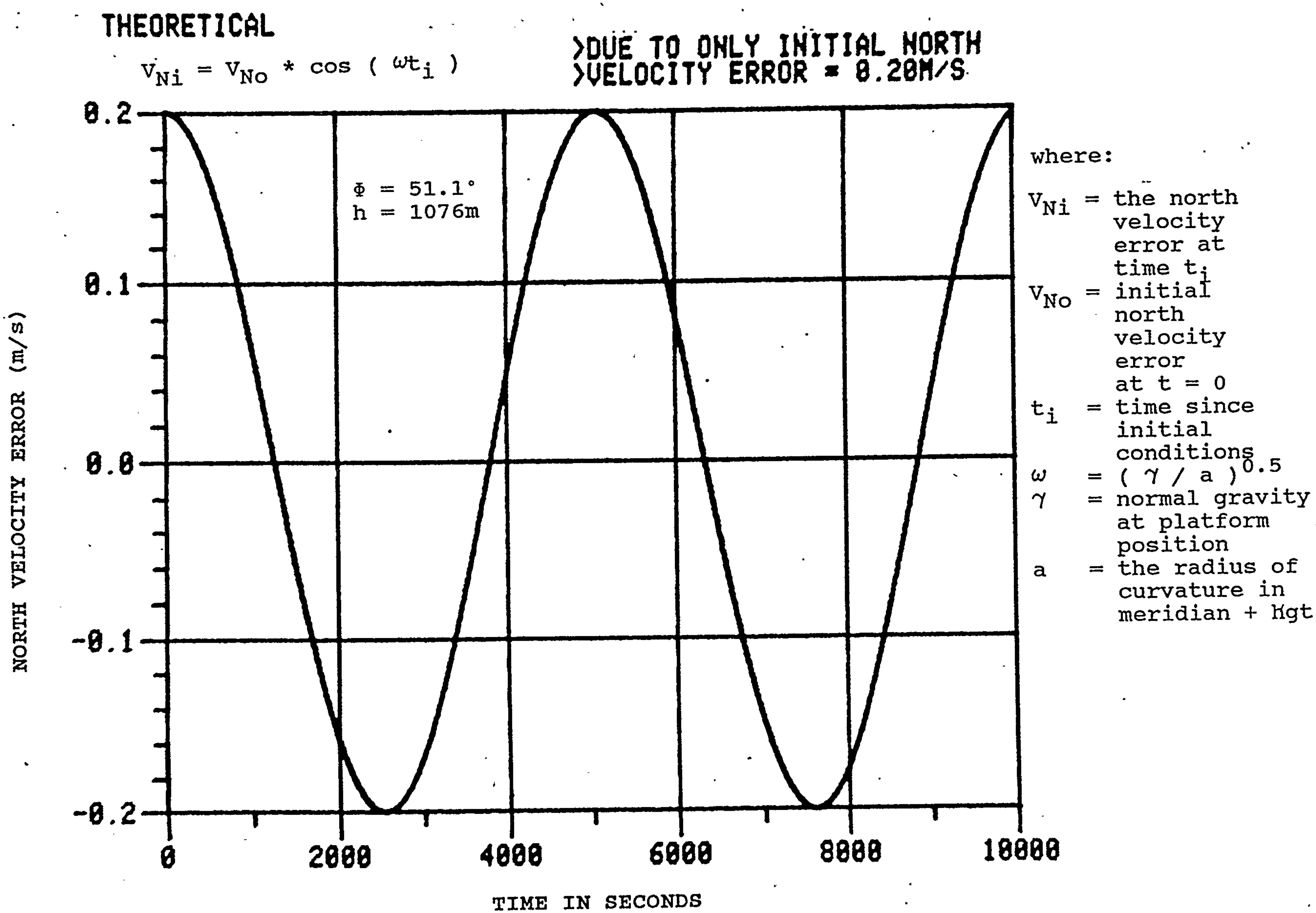

Figure 1. Theoretical Velocity Error Propagation
Due To Initial 0.2m/s Velocity Error

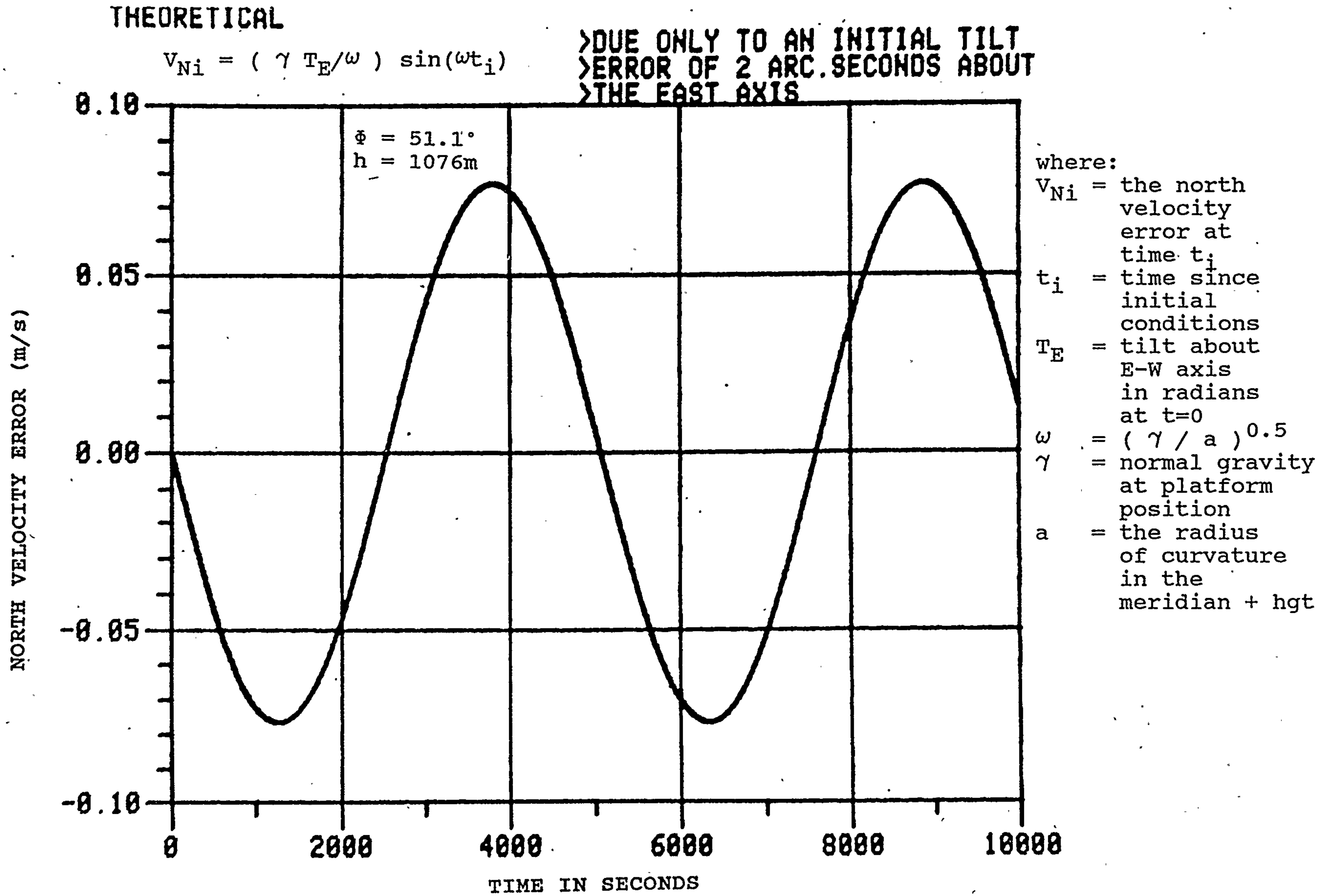

Figure 2. Theoretical Velocity Error Propagation
Due To Initial 2" Tilt Error

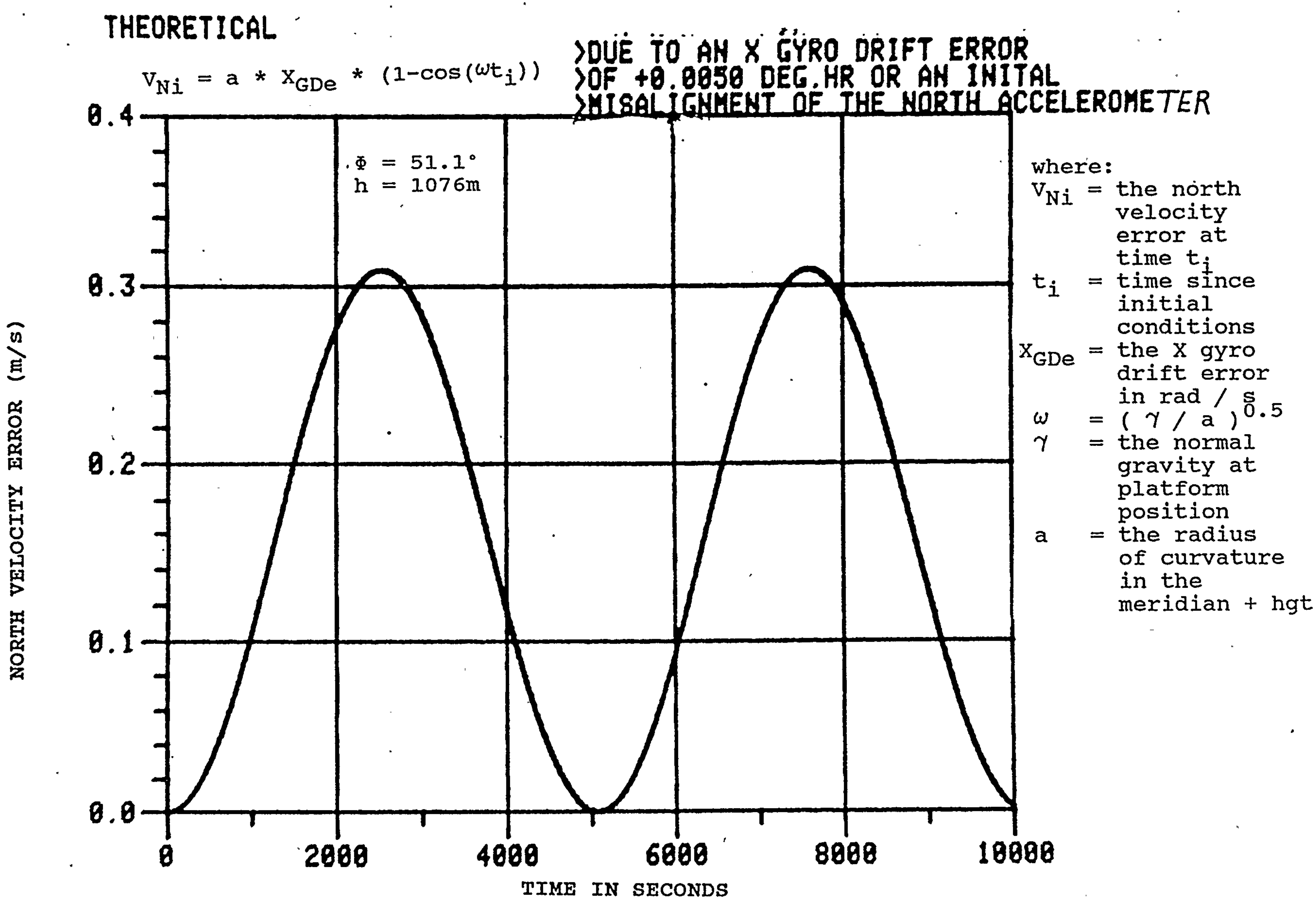

Figure 3. Theoretical Velocity Error Propagation
Due To +0.0050°/h X Gyro Drift Error

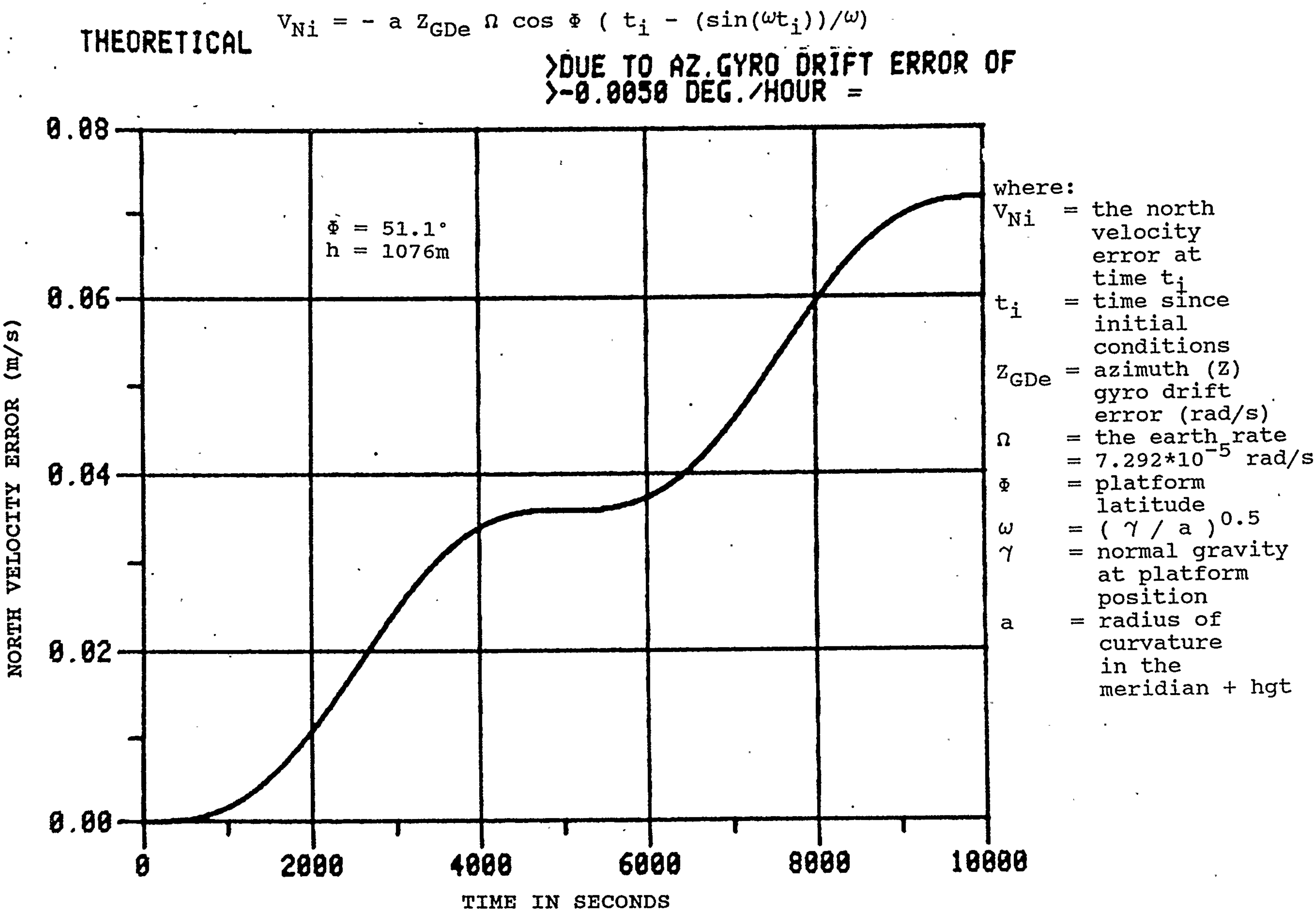

Figure 4. Theoretical Velocity Error Propagation
Due To -0.0050°/h Azimuth (Z) Gyro Drift Error

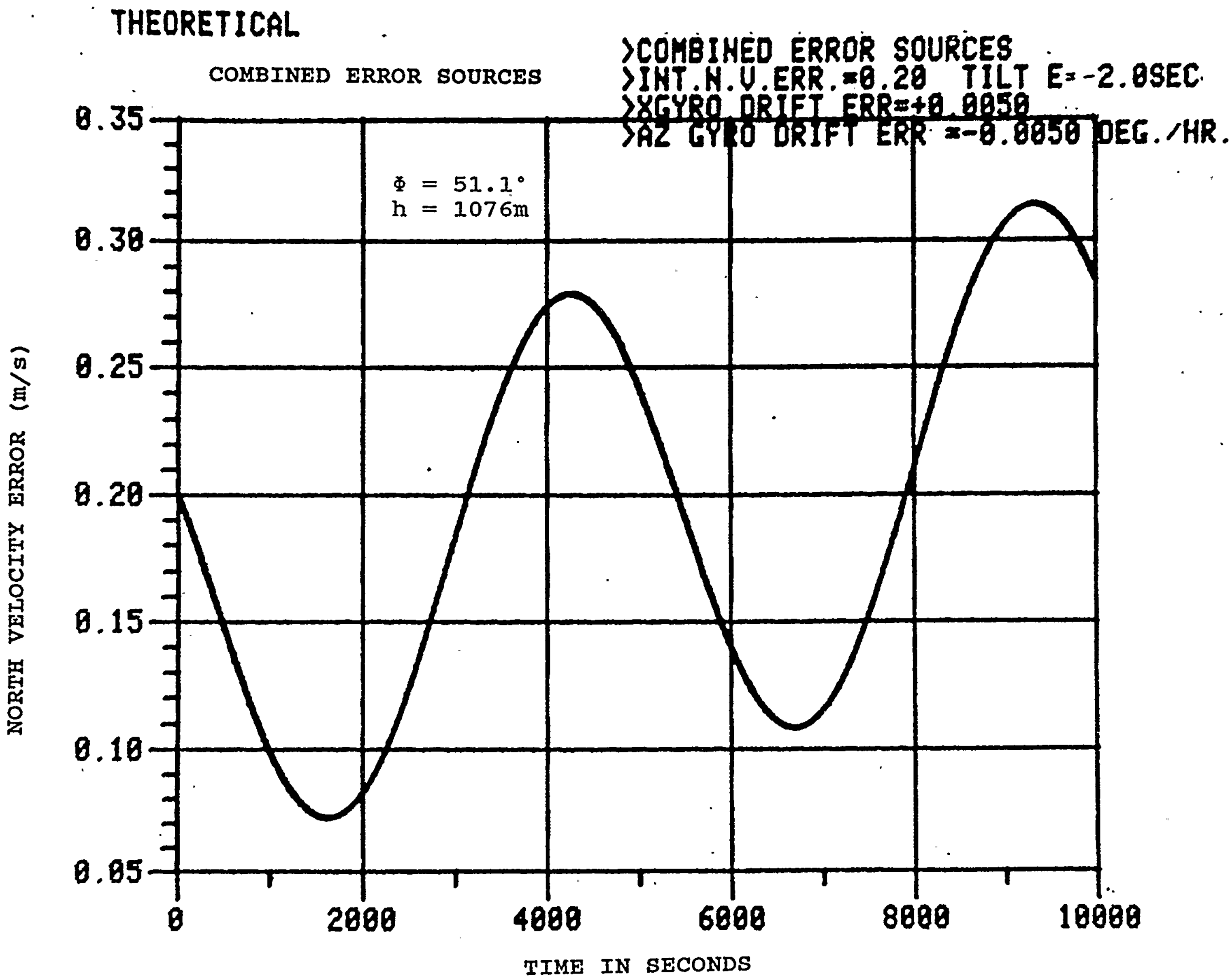

Figure 5. Theoretical Velocity Error Propagation
Due To Combination Various Error Sources

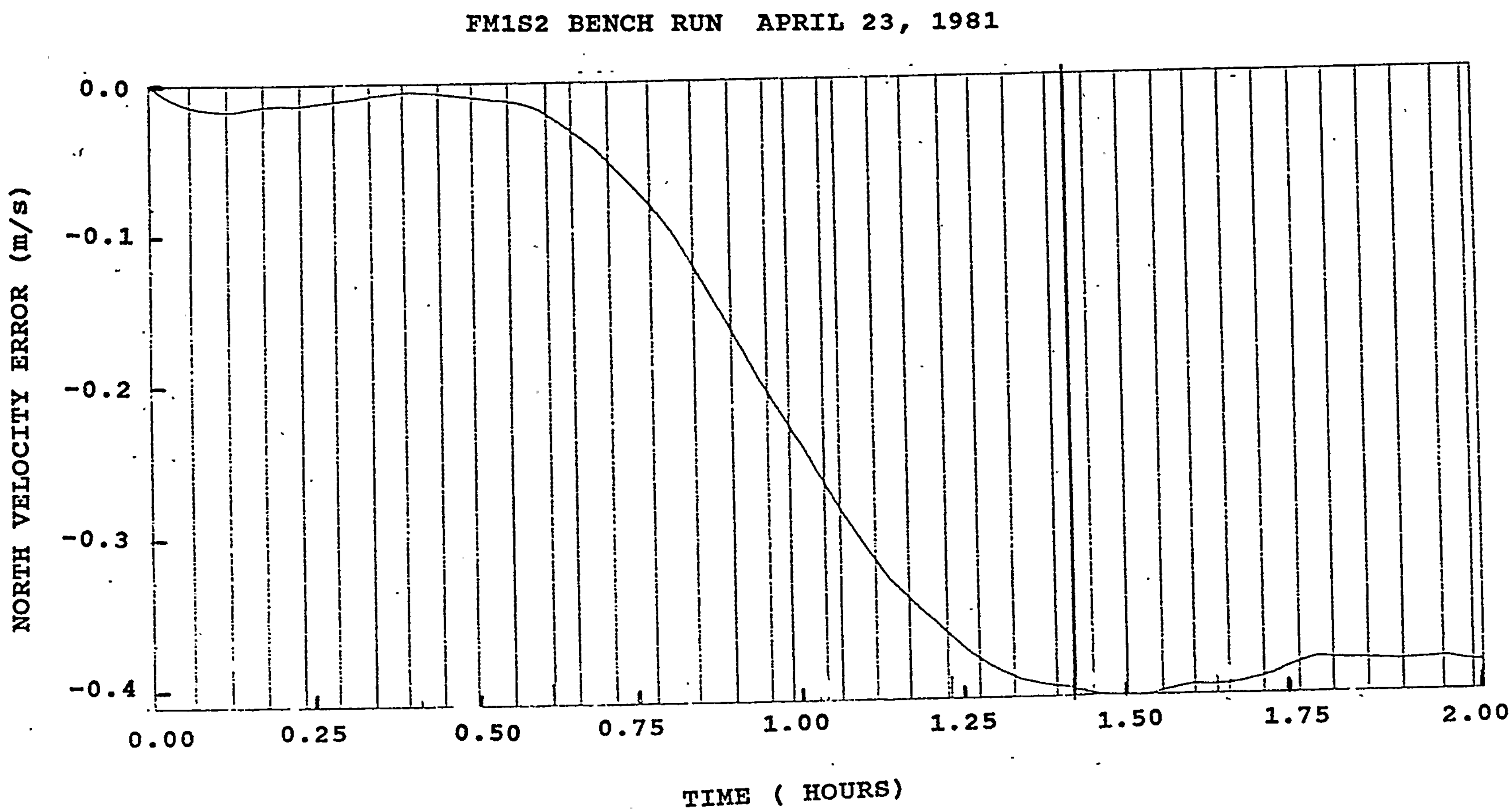

Figure 6. Actual FILS North Velocity Error Propagation

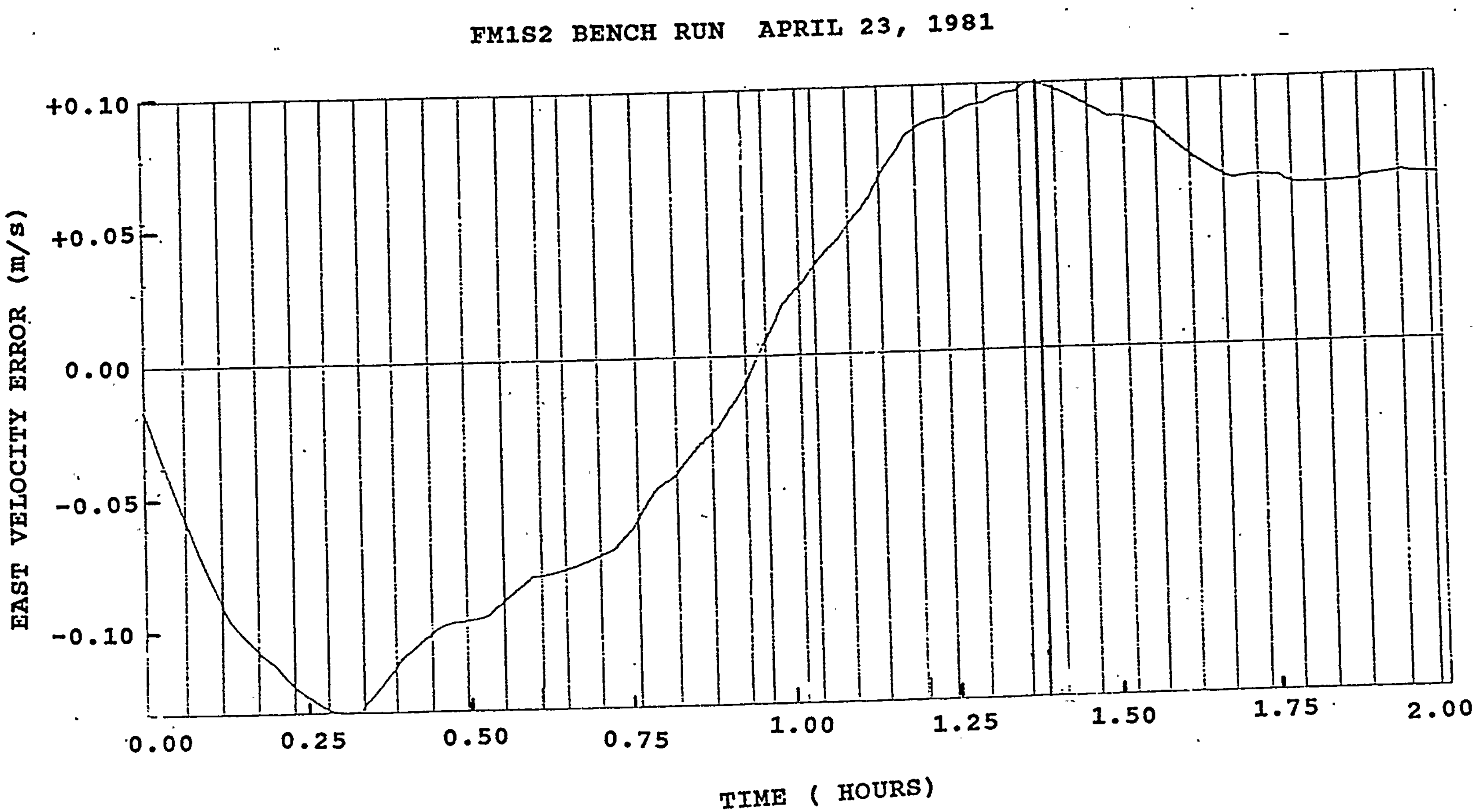

Figure 7. Actual FILS East Velocity Error Propagation

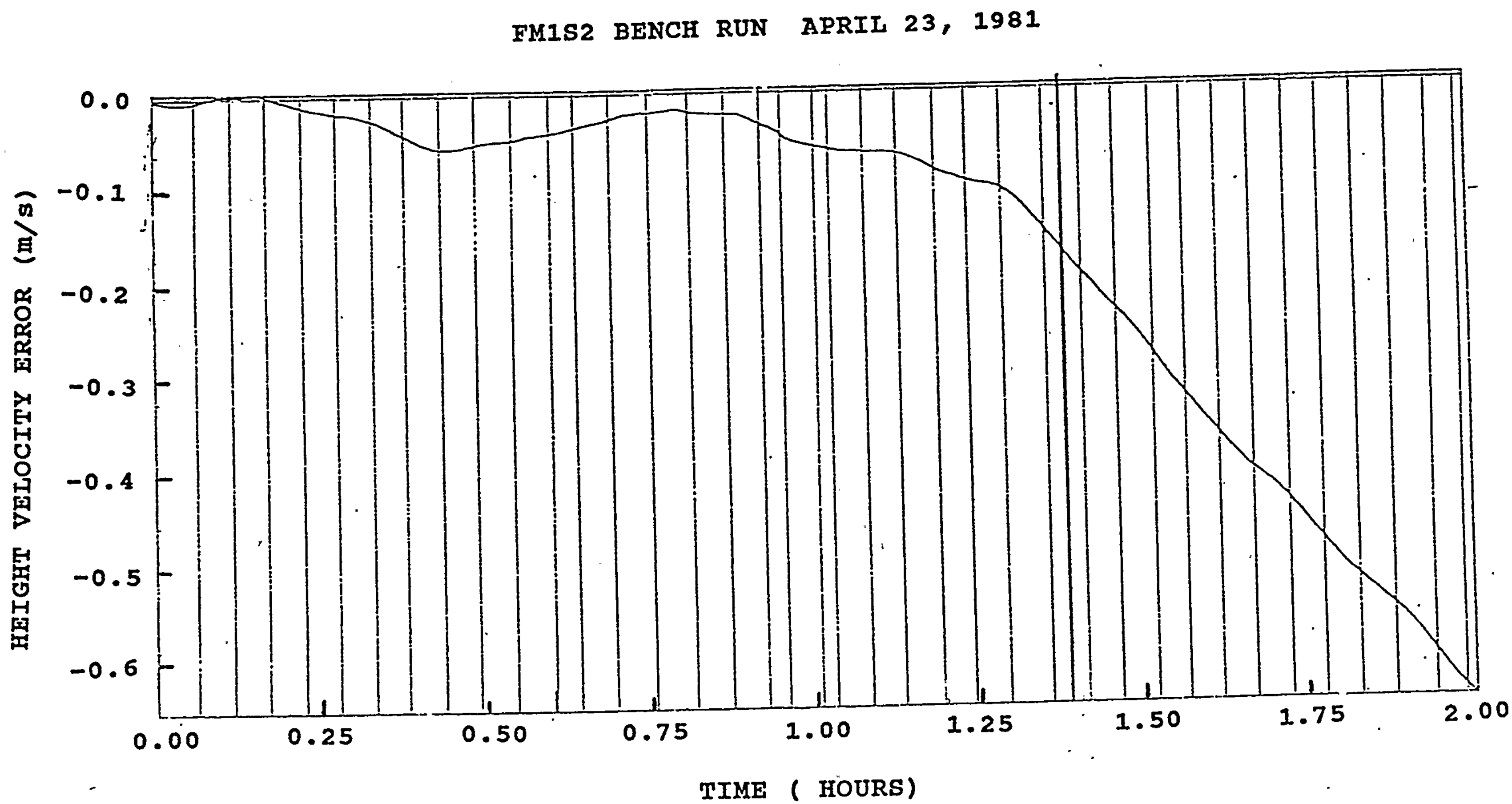

Figure 8. Actual FILS Height Velocity Error Propagation

Appendix B. Relationships Required to go from IMU coordinates to the Coordinates of an External Point or Vice Versa

Table of Contents

List of Tables

List of Figures

DEFINITION OF TERMS USED IN APPENDIX B

METHOD I - Position Determination via FILS Mirror

METHOD II - Position Determination via Vehicle Reference Point; Protractor, Chain, Plumb Bob

METHOD III - Position Determination via Vehicle Reference Point, EDM, Angle Encoders.

First System - Local Astronomic (RHS)

Second System - Grid (RHS)

Third System - Casing (RHS)

Fourth System - Intermediate Transformation (Euler Angles)

Fifth System - Unscribed Mirror (RHS)

Sixth System - Scribed Mirror (RHS)

Seventh System - Vehicle Reference Point

Eighth System - E.D.M. Offset (RHS)

AZ_G - U.T.M. grid azimuth

C - grid convergence

d1 - slope distance theodolite to mirror

d2 - slope distance theodolite to target over survey point

d3 - vertical height of target over survey point

H1 - horizontal angle between mirror, theodolite, and target

H2 - horizontal angle between T1, T2, and the VRP

H3 - horizontal angle between the 0 of the VRP protractor and the sight line from T2 to the VRP

IMU - Inertial Measuring Unit

LLISS - Local Level Inertial Survey System

RHS - Right Handed System

$R\phi$ - rotation of axes about X axis

Rk - rotation of axes about Z axis

$R\Omega$ - rotation of axes about Y axis

V1 - vertical angle of reflection of theodolite in mirror

V2 - vertical angle between theodolite and survey point target

V3 - vertical angle between the theodolite at T2 and the VRP

$Y3_m$ - distance from the IMU origin to the mirror surface (Y3 coordinate of the mirror origin (-ve in this direction)

α - rotation angle about the X5 axis required to make the Z5' axis $\parallel$ to the Z3 axis.

α_8 - the horizontal angle measured in the eighth coordinate system from the horizontal reference zero to the survey point to be measured.

β - rotation angle about Z5' axis required to make Y5" coincident with Y3

β_8 - the vertical angle measured in the eighth coordinate system from its vertical reference plane to the survey point to be measured

$\Delta\beta_8$ - the vertical angle in the eighth coordinate system from the vertical reference mark to the eighth system vertical plane.

γ - angle between Z5 and Z6 axis

ζ - horizontal angle between the projection of the Y3 axis in the horizontal plane and the Y7 axis.

η - the angle of rotation about the Z"8 axis required to make the X"8 and Y"8 axis parallel to the X3 and Y3 axes respectively

ρ - the angle of rotation about the X8 axis required to bring the Y8 axis parallel to the X3,Y3 plane.

σ - the angle of rotation about the Y'8 axis required to bring the Z'8 axis parallel to the Z3 axis

ψ - horizontal angle between grid north and the 0° mark of the protractor in the seventh system (ie. grid bearing of the 0° mark)

ϕ - pitch

Ω - roll

1. Introduction

The requirement that the IMU coordinates be established from the coordinates of an external point, or conversely, that the coordinates of an external point be established from the coordinates of the IMU origin is a necessity for the Local Level Inertial Survey System (LLISS). Because it is physically impossible or practically undesirable to require the IMU origin be made coincident with the external point of interest, it is necessary to establish a means of determining the eccentricity of the external point from the IMU origin. This eccentricity should be resolvable into three components, as for example delta grid northing, delta grid easting, and delta height.

In practice, the Ferranti LLISS has three methods of going to (or from) the IMU origin from (or to) the external point of interest. One of these methods is to use a theodolite set up exactly on a line perpendicular to the plane mirror surface affixed to the FILS IMU casing. This will be denoted as **METHOD I.** Another approach is to make measurements from a fixed point on the transportation vehicle which maintains a constant (or near constant) relationship to the IMU origin. If the measurement from this point is made with a protractor, tape, and plumb bob, it is denoted as **METHOD II. METHOD III** is making the measurement from this point with an electromagnetic distance measuring device (E.D.M.). The device described in this write up is an infrared AGA measuring unit which has had angular encoders added to its instrument support yoke.

There will be eight coordinate systems described in this writeup and the relationship between them will be given.

2. First Coordinate System (Local Astronomic)

The first coordinate system is the right handed Local Astronomic System. This is the system in which the force vector from gravitational and rotational sources are separated from forces (accelerations) due to actual movement with respect to the earths surface. This system is summarized as follows:

SYSTEM:	**FIRST COORDINATE SYSTEM (LOCAL ASTRONOMIC (RHS))**
TYPE:	ORTHOGONAL, RIGHT HANDED
X:	INSTANTANEOUS EAST (+VE EAST) (in horizontal plane)
Y:	INSTANTANEOUS NORTH (+VE NORTH) (in horizontal plane)
Z:	GRAVITY VECTOR (+VE UP)
ORIGIN:	IMU CENTER

3. **Second Coordinate System (U.T.M. Grid)**

The second coordinate system discussed is the GRID system. While this is not necessarily required for all inertial surveys it is very often used, particularly for land surveys. One advantage of this system is its near equal length scaling for all three component parts (over a small distance). The second system can be summarized as follows:

SYSTEM:	**SECOND COORDINATE SYSTEM (GRID (RHS))**
TYPE:	ORTHOGONAL, RIGHT HANDED
X:	UTM GRID EAST (+VE EAST) (in horizontal plane)
Y:	UTM GRID NORTH (+VE NORTH) (in horizontal plane)
Z:	GRAVITY VECTOR (+VE UP)
ORIGIN:	IMU CENTER

The second system is related to the first system (with a sufficient degree of accuracy for the offset distances involved) by the grid convergence angle C which is the angle between geodetic north (in this context approximated to be the same as instantaneous north) and the central meridian of the U.T.M. projection. This rotation is about the Z axis (gravity vector). It is in the second system that the delta grid northings, delta grid eastings, and height differences are determined to be directly added to the U.T.M. coordinates and the height of the I.M.U. origin (or subtracted from the external point) to obtain the U.T.M. coordinates and the height of the external point (or the I.M.U. origin). The relationship of GRID north to GEODETIC north is shown in figure 1 below.

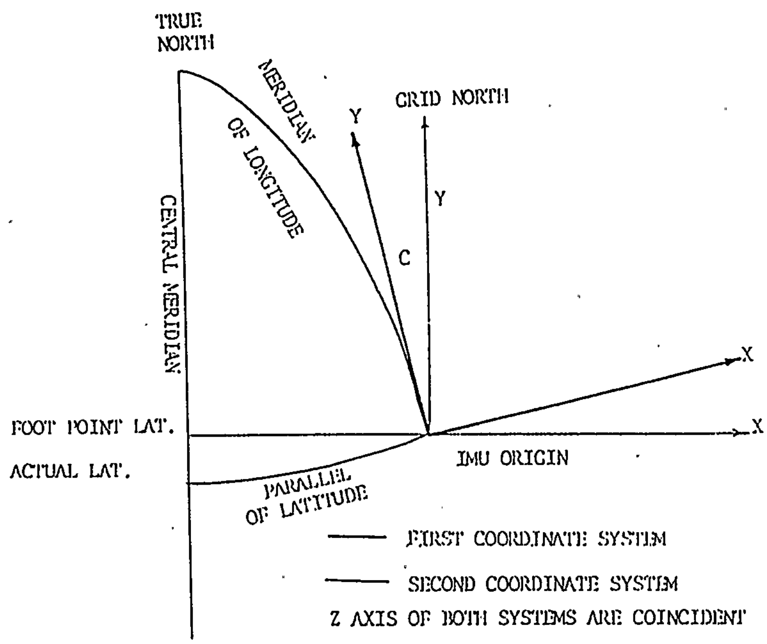

Figure 1. Relationship of Grid north to Geodetic North

4. Third Coordinate System (Casing)

Vehicle movement makes it impossible to define a constant triplet of offset values in the second system. It is therefore necessary to establish a coordinate system in which the offset triplet will remain constant no matter what orientation the vehicle assumes. The third coordinate system as defined above has this characteristic provided the FILS casing is rigidly attached to the transport vehicle. This fixed triplet is possible, irrespective of vehicle orientation, because the outer roll gimbal axis is directly attached to the FILS casing and the NULL of the outer roll gimbal axis synchro is also fixed relative to the FILS casing. (A small approximation is made as the movement of the FILS Casing relative to the Vehicle Reference Point (VRP) due to shock absorber flexure and torsion as well as vehicle flexure are present).

SYSTEM:	**THIRD COORDINATE SYSTEM (CASING (RHS))**
TYPE:	ORTHOGONAL, RIGHT HANDED
X:	REMAINING AXIS TO FORM A RIGHT HANDED, ORTHOGONAL SYSTEM
Y:	OUTER ROLL GIMBAL AXIS
Z:	AXIS IN DIRECTION OF NULL ON OUTER ROLL GIMBAL SYNCHRO
ORIGIN:	IMU CENTER

5. Fourth Coordinate System (Intermediate Transformation System)

The fourth coordinate system considered is the system in which the roll, pitch, and azimuth angles are measured. Coordinates are not given directly in this system, but rather the angles about the X,Y,Z axes (being roll, pitch, and azimuth respectively), are used to transform coordinates from the third system into the second system or vice versa.

When aligning, the Z axis is uniquely defined by the gravity vector (+VE UP), the X axis is always in the horizontal plane (ie. always perpendicular to the Z axis) and is at right angles to the Y axis. The Y axis is however, not necessarily at right angles to the XY plane and can move with time.

SYSTEM:	**FOURTH COORDINATE SYSTEM (INTERMEDIATE TRANSFORMATION)**
TYPE:	NON-ORTHOGONAL AXES VARYING WITH TIME
X:	IN HORIZONTAL PLANE AT RIGHT ANGLE TO Y AXIS
Y:	OUTER GIMBAL ROLL AXIS (-VE through the mirror)
Z:	ALIGNED TO GRAVITY VECTOR (+VE UP)
ORIGIN:	IMU CENTER

The roll, pitch, and azimuth angles picked off the FILS Synchro/Digital Converters are as shown in table 1. When the system is navigating, the X and Z axes are maintained by mathematically calculated feedback to the platform torquers to account for earth rotation and the vehicle movement. They will be somewhat in error from the gravity vertical and horizontal plane at any time. This is what produces the well known Schuler velocity error patterns.

Table 1. Intermediate Transformation System Angle Definitions

Type Of Angle	Axis About Which Rotation Takes Place	Zero Angular Reference	Comments
Roll (Ω)	Y, Outer gimbal roll axis	Vertical = 0 Angle from vertical to servo reference mark Sign: +ve right handed axis from IMU origin away from mirror side	+ve Y axis goes from mirror side => IMU origin => side opp. mirror along outer gimbal roll axis
Pitch (ϕ)	X, Axis in horizontal plane at right angles to the Y axis	Horizontal = 0 Nose = side of casing opposite mirror. +VE = Nose Up -VE = Nose Down	+ve X axis is ninety (90) degrees to right of the +VE Y axis
Azimuth (Az)	Z axis is coincident with the gravity vector. (VERTICAL) (+VE UP)	Instantaneous north +VE to the east of north.	For small offset distances encountered instantaneous and geodetic north can be considered to be coincident.

6. Coordinate Transformation Via Axes Rotations

The problem of changing from the X,Y,Z coordinates in the third system to the X,Y,Z coordinates in the second system is dealt with by a series of rotations. The first rotation of the third system is about the Y axis through a $-\Omega$ angle. The effect of this rotation is to place the X axis of what was the third system into the horizontal plane. The next rotation is about this new X axis through an angle $-\phi$. This has the effect of moving the Y axis into the horizontal plane. The Z axis of this rotated system is now coincident with the Z axis of the second system. The X and Y axis differ from the X and Y axes of the second system by the grid azimuth (Az_G). As the grid azimuth is defined positive to the east of north (which in a right handed system should be negative), the last rotation is a +K (grid azimuth) rotation.

This rotation sequence can be represented in matrix rotation form as:

$$\begin{bmatrix} X2 \\ Y2 \\ Z2 \end{bmatrix} = RK * R\phi * R\Omega \begin{bmatrix} X3 \\ Y3 \\ Z3 \end{bmatrix} \quad \text{..................B 1}$$

Where RK, $R\phi$, $R\Omega$ represent the rotations of the axes for right handed systems, these rotation matrices are shown below:

$$\underset{\text{(about Z axis)}}{RK} = \begin{bmatrix} \cos K & \sin K & 0 \\ -\sin K & \cos K & 0 \\ 0 & 0 & 1 \end{bmatrix} \quad \text{..........B 2}$$

$$\underset{\text{(about X axis)}}{R\phi} = \begin{bmatrix} 1 & 0 & 0 \\ 0 & \cos\phi & \sin\phi \\ 0 & -\sin\phi & \cos\phi \end{bmatrix} \quad \text{..........B 3}$$

$$\underset{\text{(about Y axis)}}{R\Omega} = \begin{bmatrix} \cos\Omega & 0 & -\sin\Omega \\ 0 & 1 & 0 \\ \sin\Omega & 0 & \cos\Omega \end{bmatrix} \quad \text{..........B 4}$$

The combination of these matrices in the order RK, Rϕ, RΩ yields:

$$\begin{bmatrix} [CosK*Cos\Omega+SinK*sin\phi*Sin\Omega] & [SinK*Cos\phi] & [SinK*Sin\phi*Cos\Omega-Sin\Omega*CosK] \\ [CosK*Sin\phi*Sin\Omega-SinK*Cos\Omega] & [CosK*Cos\phi] & [CosK*Sin\phi*Cos\phi+Sin\Omega*SinK] \\ [Cos\phi*Sin\Omega] & [-Sin\phi] & [Cos\phi*Cos\Omega] \end{bmatrix}$$

.... B 5

Which can be expanded to:

$$\text{(EAST) GRID} \quad X2 = (CosK*Cos\Omega + Sin\phi*SinK*Sin\Omega) * X3 + (SinK*Cos\phi) * Y3 + (SinK*Sin\phi*Cos\Omega - Sin\Omega*CosK) * Z3 \quad .... \text{B 6}$$

$$\text{(NORTH) GRID} \quad Y2 = (CosK*Sin\phi*Sin\Omega - SinK*Sin\Omega) * X3 + (CosK*Cos\phi) * Y3 + (CosK*Sin\phi*Cos\Omega - Sin\Omega*SinK) * Z3 \quad .... \text{B 7}$$

$$\text{(HEIGHT) GRID} \quad Z2 = (Cos\phi*Sin\Omega) * X3 + (-Sin\phi) * Y3 + (Cos\phi*Cos\Omega) * Z3 \quad .... \text{B 8}$$

To calculate the delta grid northing, easting, and height from the IMU center to the vehicle reference point, the following changes are made to the above equations:

$$\Omega = - \Omega \qquad \phi = - \phi \qquad K = +Az_G$$

as Cos(-A) = Cos A and Sin(-A) = -Sin A

the equations B6 to B8 become:

$$\text{Delta EAST} \quad X2 = (CosAZ_G*Cos\Omega + Sin\phi*SinAz_G*Sin\Omega) * X3 + (SinAz_G*Cos\phi) * Y3 + (Sin\Omega*CosAz_G - SinAz_G*Sin\phi*Cos\Omega) * Z3 \quad ..\text{B9}$$

$$\text{Delta NORTH} \quad Y2 = (CosAz_G*Sin\phi*Sin\Omega - SinAz_G*Cos\Omega) * X3 + (CosAz_G*Cos\phi) * Y3 - (CosAz_G*Sin\phi*Cos\Omega + Sin\Omega*SinAz_G) * Z3 \quad ..\text{B10}$$

$$\text{Delta HEIGHT} \quad Z2 = (-Cos\phi*Sin\Omega) * X3 + (Sin\phi) * Y3 + (Cos\phi*Cos\Omega) * Z3 \quad ..\text{B11}$$

The above equations are used in the calculation of the delta Easting, Delta Northing, and Delta Height components from the IMU origin to the vehicle reference point by using the constant triplet X3,Y3,Z3 determined from calibration and stored in the program, and by using the attitude value in the Roll, Pitch, and Azimuth stores of the FILS unit. Note: (the K value must first be converted into a grid azimuth Az_G by applying the convergence to the instantaneous north azimuth). In addition to this, the initial azimuth misalignment and drift with time is applied.

Altering the order in which the three rotational matrices are applied will alter the expanded rotational matrix. In the case of going from known coordinates in the second system to coordinates in the third system, the following rotations are made:

$$\begin{bmatrix} X3 \\ Y3 \\ Z3 \end{bmatrix} = R\Omega * R\phi * RK \; | \; Y2 \; | \quad \ldots\ldots\ldots\ldots\ldots\ldots \text{B 12}$$

The combined rotational matrix has the following form:

$$\begin{bmatrix} [Cos\Omega*CosK-Sin\Omega*Sin\phi*sinK] & [Cos\Omega*SinK+Sin\Omega*Sin\phi*CosK] & [-\ Sin\Omega*Cos\phi] \\ [-SinK*Cos\phi] & [CosK*Cos\phi] & [Sin\phi] \\ [Sin\Omega*CosK+Cos\Omega*Sin\phi*SinK] & [Sin\Omega*SinK-Cos\Omega*Sin\phi*CosK] & [Cos\Omega*cos\phi] \end{bmatrix}$$

$$\ldots\ldots\ldots\ldots\ldots\ldots\ldots\ldots \text{B 13}$$

Substituting B13 into B12 and expanding the terms yield:

$$\begin{aligned} X3 = &\ (Cos\Omega*CosK - Sin\Omega*Sin\phi*SinK) * X2 \\ &+ (Cos\Omega*SinK + Sin\Omega*Sin\phi*CosK) * Y2 \\ &- (Sin\Omega*Cos\phi) * Z2 \quad \ldots\ldots\ldots\ldots\ldots\ldots \text{B 14} \end{aligned}$$

$$\begin{aligned} Y3 = &\ (-SinK*Cos\phi) * X2 \\ &+ (CosK*Cos\phi) * Y2 \\ &+ (Sin\phi) * Z2 \quad \ldots\ldots\ldots\ldots\ldots\ldots \text{B 15} \end{aligned}$$

$$\begin{aligned} Z3 = &\ (Sin\Omega*CosK + Cos\Omega*Sin\phi*SinK) * X2 \\ &+ (Sin\Omega*SinK - Cos\Omega*Sin\phi*CosK) * Y2 \\ &+ (Cos\Omega*Cos\phi) * Z2 \quad \ldots\ldots\ldots\ldots\ldots\ldots \text{B 16} \end{aligned}$$

To calculate the fixed coordinate triplet X3,Y3,Z3 from the IMU origin to the vehicle reference point if the delta northing, easting and height are known, the following changes are made to the above equations:

$$\Omega = -\Omega \qquad \phi = +\phi \qquad K = -Az_G$$

as $\quad Cos(-A) = Cos(A) \quad$ and $\quad Sin(-A) = -Sin(A)$

equations B14 to B16 become:

$$\left[\begin{array}{l} X3 = (\, Cos\Omega * CosAz_G + Sin\Omega * Sin\phi * sinAz_G \,) * X2 \\ \quad - (\, Cos\Omega * SinAz_G - Sin\Omega * Sin\phi * CosAz_G \,) * Y2 \\ \quad - (\, Sin\Omega * Cos\phi \,) * Z2 \\[1ex] Y3 = (\, SinAz_G * Cos\phi \,) * X2 \\ \quad + (\, CosAz_G * Cos\phi \,) * Y2 \\ \quad + (\, Sin\phi \,) * Z2 \\[1ex] Z3 = (\, Sin\Omega * CosAz_G - Cos\Omega * Sin\phi * SinAz_G \,) * X2 \\ \quad - (\, Sin\Omega * SinAz_G + Cos\Omega * Sin\phi * CosAz_G \,) * Y2 \\ \quad + (\, Cos\Omega * Cos\phi \,) * Z2 \end{array}\right] \begin{array}{l} \\ \\ ..B17 \\[1ex] \\ \\ ..B\ 18 \\[1ex] \\ \\ ..B\ 19 \end{array}$$

The above equations are not in the main Fils post processing programs as they are only necessary to determine the offset coordinates X3,Y3,Z3 which should be constant for any vehicle if the FILS unit is rigidly fixed to the vehicle (Ignoring the small amount of dynamic displacement due to the shock absorption system used and vehicle flexture).

7. Fifth Coordinate System (Unscribed Mirror System)

METHOD I is used to transfer coordinates from the IMU origin to a survey point or vice versa by use of a theodolite and the plane mirror which is mounted on the FILS IMU casing. If this mirror surface were exactly perpendicular to the line defined by the outer roll gimbal axis (the Y axis of the third system), it could serve directly as an azimuth reference with no further calculations required. There is however, invariably a small angular deviation from this situation due to the physical mounting restrictions. It is therefore necessary to define a fifth coordinate system. Whether it is necessary to apply this system will depend on the type of work being done, and the length of the offset from the mirror surface.

A summary of the fifth system is as follows:

SYSTEM: **FIFTH COORDINATE SYSTEM (UNSCRIBED MIRROR SYSTEM)**
TYPE: ORTHOGONAL, RIGHT HANDED
X: IN PLANE OF MIRROR TO FORM RIGHT HANDED SYSTEM
Y: PERPENDICULAR TO THE REFLECTING SURFACE (+VE towards IMU)
Z: IN THE PLANE OF THE MIRROR ALONG THE PROJECTION OF THE +VE Z AXIS OF THE THIRD SYSTEM
ORIGIN: AT THE INTERSECTION OF THE OUTER ROLL GIMBAL AXIS AND THE MIRROR SURFACE.

Because of the definition of the Z axis as a projection of the Z axis of the third system in the XY plane of the fifth system, it is necessary to apply only two rotations to the fifth system to make its axes parallel to the corresponding axes in the third system. This is shown in figures 2 and 3.

The first axis rotation would be around the X5 axis in order to make the Z5' axis parallel to the Z axis of the third system. Z5' is used to denote the new z axis of the fifth system following the axis rotation about X5. Let this rotation angle be denoted as α.

The second rotation would be about the Z5' axis (now parallel to the Z3 axis) is such a way as to make the Y5" axis coincident with the Y3 axis. Let this second rotational angle be denoted as β. This rotation sequence is graphically illustrated in figure 4.

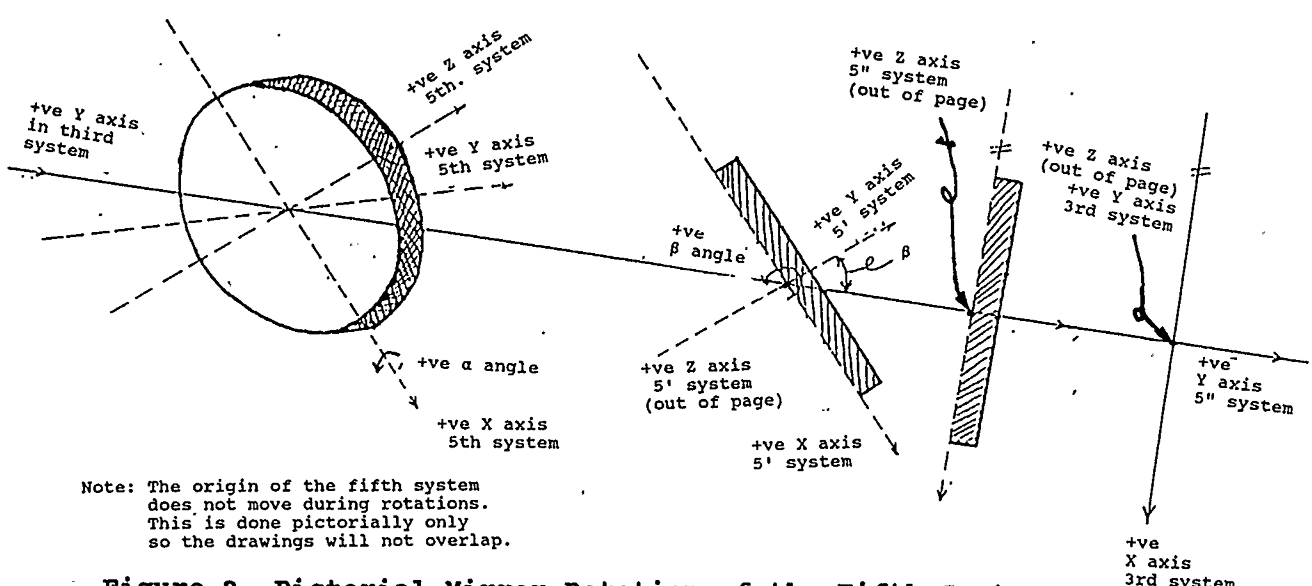

Figure 2. Pictorial Mirror Rotation of the Fifth System

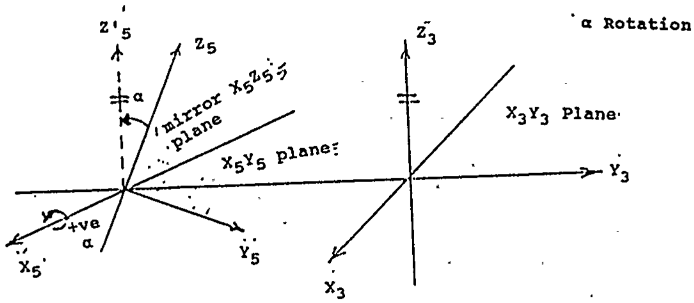

First rotation about X_5 axis brings X_5Y_5 plane into X_3Y_3 plane

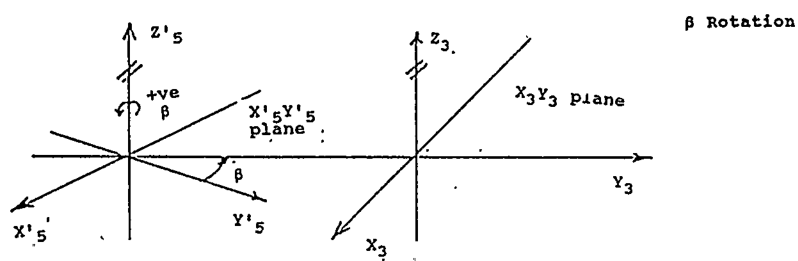

Second rotation about Z'_5 axis brings the +ve Y'_5 axis coincident with the +ve Y_3 axis

Figure 3. Cartesian Representation Of α and β Rotat

The following relationship then holds between the fifth and the third system:

$$\begin{bmatrix} X3 \\ Y3 \\ Z3 \end{bmatrix} = R_{Z5'}(\beta)\ R_{X5}(\alpha) \begin{bmatrix} X5 \\ Y5 \\ Z5 \end{bmatrix} + \begin{bmatrix} 0 \\ Y3_M \\ 0 \end{bmatrix} \quad \ldots\ldots \text{ B 20}$$

where $Y3_M$ is the Y coordinate of the fifth system origin in terms of the third system. Letting K=β and ϕ=α in equation B-2 and B-3 resepectively yields:

$$R_{Z5'}(\beta) = \begin{bmatrix} \text{Cos}\beta & \text{Sin}\beta & 0 \\ -\text{Sin}\beta & \text{Cos}\beta & 0 \\ 0 & 0 & 1 \end{bmatrix} \ldots \text{ B 21} \qquad R_{X5}(\alpha) = \begin{bmatrix} 1 & 0 & 0 \\ 0 & \text{Cos}\alpha & \text{Sin}\alpha \\ 0 & -\text{Sin}\alpha & \text{Cos}\alpha \end{bmatrix} \ldots \text{ B 22}$$

Therefore:

$$R_{Z5'}(\beta) * R_{X5}(\alpha) = \begin{bmatrix} (\ \text{Cos}\beta) & (\text{Sin}\beta*\text{Cos}\alpha) & (\text{Sin}\beta*\text{Sin}\alpha) \\ (-\text{Sin}\beta) & (\text{Cos}\beta*\text{Cos}\alpha) & (\text{Cos}\beta*\text{Sin}\alpha) \\ 0 & (-\text{Sin}\alpha) & (\text{Cos}\alpha) \end{bmatrix} \ldots \text{ B23}$$

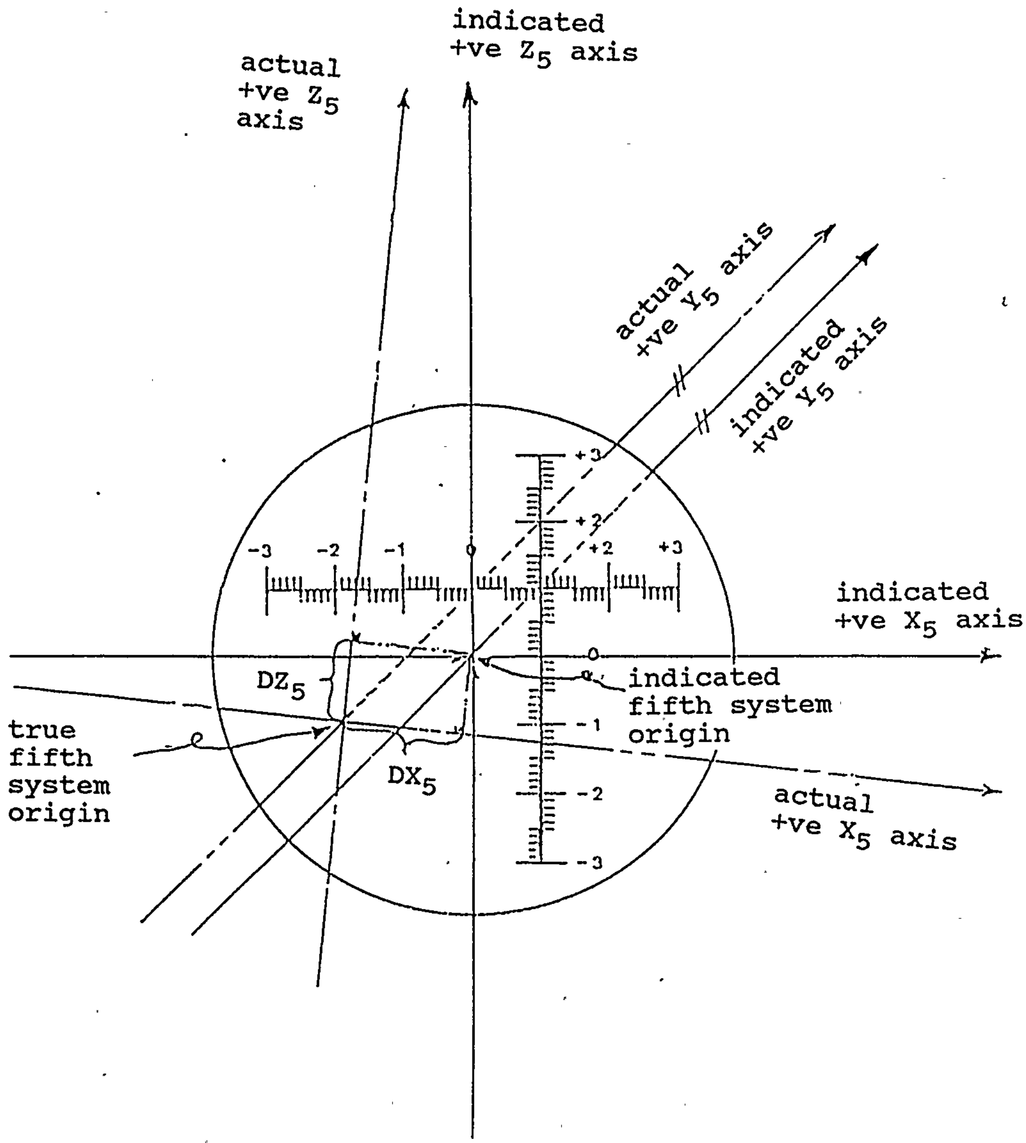

Figure 4. Mirror Engraving Appearing on Some FILS units

Equation B20 in expanded form becomes:

$X3 = (\cos\beta)*X5 + (\sin\beta*\cos\alpha)*Y5 + (\sin\beta*\sin\alpha)*Z5$	.. B 24
$Y3 = (-\sin\beta)*X5 + (\cos\beta*\cos\alpha)*Y5 + (\cos\beta*\sin\alpha)*Z5 + Y3_M$	.. B 25
$Z3 = (-\sin\alpha)*Y5 + (\cos\alpha)*Z5$	.. B 26

The problem with the fifth system is that while a parallel to the Y5 axis is easily defined in a physical sense by the mirror surface, the orientation of the X and Z axis, and the exact origin on the mirror surface are not directly apparent other than through the scribed lines on the mirror surface as shown in figure 4. (NOTE: These lines are not present on all FILS units). These are only sufficient to indicate the origin and the general direction of the axes. In order to initially determine the angle α and β it is necessary to develop a relationship between these angles and the angles which can be measure by a theodolite. For this purpose, the following terms are defined:

AZ_{G3} = the grid azimuth of the Y3 axis (system output)

AZ_{G5} = the grid azimuth of the Y5 axis (theodolite measure)

$DAZ_{5-3} = AZ_{G5} - AZ_{G3}$

V_3 = the vertical angle (pitch) of the Y3 axis (system output)

V_5 = the vertical angle (pitch) of the Y5 axis (theodolite measure)

$DV_{5-3} = V_5 - V_3$

The angular values DAZ_{5-3} and DV_{5-3} can be determined by subtracting the value of the grid azimuth and pitch angle as given by the FILS from the grid azimuth and vertical angle respectively as determined with the theodolite, a reference grid azimuth, and the FILS mirror. Knowing DAZ_{5-3} and DV_{5-3} the angles α and β can be determined if the roll angle Ω and the pitch angle ϕ are known.

The angles DAZ_{5-3} and DV_{5-3} are independent of the actual grid azimuth of the perpendicular to the mirror. For this reason, it is valid to assign this line a grid azimuth of exactly zero degrees. With this in mind, the angles α and β can be determined as follows:

Since the DAZ_{5-3} is measured in the horizontal plane and the DV_{5-3} in the vertical plane, a unit vector can be defined in the second system around zero degrees grid north such that the X,Y,Z components (denoted as DX2,DY2,DZ2 to signify they are a result of the DAZ_{5-3} and DV_{5-3} angle) are given in equation B27.

$$\begin{bmatrix} DX2 \\ DY2 \\ DZ2 \end{bmatrix} = \begin{bmatrix} \mathrm{Sin}(-DAZ_{5-3})*\mathrm{Cos}(DV_{5-3}) \\ \mathrm{Cos}(-DAZ_{5-3})*\mathrm{Cos}(DV_{5-3}) \\ \mathrm{Sin}(DV_{5-3}) \end{bmatrix} \quad \ldots\ldots\ldots\ldots \text{B 27}$$

This is shown diagrammatically in figure 5.

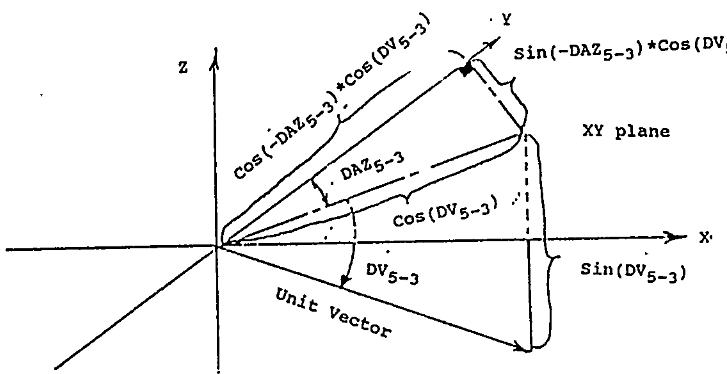

Figure 5. Diagrammatical presentation of the DAZ_{5-3} and DV_{5-3} angles

NOTE:: the minus sign is placed in front of the DAZ_{5-3} terms prior to taking the sine and cosine because the second system is a right handed system which implies that a positive azimuth angle goes to the west of north (or counterclockwise) while a grid azimuth is measured as positive to the east of north (or clockwise).

To get from the second system to the third system, rotations about the X2 axis by the pitch angle ϕ and about the Y2' axis (the outer roll gimbal axis) by the roll angle Ω are required. This sequence is given by the matrix equation:

$$\begin{bmatrix} DX3 \\ DY3 \\ DZ3 \end{bmatrix} = R_{Y2'}(\Omega)\ R_{X2}(\phi) \begin{bmatrix} DX2 \\ DY2 \\ DZ2 \end{bmatrix} \quad \ldots\ldots\ldots\ldots\ldots\ldots\ldots \text{B 28}$$

Using equations B3 and B4 for right handed systems yields:

$$R_{Y2'}(\Omega)\ R_{X2}(\phi) = \begin{bmatrix} Cos\Omega & Sin\Omega*Sin\phi & -Sin\Omega*Cos\phi \\ 0 & Cos\phi & Sin\phi \\ Sin\Omega & -Cos\Omega*Sin\phi & Cos\Omega*Cos\phi \end{bmatrix} \quad \ldots\ldots \text{ B 29}$$

Placing B29 into B28 and expanding yields:

$$DX3 = (Cos\Omega)*DX2 + (Sin\Omega*Sin\phi)*DY2 - (Sin\Omega*Cos\phi)*DZ2 \quad \ldots\ldots \text{ B 30}$$

$$DY3 = (Cos\phi)*DY2 + (Sin\phi)*DZ2 \quad \ldots\ldots \text{ B 31}$$

$$DZ3 = (Sin\Omega)*DX2 - (Cos\Omega*Sin\phi)*DY2 + (Cos\Omega*Cos\phi)*DZ2 \quad \ldots\ldots \text{ B 32}$$

From these coordinates the angles β (being the rotational angle about the Z3 axis required to make the unit vector fall in the Z3 Y3 plane) can be computed. That is:

$$\boxed{\beta = -\ Tan^{-1}\ (\ DX3\ /\ DY3\ )} \quad \ldots\ldots\ldots\ldots\ldots\ldots\ldots \text{ B 33}$$

Once the angle β has been determined, it is used to transform the DX3,DY3,DZ3 coordinates into DX3',DY3',DZ3' coordinates by the relationship:

$$\begin{bmatrix} DX3' \\ DY3' \\ DZ3' \end{bmatrix} = R_{Z3}(-\beta) \begin{bmatrix} DX3 \\ DY3 \\ DZ3 \end{bmatrix} \quad \ldots\ldots\ldots\ldots\ldots\ldots\ldots\ldots \text{ B 34}$$

Substituting in the relationship given by B2 yields:

$$\begin{bmatrix} DX3' \\ DY3' \\ DZ3' \end{bmatrix} = \begin{bmatrix} Cos\beta & -Sin\beta & 0 \\ Sin\beta & Cos\beta & 0 \\ 0 & 0 & 1 \end{bmatrix}$$

Expanding B35 yields:

$$\begin{bmatrix} DX3' \\ DY3' \\ DZ3' \end{bmatrix} = \begin{bmatrix} (Cos\beta)*DX3 - (Sin\beta)*DY3 \\ (Sin\beta)*DX3 + (Cos\beta)*DY3 \\ DZ3 \end{bmatrix} \quad \begin{matrix} \ldots\ldots\ldots\ldots\ldots\ldots \text{ B 36} \\ \ldots\ldots\ldots\ldots\ldots\ldots \text{ B 37} \\ \ldots\ldots\ldots\ldots\ldots\ldots \text{ B 38} \end{matrix}$$

By virtue of the fact that the β angle was calculated such that a rotation about the Z3 axis by (-β) would make the unit vector fall in the Z3' Y3' plane, the value of Dy3' should be zero.

The final angle α can now be calculated using the relationship:

$$\boxed{\alpha = -\mathrm{Tan}^{-1}\ (\ DZ3'\ /\ DX3'\ )} \qquad \ldots\ldots\ B\ 39$$

The angles α and β have now been determined and can be input as mirror harmonizing terms. These terms are subsequently used to supply the correct azimuth and vertical angle of a line defined by the perpendicular to the mirror surface.

The problem is now changed to one of determining the DHOR and DVERT angles caused by the α and β mirror misalignment angles for different roll and pitch angles. Again, start with a unit vector totally along the Y5 axis. This vector must then be converted into its component parts in the Y3 system (less the origin shift along the Y3 axis). This is given by equations B24 to B26.

Therefore:

$$DX3 = (\mathrm{Cos}\beta)*0 + (\mathrm{Sin}\beta*\mathrm{Cos}\alpha)*1 + (\mathrm{Sin}\beta*\mathrm{Sin}\alpha)*0$$

$$DY3 = (-\mathrm{Sin}\beta)*0 + (\mathrm{Cos}\beta*\mathrm{Cos}\alpha)*1 + (\mathrm{Cos}\beta*\mathrm{Sin}\alpha)*0$$

$$DZ3 = (-\mathrm{Sin}\alpha)*1 + (\mathrm{Cos}\alpha)*0$$

That is:

$$DX3 = \mathrm{Sin}\beta * \mathrm{Cos}\alpha \qquad \ldots\ldots\ldots\ldots\ B\ 40(a)$$

$$DY3 = \mathrm{Cos}\beta * \mathrm{Cos}\alpha \qquad \ldots\ldots\ldots\ldots\ B\ 40(b)$$

$$DZ3 = -\mathrm{Sin}\alpha \qquad \ldots\ldots\ldots\ldots\ B\ 40(c)$$

These coordinates must now be determined in the second system. This is accomplished by using a simplified form of equations B6 to B8. Since a rotation in azimuth between the second and third systems does not affect the DHOR and DVERT angles caused by the α and β mirror rotations, the following equations can be set up:

$$\begin{bmatrix} X2 \\ Y2 \\ Z2 \end{bmatrix} = R(\phi)\ R(\Omega) \begin{bmatrix} X3 \\ Y3 \\ Z3 \end{bmatrix} \qquad \ldots\ldots\ldots\ldots\ldots\ldots\ B\ 40(d)$$

$$\begin{bmatrix} X2 \\ Y2 \\ Z2 \end{bmatrix} = \begin{bmatrix} 1 & 0 & 0 \\ 0 & \text{Cos}\phi & \text{Sin}\phi \\ 0 & -\text{Sin}\phi & \text{Cos}\phi \end{bmatrix} \cdot \begin{bmatrix} \text{Cos}\Omega & 0 & -\text{Sin}\Omega \\ 0 & 1 & 0 \\ \text{Sin}\Omega & 0 & \text{Cos}\Omega \end{bmatrix} \begin{bmatrix} X3 \\ Y3 \\ Z3 \end{bmatrix} \quad .. \text{ B } 40(e)$$

To calculate the grid northing, easting, and height, the following changes are made to the above equation:

$$\Omega = -\Omega \qquad \phi = -\phi$$

as Cos(-A) = Cos(A) and Sin(-A) = -Sin(A) and X3,Y3,Z3 are DX3,DY3,DZ3 the equation becomes:

$$\begin{bmatrix} DX2 \\ DY2 \\ DZ2 \end{bmatrix} = \begin{bmatrix} \text{Cos}\Omega & 0 & \text{Sin}\Omega \\ \text{Sin}\phi*\text{Sin}\Omega & \text{Cos}\phi & -\text{Sin}\phi*\text{Cos}\Omega \\ -\text{Cos}\phi*\text{Sin}\Omega & \text{Sin}\phi & \text{Cos}\phi*\text{Cos}\Omega \end{bmatrix} \begin{bmatrix} \text{Sin}\beta*\text{Cos}\alpha \\ \text{Cos}\beta*\text{Cos}\alpha \\ -\text{Sin}\alpha \end{bmatrix} \quad .. \text{ B } 40(f)$$

In its expanded form this becomes:

$$DX2 = \text{Cos}\Omega*\text{Sin}\beta*\text{Cos}\alpha - \text{Sin}\Omega*\text{Sin}\alpha \quad .... \text{ B } 40(g)$$

$$DY2 = \text{Sin}\phi*\text{Sin}\Omega*\text{Sin}\beta*\text{Cos}\alpha + \text{Cos}\phi*\text{Cos}\beta*\text{Cos}\alpha + \text{Sin}\phi*\text{Cos}\Omega*\text{Sin}\alpha \quad .\text{B } 40(h)$$

$$DZ2 = -\text{Cos}\phi*\text{Sin}\Omega*\text{Sin}\beta*\text{Cos}\alpha + \text{Sin}\phi*\text{Cos}\beta*\text{Cos}\alpha - \text{Cos}\phi*\text{Cos}\Omega*\text{Sin}\alpha \quad .\text{B } 40(i)$$

$$DXY2 = DX2 * DY2 \quad ....\text{B } 40(j)$$

$$\boxed{\begin{aligned} DHOR &= \text{Tan}^{-1} (DX2 / DY2) \\ DVERT &= \text{Tan}^{-1} (DZ2 / DXY2) \end{aligned}} \quad \begin{aligned} &......\text{B } 40(k) \\ &......\text{B } 40(l) \end{aligned}$$

8. Sixth Coordinate System (Scribed Mirror System)

From figure 4 it can be seen that a sixth coordinate system can be defined.

SYSTEM: **SIXTH COORDINATE SYSTEM (SCRIBED MIRROR SYSTEM)**
TYPE: ORTHOGONAL, RIGHT HANDED
X: AXIS SCRIBED ON MIRROR SURFACE
(+VE AXIS ≈ ‖ TO +VE x AXIS OF SYSTEM 5)
Y: PERPENDICULAR TO THE REFLECTING SURFACE (+VE towards IMU)
Z: AXIS SCRIBED ON MIRROR SURFACE
(+VE AXIS ≈ ‖ TO +VE Z AXIS OF SYSTEM 5)
ORIGIN: POINT ON MIRROR SURFACE AT INTERSECTION OF LINES PARALLEL TO THE SCRIBED X AND Z LINES RESPECTIVELY AND GOING THROUGH SCRIBED ZERO POSITIONS ON THE Z AND X AXIS RESPECTIVELY.

A few assumptions are made at this point. These are as follows.

ASSUMPTIONS:
1) THE MIRROR SURFACE IS PERFECTLY FLAT
2) THE SCRIBED LINES PARALLEL TO THE X AND Z AXIS RESPECTIVELY INTERSECT AT RIGHT ANGLES.

The first assumption implies that the Y axis of the sixth system is parallel to the Y axis of the fifth system. The second assumption is made so the system can be considered orthogonal. Both of these assumptions are realistic in nature considering the limited use to which this system will be put.

Let the angle γ represent the amount by which the Z6 axis must be rotated about the positive Y6 axis such that the rotated Z6 axis (denoted by Z6') will be parallel with the Z5 axis. See figure 6 below:

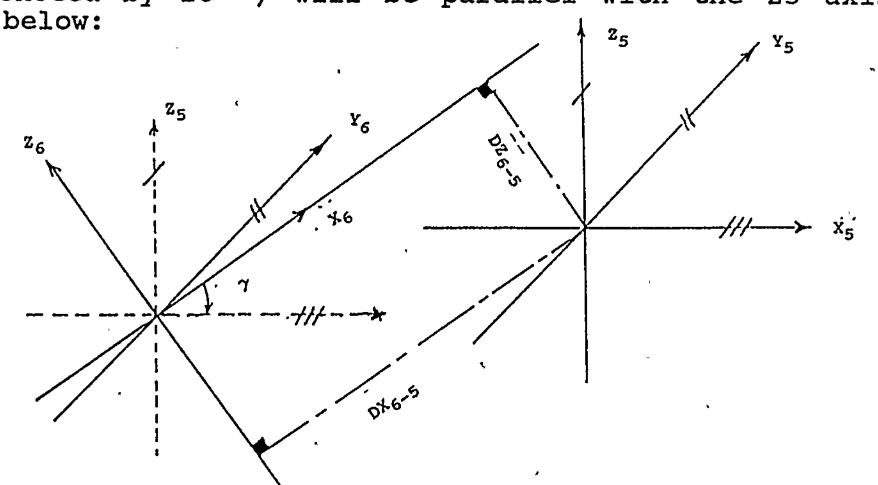

Figure 6. : γ Angle rotation in the sixth coordinate system

Therefore the relationship between coordinates in the sixth and fifth system is give by:

$$\begin{bmatrix} X5 \\ Y5 \\ Z5 \end{bmatrix} = R_{Y6}(\gamma) \begin{bmatrix} X6 \\ Y6 \\ Z6 \end{bmatrix} + \begin{bmatrix} DX_{6-5} \\ 0 \\ DZ_{6-5} \end{bmatrix} \qquad \text{.......... B 41}$$

Replacing $RY_6(\gamma)$ of equation B41 by its expanded form given in equation B4 yields:

$$\begin{bmatrix} X5 \\ Y5 \\ Z5 \end{bmatrix} = \begin{bmatrix} \text{Cos}\gamma & 0 & -\text{Sin}\gamma \\ 0 & 1 & 0 \\ \text{Sin}\gamma & 0 & \text{Cos}\gamma \end{bmatrix} \begin{bmatrix} X6 \\ Y6 \\ Z6 \end{bmatrix} + \begin{bmatrix} DX_{6-5} \\ 0 \\ DZ_{6-5} \end{bmatrix} \qquad \text{..... B 42}$$

This Yields:

$$X5 = (\text{Cos}\gamma)*X6 - (\text{Sin}\gamma)*Z6 + DX_{6-5} \qquad \text{...... B 43}$$

$$Y5 = Y6 \qquad \text{....... B 44}$$

$$Z5 = (\text{Sin}\gamma)*X6 + (\text{Cos}\gamma)*Z6 + DZ_{6-5} \qquad \text{....... B 45}$$

For most practical purposes the angle γ and the offsets DX_{6-5} and DZ_{6-5} will be so small as to be insignificant. In this situation, the fifth and sixth system can be said to be identical.

9. Seventh Coordinate System (Vehicle Reference Point System)

For ease of operation in the field, the measurements which are made from the vehicle reference point (VRP) are made in a coordinate system described as follows:

SYSTEM: **SEVENTH COORDINATE SYSTEM (VEHICLE REFERENCE POINT SYSTEM)**
TYPE: ORTHOGONAL, RIGHT HANDED
X: IN HORIZONTAL PLANE TO FORM A RIGHT HANDED SYSTEM
Y: IN HORIZONTAL PLANE, +VE DIRECTION DEFINED BY 0° ON PROTRACTOR
Z: ALONG GRAVITY VECTOR, +VE UP
ORIGIN: VEHICLE REFERENCE POINT

This coordinate system is illustrated in figure 7.

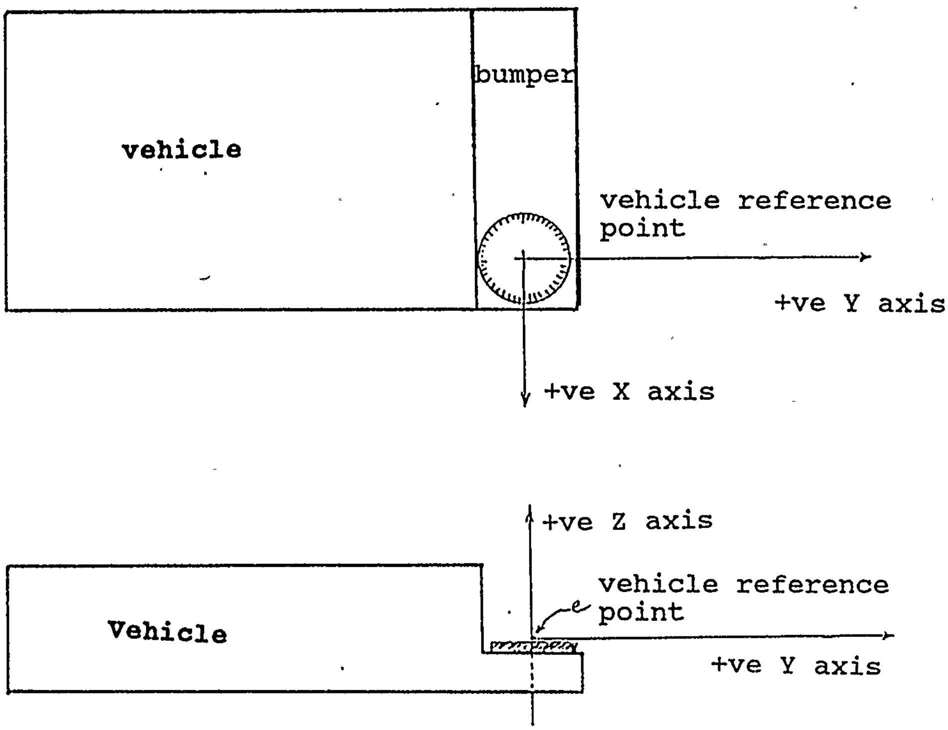

Figure 7. Vehicle Reference Point System

In this system, the person measuring the offset to or from a survey point would measure the horizontal distance d_h to the point, the vertical distance d_v to the point, and the angle made in the horizontal plane from the vehicle reference point to the survey point with respect to the zero mark on the protractor system ϵ_h.

Comparing this seventh system (vehicle reference point system) with the second system (grid right handed system), it can be seen that the X and Y axes of both systems are in the horizontal plane and the Z axes are both along the gravity vertical (+ve up). The seventh system can therefore be related to the second system by a single rotation about the Z axis and a translation of the origin. Let ψ denote the horizontal angle between the Y axis of the second system (ie. U.T.M. grid north) and the Y axis of the seventh system. This is shown in figure 8.

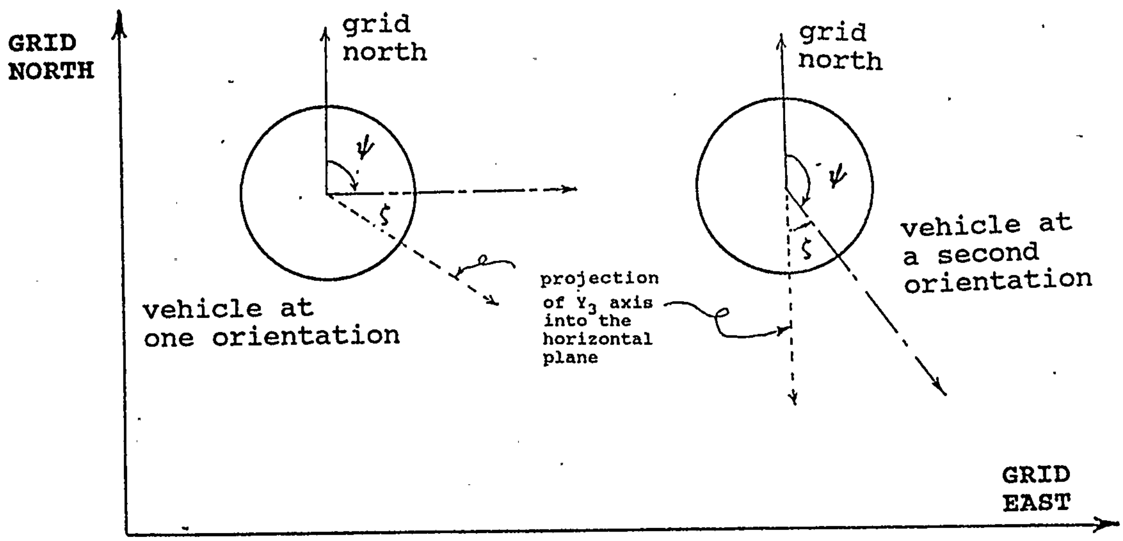

NOTE: The ψ angle changes as the orientation of the vehicle changes, but the ζ angle remains constant.

Figure 8. Angular Relationship of Protractor and Grid North

From this figure, it is apparent that as the vehicle moves the angle ψ changes. To find the angle ψ it is necessary to link the Y7 axis with another system which will maintain a constant relationship to it. The third system is again the linking system. As its Y axis is fixed to the FILS IMU casing, and the casing is fixed to the vehicle, a constant angular relationship is maintained between the Y7 axis and the projection of the Y3 axis into the horizontal plane. Let the angle from the projection of the Y3 axis onto the horizontal plane of the Y7 axis be denoted as ζ. As the grid azimuth of the Y3 axis is known, the grid azimuth of the Y7 axis (ψ) can be determined as shown in equation B46.

$$\psi = AZ_{GRID}(Y3) - \zeta \quad \text{......... B 46}$$

The offsets from the vehicle reference point to the survey point in the second system are them given by:

$$\begin{bmatrix} DX2 \\ DY2 \\ DZ2 \end{bmatrix}_{VRP \Rightarrow SP} = \begin{bmatrix} \mathrm{Cos}(-\psi) & \mathrm{Sin}(-\psi) & 0 \\ -\mathrm{Sin}(-\psi) & \mathrm{Cos}(-\psi) & 0 \\ 0 & 0 & 1 \end{bmatrix} \begin{bmatrix} X7 \\ Y7 \\ Z7 \end{bmatrix} \quad \text{...... B 47}$$

The minus sign in front of the grid azimuth ψ is due to the fact that the +ve grid azimuth is in the clockwise direction whereas the seventh system is right handed and has a positive rotation about the Z axis in a counterclockwise direction.

As $\mathrm{Cos}(-A) = \mathrm{Cos}(A)$ and $\mathrm{Sin}(-A) = -\mathrm{Sin}(A)$

equation B47 can be expanded to the form shown in equations B48 to B50 as follows:

$$DX2_{VRP=>SP} = \mathrm{Cos}(\psi)*X7 - \mathrm{Sin}(\psi)*Y7 \qquad \text{............ B 48}$$

$$DY2_{VRP=>SP} = \mathrm{Sin}(\psi)*X7 + \mathrm{Cos}(\psi)*Y7 \qquad \text{............ B 49}$$

$$DZ2_{VRP=>SP} = Z7 \qquad \text{............ B 50}$$

The values of X7 and Y7 are determined from the measured horizontal distance d_h and the horizontal angle ϵ_h as shown in the following equations B51 and B52.

$$X7 = d_h * \mathrm{Sin}\ \epsilon_h \qquad \text{........... B 51}$$

$$Y7 = d_h * \mathrm{Cos}\ \epsilon_h \qquad \text{........... B 52}$$

The vertical distance d_v is parallel to the Z7 axis. Therefore, the Z7 coordinate is equal to the d_v distance if a minus is used to denote distances lower than the vehicle reference point and a positive to denote distances above the vehicle reference point. In equation form this is given by:

$$Z7 = d_v \qquad \text{.......... B 53}$$

10. METHOD I IMU => SURVEY POINT VIA MIRROR AND THEODOLITE

For METHOD I the following data is used.

Externally measured values: d_1, d_2, d_3, $\sphericalangle H_1$, $\sphericalangle V_2$.

Calibrated values: α, β, $Y3_M$

Internally measured values: AZ_G, ϕ, Ω

The DHOR and DVERT angles as determined by equations B40(k) and B40(l) are applied to the AZ_G and pitch angles given by the system to obtain the correct azimuth and pitch of the mirror reference line. With this established, the d_1, d_2, d_3 distances are converted into their grid northing, easting, and height components. This would give the coordinate differences in the second system from the fifth system origin to the survey point. If the angles α and β are very small, the distance d_1 can be treated as $(d_1 + |Y3_M|)$ and the coordinate differences will be in the second system from the IMU origin to the survey point. See figures 10 and 11 for a diagrammatic presentation of d_1, d_2, d_3, $\sphericalangle H_1$, $\sphericalangle V_2$, $Y3_M$.

11. METHOD II IMU => SURVEY POINT VIA VEHICLE REFERENCE POINT

For METHOD II the following data is used.

Externally measured values: d_h, d_v, ϵ_h

Calibrated values: X3, Y3, Z3, ζ

Internally measured values: AZ_G, ϕ, Ω

Combining equations B9 to B11 with equations B48 to B50 yields:

$$
\boxed{
\begin{aligned}
DE_{SP} = \; & (\cos AZ_G*\cos\Omega + \sin\phi*\sin AZ_G*\sin\Omega) * X3 \\
+ & (\sin AZ_G*\cos\phi) * Y3 \\
+ & (\sin\Omega*\cos AZ_G - \sin AZ_G*\sin\phi*\cos\Omega) * Z3 \\
+ & (\cos\psi) * X7 - (\sin\psi) * Y7 \\
\\
DN_{SP} = \; & (\cos AZ_G*\sin\phi*\sin\Omega - \sin AZ_G*\cos\Omega) * X3 \\
+ & (\cos AZ_G*\cos\Omega) * Y3 \\
- & (\cos AZ_G*\sin\phi*\cos\Omega + \sin\Omega*\sin AZ_G) * Z3 \\
+ & (\sin\psi) * X7 + (\cos\psi) * Y7 \\
\\
DHT_{SP} = \; & (-\cos\phi*\sin\Omega) * X3 + (\sin\phi) * Y3 \\
+ & (\cos\phi*\cos\Omega) * Z3 + Z7
\end{aligned}
}
$$

......B 54

.....B 55

.....B 56

The sense of these delta values is from the IMU origin to the survey point. The value of ψ is obtained from equation B46. The equations B54 to B56 can be written as:

$$
\boxed{
\begin{aligned}
DE_{SP} &= DE_{VRP} + \cos\psi * X7 - \sin\psi * Y7 \\
DN_{SP} &= DN_{VRP} + \sin\psi * X7 + \cos\psi * Y7 \\
DHT_{SP} &= DHT_{VRP} + Z7
\end{aligned}
}
$$

12. Calibration Procedures For Method II

The distance $Y3_M$ should be readily available from working drawing to the required precision (its values is approximately 14.5 Cm.). The angles α and β are obtained by measuring known grid azimuth lines with a theodolite and then aligning the theodolite crossbars on their reflection in the mirror. The horizontal and vertical angles are read along with the system roll, pitch, and azimuth. α is given by equations B39 and β by equation B33. To determine the X3, Y3, Z3 constant vehicle offsets, a measurement of the vehicle reference point is done via the theodolite and mirror as shown in figures 9 and 10 . The actual X3, Y3, Z3 values are calculated using equations B17 to B19. For very accurate work, equations B24 to B26 would also have to be considered. The measurement of the H3 angle allows for the calculation of ζ.

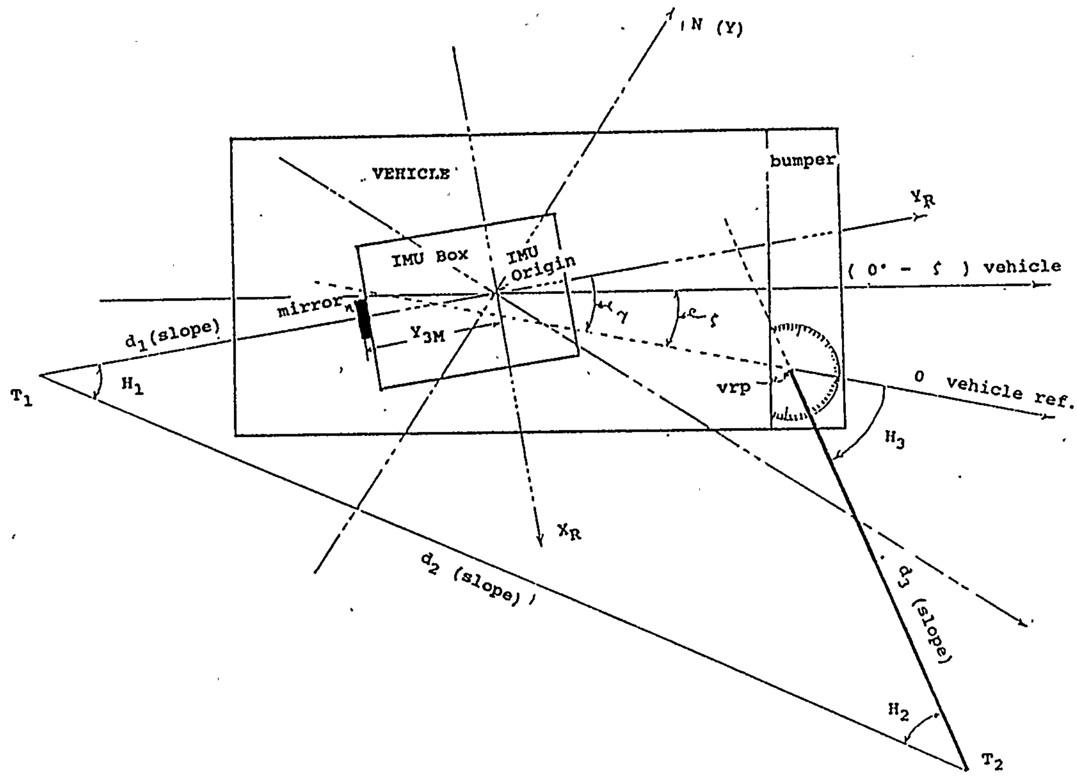

Figure 9. Top View of VRP Calibration Layout METHOD II

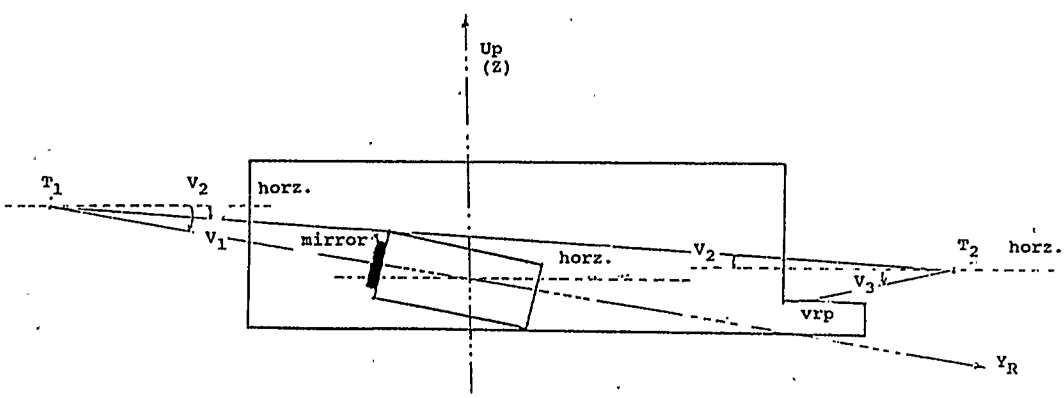

Figure 10. Side View of VRP Calibration Layout METHOD II

13. Offset Calculations using EDM Equipment

The description in this section is for a specific configuration of EDM offset measuring unit as used by NORTECH SURVEYS for long distance offsets. It comprises of a distance measuring unit mounted on a yoke which has angular encoders on it. These angular encoders read the change in angle from a stop, and not an absolute angle. For a different type of EDM measuring unit, a different set of equations may have to be developed.

The infra red measuring unit (AGA) is set in a yoke as shown in figure 11 below. The intersection of the two rotational axis define the origin of this local coordinate system.

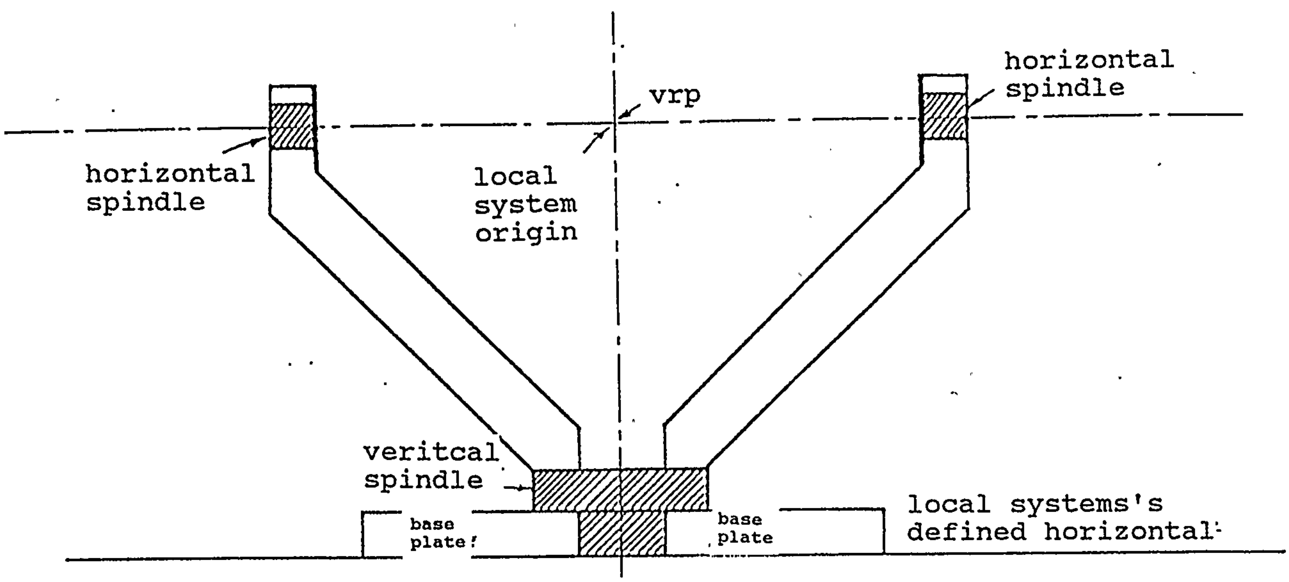

Figure 11. EDM Yoke Local Coordinate System

The local system's horizontal and vertical axes as defined are not required to be mounted at any specific orientation with respect to either the locally defined gravity vector and horizon, or the roll, pitch, and azimuth axis of the inertial unit. It is necessary however to calibrate the following parameters once the yoke is mounted with a fixed relationship to the inertial unit.

1) Offsets from the IMU centre to the Local System Origin (VRP) in terms of X3, Y3, Z3. NOTE: the subscript "3" is used here to conform with the third system (casing right handed system) previously referred to in this Appendix.

2) The angle ρ of rotation about the X8 axis required to bring the Y8' axis parallel to the X3 Y3 plane.

3) The angle of σ of rotation about the Y8 axis required to bring the Z'8 axis parallel to the Z3 axis.

4) The angle η of rotation about the Z"8 axis required to make the X"8 and Y"8 axes parallel to the x3 and y3 axis respectively.

5) The angle $\Delta\beta 8$ from the vertical reference point (zero) of system 3 to the plane defined by the X8 and Y8 axes.

In terms of the yoke system (system # 8) the coordinates are derived from the measured slope distance d_8; the horizontal angle α_8 measured in the X8 Y8 plane; the vertical angle β_8 measured in a plane perpendicular to the x8 y8 plane from the vertical stop point to the target; and the calibrated angle $\Delta\beta_8$.

The system #8 coordinates are then defined as:

$$X8 = d_8 * \text{Cos} (\beta_8 - \Delta\beta_8) * \text{Sin} (\alpha_8) \qquad \text{.........} \text{ B 57}$$

$$Y8 = d_8 * \text{Cos} (\beta_8 - \Delta\beta_8) * \text{Cos} (\alpha_8) \qquad \text{.........} \text{ B 58}$$

$$Z8 = d_8 * \text{Sin} (\beta_8 - \Delta\beta_8) \qquad \text{.........} \text{ B 59}$$

This coordinate system and its components are shown in figure 12.

The coordinates derived in system #8 must be transformed into system #3 coordinates by rotating the axis of system #8 to a position parallel with the axis of system #3 and applying the offsets, in terms of system #3 coordinates, from the IMU (system #3) origin to the VRP (system #8) origin . These rotation angles and translation distances are fixed and are determined by calibration. The order of rotation is assumed to be first about the X8 axis and then about the Y'8 axis to bring the Z8 axis parallel to the Z3 axis, finally about the Z"8 axis (the Z8 axis has been rotated twice hence Z"8) to bring the X"8 axis parallel to the X3, Y3 axis. The system #3 to system #8 offset coordinates (origin to origin) are then applied as translation terms. The resulting transformation is shown first in matrix rotation form, and then in its expanded form.

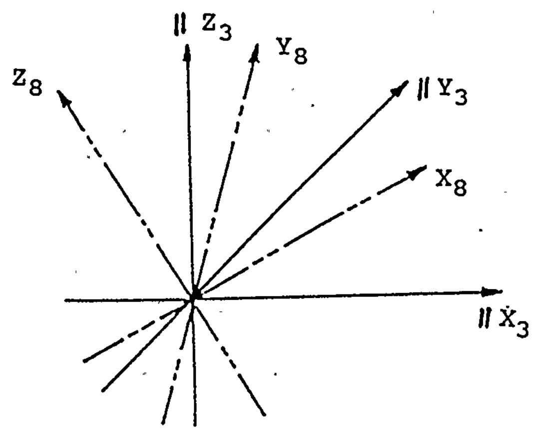

a) Initial Orientations:

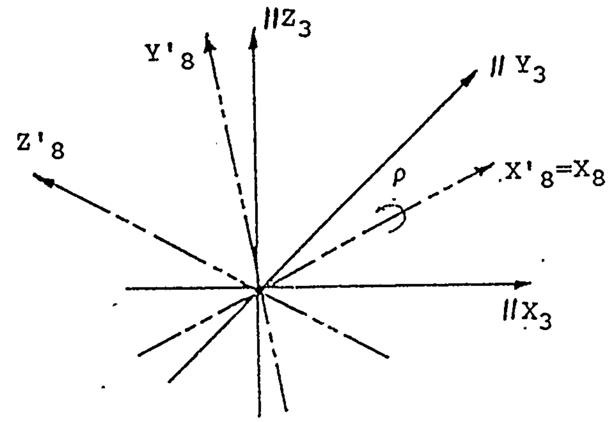

b) Y_8 axis is rotated by an angle ρ about the X_8 axis such that the Y_8 axis lies in a plane parallel to the X_3 Y_3 plane.

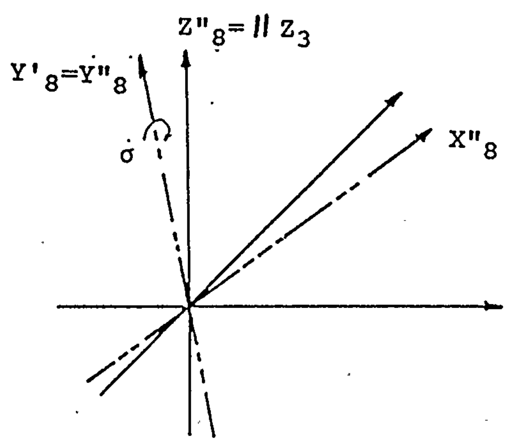

c) X''_8 axis is rotated by an angle σ around the Y'_8 axis such that the X'_8 axis lies in a plane parallel to the X_3 Y_3 plane. This will also make the Z''_8 axis parallel to the Z_3 axis.

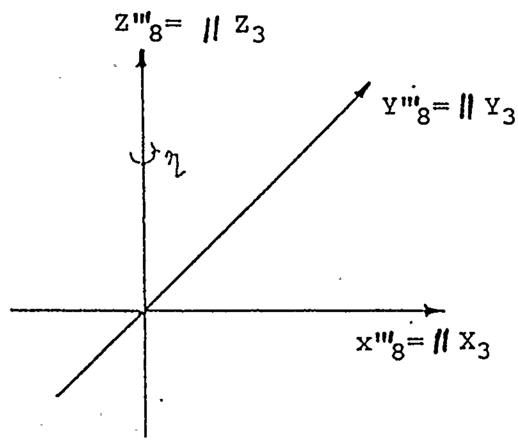

d) A rotation of η is made about the Z''_8 axis such that the X''_8 and Y''_8 axis are parallel with the X_3 and Y_3 axis.

Figure 12. System 8 Rotational Sequences

$$\begin{bmatrix} X3 \\ Y3 \\ Z3 \end{bmatrix}_{Pt.} = \begin{bmatrix} \cos\eta & \sin\eta & 0 \\ -\sin\eta & \cos\eta & 0 \\ 0 & 0 & 1 \end{bmatrix} \begin{bmatrix} \cos\sigma & 0 & -\sin\sigma \\ 0 & 1 & 0 \\ \sin\sigma & 0 & \cos\sigma \end{bmatrix} \begin{bmatrix} 1 & 0 & 0 \\ 0 & \cos\rho & \sin\rho \\ 0 & -\sin\rho & \cos\rho \end{bmatrix} \begin{bmatrix} X8 \\ Y8 \\ Z8 \end{bmatrix}_{Pt.} + \underset{\text{Sys. \#8 Origin}}{\begin{bmatrix} X3 \\ Y3 \\ Z3 \end{bmatrix}}$$

Expanding the matrix form above yields:

$$\boxed{\begin{aligned} X3_{Pt.} = {} & (\cos\eta*\cos\sigma) * X8 \\ & + (\sin\eta*\cos\rho + \cos\eta*\sin\sigma*\sin\rho) * Y8 \\ & + (\sin\eta*\sin\rho - \cos\eta*\sin\sigma*\cos\rho) * Z8 \\ & + X3 \\[1ex] Y3_{Pt.} = {} & (-\sin\eta*\cos\sigma) * X8 \\ & + (\cos\eta*\cos\rho - \sin\eta*\sin *\sin\rho) * Y8 \\ & + (\cos\eta*\sin\rho + \sin\eta*\sin\sigma*\cos\rho) * Z8 \\ & + Y3 \\[1ex] Z3_{Pt.} = {} & (\sin\sigma) * X8 - (\cos\sigma*\sin\rho) * Y8 \\ & + (\cos\sigma*\cos\rho) * Z8 + Z3 \end{aligned}}$$

.... B 60

.... B 61

.... B 62

To obtain the $X3_{Pt}$, $Y3_{Pt.}$, $Z3_{Pt.}$ offsets in terms of U.T.M. coordinates, equations B9 to B11 are used exchanging $X3_{Pt.}$, $Y3_{Pt.}$, $Z3_{Pt.}$ as computed above for X3, Y3, Z3 as expressed in the aforementioned equations.

If the offsets are to be determined in geographic coordinates, this can be accomplished by using equations B9 to B11 with the following modifications:

1.) Replace grid azimuth by true azimuth.

2.) Convert the De into angular measurement by dividing DE by $(R_v + h) * (\cos (\text{Latitude}))$.
where R_v is the radius of curvature in the prime vertical and h is the height above the reference ellipsoid (h will have no significant affect for short offsets).

3.) Convert the Dn into angular measurement by dividing DN by $(R_m + h)$
where R_m is the radius of curvature in the meridian and h is as specified above.

Appendix C. FILS MK_II Addressable Stores

The FILS MARK II system stores its data data in 16 bit registers which are addressed by setting the sector 01_8 to 17_8, that is 1 through 15 decimal. Each of these sectors contains words 00_8 to 35_8, that is 00 to 29 decimal. Therefore a store address of 0435 (which is an octal number) would be sector 04_8 ,store 35_8. The stores 36_8 and 37_8, known as stores P and Q, are sector independent and are used for transfering data.

The scaling of the most important terms is as follows:

All angles are held with MSB = 180°
except for the latitude and longitude residues
which are in terms of linear distance.

Latitude residue LSB		= 9.1761868 * 10^{-4} metres
Longitude residue LSB		= 9.1761868 * 10^{-4} metres
Torquer increment, X and Y gyros		= 0.48523 sec.
Torquer increment, Z gyro		= 7.76368 sec. = 16*(X)
Velocity reset		= 0.02286 m/sec.
Delta Time		= 0.0200704 sec.
Radius = Ro + Delta R;	Ro	= 6390871.555 m.
Delta R MSB		= 199714.7361 m.
Σ updates LSB		= 0.058727596 m.
Total Velocity	MSB	= 93.63456 m/sec.
		= 182.01 Knots
	LSB	= 0.0028575 m/sec.
Alignment velocity averages	MSB	= 46.81728 m/sec.
	LSB	= 0.00142875 m/sec.
0.6 sec. velocity averages	MSB	= 93.63456 m/sec.
	LSB	= 0.0028575 m/sec.
Update Velocity averages	MSB	= 5.85216 m/sec.
	LSB	= 0.00017859375 m/sec.
Height	MSB	= 30,790.17386 m.
	LSB	= 0.9396415361 m.
Height residue	MSB	= 3.758566145 m.
	LSB	= 0.0001470233 m.
Gravity residue	LSB	= 1.737882653*10^{-4} m.s^{-2}
which is approximately		= 1.7 milligals
Gyro Drift	MSB	= 24.182784°/hr.
	LSB	= 00.000738°/hr.
Interval timer	LSB	= 0.0802816 sec.
	MSB	= 2630.667469 sec.
Total Time	LSB	= 0.6422528 sec.
	MSB	= 21045.340 sec.
		= 5 hrs. 50 min. 45.34 sec.

These upper and lower value can be very significant in establishing limitation for the system as it operates in fixed point arithmatic.

The following pages present the INS data storage allocation charts, one page for each sector starting at sector 01_8 and going to sector 17_8.

SECTOR 01 (01 DEC.)	INS-DATA STORAGE ALLOCATION CHART				
STORE ADDRESS	DATA QUANTITY	SYMBOL	LSB SCALING	OVERFLOW RANGE	COMMENTS
0100	EDM Input Data	BUF2			
0101		BUF1			
0102		BUF4			
0103		BUF3			
0104		BUF6			
0105		BUF5			
0106	Next Point Northing	NPNTH			
0107					
0110	Next Point Easting	NPE			
0111					
0112	Surveyed Point Northing	SPNTH			
0113					
0114	Surveyed Point Easting	SPE			
0115					
0116	Align Point Northing	APN			
0117					
0120	Align Point Easting	APE			
0121					
0122					
0123					
0124					
0125					
0126	EDM Table Pointer	INCNT			
0127	GRID Zone	ZONE			
0130					
0131					
0132	VRP Northing	PNORTH			
0133					
0134	VRP Easting	PEAST			
0135					

SECTOR 02 (02 DEC.)	INS-DATA STORAGE ALLOCATION CHART				
STORE ADDRESS	DATA QUANTITY	SYMBOL	LSB SCALING	OVERFLOW RANGE	COMMENTS
0200	Protractor Harmonization Ang	EPS			
0201	IMU-VRP X Offset	XV			
0202	IMU-VRP Y Offset	YV			
0203	IMU-VRP Z Offset	ZV			
0204	EDM Harmonization Ang. P	RHO			
0205	EDM Harmonization Ang. σ	STG			
0206	EDM Harmonization Ang. η	NU			
0207	EDM Harminization Ang. DB8	DB8			
0210	Meridional Radius A coeff.	AM			S.F. 35
0211					
0212	Tangential Radius A coeff.	AT			S.F. 37
0213					
0214	Meridional Radius B coeff.	BM			S.F. 36
0215	Tangential Radius B coeff.	BT			S.F. 38
0216					
0217					
0220					
0221	Grid Selector	SELECT			
0222	(Z Scale Factor)				
0223	Y Accelerometer Misalignment	ORTHN			
0224	Mirror Harmonization Angle	MIRROR			
0225	Free Air Corr. for Gravity	FREEAIR			
0226	X Accelerometer Misalignment	ENORTH			
0227	Z Accel. Mis. about Y axis	ZNORTH			
0230	Z Accel. Mis. about X axis	ZEORTH			
0231	X Scale Factor	XSCALE			
0232	Y Scale Factor	YSCALE			
0233	X Gyro Drift	XDRIFT	.000738°/hr.	24.182784°/hr.	
0234	Y Gyro Drift	YDRIFT	.000738°/hr.	24.182784°/hr.	
0235	Z Gyro Drift	ZDRIFT	.000738°/hr.	24.182784°/hr.	

SECTOR 03 (03 DEC.)	INS-DATA STORAGE ALLOCATION CHART				
STORE ADDRESS	DATA QUANTITY	SYMBOL	LSB SCALING	OVERFLOW RANGE	COMMENTS
0300					
0301					
0302					
0303					
0304					
0305					
0306					
0307					
0310	Segment J2				
0311	Data Preparation				
0312	Buffer				
0313					
0314					
0315					
0316					
0317					
0320					
0321					
0322					
0323					
0324					
0325	W.S.				
0326	W.S.				
0327	W.S.				
0330	Data Checksum	CHECKS			
0331		CTLIM			
0332		CTOUT			
0333		CTINP			
0334		POINT			
0335	Data Dump Status	STATUS			

SECTOR 04 (04 DEC.) INS-DATA STORAGE ALLOCATION CHART

STORE ADDRESS	DATA QUANTITY	SYMBOL	LSB SCALING	OVERFLOW RANGE	COMMENTS
0400	Azimuth Rate	AZ RATE			
0401	Current Est. of Gravity Err.	GERROR			
0402	Next Point Latitude	NPLAT			
0403					
0404	Next Point Longitude	NPLONG			
0405					
0406	Predicted VRP Latitude	PLAT	$\pi * 2^{-15}$		
0407			$\pi * 2^{-31}$		
0410	Predicted VRP Longitude	PLONG	$\pi * 2^{-15}$		
0411			$\pi * 2^{-31}$		
0412	Predicted VRP Height	PHEIGHT	0.9396415365m		
0413			$0.9..* 2^{-16}$		
0414	Survey Point Lat. Residue	SPLATRES			
0415	Survey Point Lng. Residue	SPLONGRES			
0416	Frozen 0.6 se. Z Velocity	VZAV	0.00285757m/s	93.63456 m/s	
0417					
0420	ZCH	ZCH			
0421					
0422	Z1H	Z1H			
0423					
0424	Z2H	Z2H			
0425					
0426	Latitude Residue	LATRES	9.1761868E-4m.	4.7049184E-6 rad.	
0427			$9.1..E-4*2^{-16}m$		
0430	Longitude Residue	LONGRES	9.1761868E-4m.	4.7049184E-6rad/cos$pred.	
0431			$9.1..E-4*2^{-16}m$		
0432	Number of Z Torque Pulses	AZTORQ	7.76368 sec.		= 16 * 0.48523 sec.
0433	Number of X Torque Pulses	XTORQ	0.48523 sec.		
0434	Number of Y Torque Pulses	YTORQ	0.48523 sec.		
0435	Last Gravity Error	GERR			

SECTOR 05 (05 DEC.)	INS-DATA STORAGE ALLOCATION CHART				
STORE ADDRESS	DATA QUANTITY	SYMBOL	LSB SCALING	OVERFLOW RANGE	COMMENTS
0500	Computer OK Counter	COMPOK			
0501	Last Vz 20 sec. Average	VZ1	1.7859375^{-4} m/s	5.85216 m/s	
0502	Previous Vz 20 sec. Average	VZ2	1.7859375^{-4} m/s	5.85216 m/s	
0503	Gravity Residue	GRES	1.737882653^{-5} m/s^2	0.569469388 m/s^2	≈ 1.7 mgals
0504	Z Velocity Residue	VZRES			
0505					
0506	VZ in Align/Update	VZSUM			
0507					
0510	VZ for 0.6 sec. Average	VZ6			
0511					
0512	VZ 5 sec. Update Average 1	VZAV1			
0513	VZ 5 sec. Update Average 2	VZAV2			
0514	VZ 5 sec. Update Average 3	VZAV3			
0515	VZ 5 sec. Update Average 4	VZAV4			
0516					
0517					
0520	Height Residue	HEIGHTL	$1.1470233E^{-4}$ m	3.758566145 m.	
0521			$1.7502187E^{-9}$ m		
0522	Z Capacitor Trim w.s.	ZWS			
0523					
0524	Z Encoding Capacitor Scale	ZSF			
0525					
0526					
0527	Height	HEIGHTM	0.9396415365m	30790.17387 m.	
0530	Total Vz	VZ			
0531					
0532	Initial Capacitor Voltage Z	VZE			
0533	Cross Product Velocity Z	VZX	.3/32 ft/sec.		= 0.00285750 m./sec.
0534	Z Cross Product Acceleration	CPA			
0535					

SECTOR 06 (06 DEC.)			INS-DATA STORAGE ALLOCATION CHART		
STORE ADDRESS	DATA QUANTITY	SYMBOL	LSB SCALING	OVERFLOW RANGE	COMMENTS
0600	S/D Multiplier 1 Output	MULT1OP			
0601	S/D Multiplier 2 Output	MULT2OP			
0602	S/D Channel Address	CHADD			
0603	W.S.				
0604	Pitch	PITCH	$\pi * 2^{-15}$		LSB ≈ 19.775 sec.
0605	Roll	ROLL	$\pi * 2^{-15}$		LSB ≈ 19.775 sec.
0606	Station Number	STATION			
0607			0.00125		LSB=1/800th. stn.#
0610	Time Since Mode Change	TOTIM	0.6422528 sec	≈ 5.8459 Hrs.===	21,045.33975 seconds
0611	Stores Test Failure Count	FAILCNT			
0612	Failing Store Address	FAILADD			
0613	Offset Range	OFFR			
0614	Offset Delta Height	OFFH			
0615	Offset Angle	OFFA			
0616	Z Predictor Coefficient A	AH	$1.7859375E^{-4}$	5.85216 m/s	
0617	Z Predictor Coefficient B	BH	$1.7859375E^{-4}$	5.85216 m/s	
0620	Z Predictor Coefficient C	CH	$1.7859375E^{-4}$	5.85216 m/s	
0621	Old Interval Timer	TO	0.0802816 sec	2630.667469sec	
0622		AN	$1.7859375E^{-4}$	5.85216 m/s	
0623		BN	$1.7859375E^{-4}$	5.85216 m/s	
0624		CN	$1.7859375E^{-4}$	5.85216 m/s	
0625		AE	$1.7859375E^{-4}$	5.85216 m/s	
0626		BE	$1.7859375E^{-4}$	5.85216 m/s	
0627		CE	$1.7859375E^{-4}$	5.85216 m/s	
0630	Start Level 0 Count	ISOCNT			
0631	Penultimate Interval Timer	T1	0.0802816 sec	2630.667469sec	
0632	Offset Vertical Angle	VANGLE			
0633	Stores Test Address	TESTADD			
0634	Line / Pass Designation	LINEPASS			
0635					

SECTOR 07 (07 DEC.)	INS-DATA STORAGE ALLOCATION CHART				
STORE ADDRESS	DATA QUANTITY	SYMBOL	LSB SCALING	OVERFLOW RANGE	COMMENTS
0700	Calibrate Count	CALCNT			
0701	X Axis Drift	EWDRIFT			
0702	Y axis Drift	NSDRIFT			
0703	Calibrate Timer				
0704	Heading Filter Z0	Z0B			
0705					
0706	Heading Filter Z1	Z1B			
0707					
0710	Drift Filter Z0	Z0D			
0711					
0712	Present Drift Estimate (Y)	DRIFT1			
0713	Last Drift Estimate (Y)	DRIFT2			
0714	Present Z Drift Estimate	ZRATE1			
0715	Last Z Drift Estimate	ZRATE2			
0716					
0717					
0720					
0721					
0722					
0723					
0724	Longitude Scale Factor	LONGSF			For Position Integration
0725					LSH Always Appears = 0
0726	CDP Input Data 1	CDPINC			
0727	CDP Input Data 2	CDPIND			
0730	BITE Status	BITEA			
0731	BITE Status on Switch-Off	BITEB			
0732	Test Data	TESTDATA			
0733	Test Timer	TESTIM	0.02007045 s.	≈ 10.96 min.	
0734	Program Checksum	CHECK			
0735	V24 Interface Prom Checksum				BITE status if not CS0

SECTOR 10 (08 DEC.)	INS-DATA STORAGE ALLOCATION CHART				
STORE ADDRESS	DATA QUANTITY	SYMBOL	LSB SCALING	OVERFLOW RANGE	COMMENTS
1000					
1001					
1002					
1003					
1004					
1005	LEVEL 2				
1006	Working Stores 50Hz.Interrupt				
1007					
1010					
1011					
1012					
1013					
1014	Vn Residue	VNRES			
1015					
1016	E/W Gyro Torque Residue	TILTERES			
1017	N/S Gyro Torque Residue	TILTNRES			
1020	Azimuth Torque Residue DL.	AZRES	1.94092 sec.		$7.76368*2^{-2}$
1021			$1.94092*2^{-16}$		≈ 2.9616E-5
1022	Cosine (Latitude) DL.	COSLAT	2^{-15}		
1023			2^{-31}		
1024					
1025	Sine (Latitude)	SINLAT	2^{-15}		
1026	Meridional Radius & Height	RM			
1027	Tangential Radius & Height	RT			
1030	Coriolis Rate	CORATE			
1031					
1032	VE Residue	VERES			
1033					
1034	Acceleration East	EACL			
1035	Acceleration North	NACL			

SECTOR 11 (09 DEC.)	INS-DATA STORAGE ALLOCATION CHART				
STORE ADDRESS	DATA QUANTITY	SYMBOL	LSB SCALING	OVERFLOW RANGE	COMMENTS
1100					
1101					
1102					
1103					
1104					
1105					
1106					
1107		TM1			
1110	LEVEL 0	TM2			
1111	Working Stores (Main Prog)	TM3			
1112		TM4			
1113		TM5			
1114		TM6			
1115		TM7			
1116		TM8			
1117		TM9			
1120					
1121					
1122		SINROL			
1123		COSROL			
1124		SINPIT			
1125		X1/COSPIT			
1126		Y1/SINAZ			
1127		Z1/COSAZ			
1130	CDP Control Word	CONTROL			
1131	CDP Look Up Table Offset	OFFSET			
1132	CDP Input BCD Characters	CDPBCD 1			
1133	CDP Input BCD Characters	CDPBCD 2			
1134	1st. Input Character	BCD			
1135	CDP Input BCD Characters	CDPBCD 3			

SECTOR 12 (10 DEC.)		INS-DATA STORAGE ALLOCATION CHART			
STORE ADDRESS	DATA QUANTITY	SYMBOL	LSB SCALING	OVERFLOW RANGE	COMMENTS
1200	Number of Resets, E Channel	VEI	0.3/4 ft/sec	749.07648 m/s	LSB = 0.02286 m/s
1201	Number of Resets, N Channel	VNI	0.3/4 ft/sec	749.07648 m/s	LSB = 0.02286 m/s
1202	Number of Resets, Z Channel	VZI	0.3/4 ft/sec	749.07648 m/s	LSB = 0.02286 m/s
1203	Last Z Position Correction	DELH	0.058 m.	1,900.544m.	
1204	Total Z Position Correction	HZUPT			
1205			0.058 m.	1,900.544m.	
1206	Uncorrected Latitude	LAT	$\pi * 2^{-15}$		
1207			$\pi * 2^{-31}$		
1210	Uncorrected Longitude	LONG	$\pi * 2^{-15}$		
1211			$\pi * 2^{-31}$		
1212	Alignment Point Latitude	ILATM			
1213					
1214	Alignment Point Longitude	ILONGM			
1215					
1216	Alignment Point Height	IHTM	0.9396415365m.	30790.17387 m.	
1217					
1220	Surveyed Point Latitude	SLAT			
1221					
1222	Surveyed Point Longitude	SLONG			
1223					
1224	X Encoding Capacitor Scale	XSF			
1225	Y Encoding Capacitor Scale	YSF			
1226	Surveyed Point Height	SHTM			
1227		SHTL			
1230	Total Y Position Correction	NZPUT	$0.058*2^{16}$ m.	124,554,051.6m	
1231			0.058 m.		
1232	Total X Position Correction	EZUPT	$0.058*2^{16}$ m.	124,554,051.6m	
1233			0.058 m.		
1234	Last Y Position Correction	DELN	0.058 m.	1900.544 m.	
1235	Last X Position Correction	DELE	0.058 m.	1900.544 m.	

SECTOR 13 (11 DEC.)	INS-DATA STORAGE ALLOCATION CHART				
STORE ADDRESS	DATA QUANTITY	SYMBOL	LSB SCALING	OVERFLOW RANGE	COMMENTS
1300	VN 5 sec. Update Average	VNAV 1			
1301	VN 5 sec. Update Average	VNAV 2			
1302	VN 5 sec. Update Average	VNAV 3			
1303	VN 5 sec. Update Average	VNAV 4			
1304	VE 5 sec. Update Average	VEAV 1			
1305	VE 5 sec. Update Average	VEAV 2			
1306	VE 5 sec. Update Average	VEAV 3			
1307	VE 5 sec. Update Average	VEAV 4			
1310	Last VN 20 sec. Average	VN 1			
1311	Previous VN 20 sec. Average	VN 2			
1312	Last VE 20 sec. Average	VE 1			
1313	Previous VE 20 sec. Average	VE 2			
1314	Previous Update Interval	PREVINT	0.0802816 sec		
1315	Present Update Interval	PRESINT	0.0802816 sec	2630.6675 sec.	
1316	20 sec. Counter	TWENTYSEC			
1317	5 sec. Counter	TWOSEC			
1320		CDP1			
1321		CDP2			
1322		CDP3			
1323	CDP Data Preparation	CDP4			
1324	Buffers	CDP5			
1325		CDP6			
1326		CDP7			
1327		CDP8			
1330	Cross Product Velocity Y	VNX	.3/32 ft./s.		
1331	Cross Product Velocity X	VEX	.3/32 ft./s.		
1332	Initial Capacitor Voltage Y	VNE			
1333	Initial Capacitor Voltage X	VEE			
1334	N Counter (Align Filter)	NCOUNT			
1335	M Counter (Align Filter)	MCOUNT			

SECTOR 14 (12 DEC.)	INS-DATA STORAGE ALLOCATION CHART				
STORE ADDRESS	DATA QUANTITY	SYMBOL	LSB SCALING	OVERFLOW RANGE	COMMENTS
1400	Total VN	VNTOT	2.8575E-3 m/s	93.63456 m/s	
1401			4.3601989E-8		
1402	Total VE	VETOT	2.8575E-3 m/s	93.63456 m/s	
1403					
1404					
1405					
1406	0.6 second timer	PT6SEC	0.0200704 sec		
1407	CDP Status Number	CDPSTATUS			
1410	CDP Fault Number	CDPFAULT			
1411	Stores Inspect Address	STORCODE			
1412	Frozen 5 sec. Velocity Y	VN5			
1413					
1414	Frozen 5 sec. Velocity X	VE5			
1415					
1416	Grid Convergence	CONV			
1417	Program Discretes 1	STATUS A			
1420	Program Discretes 2	STATUS B			
1421	Program Discretes 3	STATUS C			
1422	Control Word 1	STATUS D			
1423	Control Word 2	STATUS E			
1424	VN in Align/Update	VNSUM			
1425					
1426	VE in Align/Update	VESUM			
1427					
1430	VN for 0.6 sec. Average	VN6			
1431					
1432	VE for 0.6 sec. Average	VE6			
1433					
1434	Frozen 5 sec. Velocity Z	VZ5			
1435					

SECTOR 15 (13 DEC.)	INS-DATA STORAGE ALLOCATION CHART				
STORE ADDRESS	DATA QUANTITY	SYMBOL	LSB SCALING	OVERFLOW RANGE	COMMENTS
1500	Azimuth	AZ	$\pi * 2^{-15}$		
1501	Memorized Azimuth	MEMAZ	$\pi * 2^{-15}$		
1502	Coarse Azimuth	COARSEAZ	$\pi * 2^{-15}$		
1503	Grid Az. of Mirror	GRIDAZ	$\pi * 2^{-15}$		
1504	Filtered Az. (+ mirror)	FILAZ	$\pi * 2^{-15}$		
1505					
1506	X Capacitor Trim w.s.				
1507					
1510	Y Capacitor Trim w.s				
1511					
1512	Capacitor Trim Counter				
1513					
1514	Az. Error Torque Down Count	MODPHI			
1515	Tilt Y Torque Down Count	MODTILTN			
1516	Tilt X Torque Down Count	MODTILTE			
1517	Heading Error	PHI			
1520	Last Tilt Y	TILTN			
1521	Last Tilt X	TILTE			
1522	Z0N	Z0N			
1523					
1524	Z1N	Z1N			
1525					
1526	Z2N	Z2N			
1527					
1530	Z0E	Z0E			
1531					
1532	Z1E	Z1E			
1533					
1534	Z2E	Z2E			
1535					

SECTOR 16 (14 DEC.)	INS-DATA STORAGE ALLOCATION CHART				
STORE ADDRESS	DATA QUANTITY	SYMBOL	LSB SCALING	OVERFLOW RANGE	COMMENTS
1600	Range				
1601					
1602	Bearing		$\pi * 2^{-15}$		
1603					
1604	Frozen 0.6 sec. Latitude	LAT 6	$\pi * 2^{-15}$		
1605			$\pi * 2^{-31}$		CHANGES AT $\pi * 2^{-20}$
1606	Frozen 0.6 sec. Longitude	LONG 6	$\pi * 2^{-15}$		
1607			$\pi * 2^{-31}$		CHANGES AT $\pi * 2^{-20}$
1610	Frozen 0.6 sec. Lat. Residue	LATR 6	$9.1761868*10^{-4}$	m.	MOD LAT6 AT ≈ 20867 BITS
1611	Frozen 0.6 sec. Lng. Residue	LONGR 6	$9.1761868*10^{-4}$	m.	LONG6 AT ≈ 20867 / COSΦ
1612	Frozen 0.6 sec. Height	HT 6	.9396415365m	30790.17387m	
1613	Frozen 0.6 sec. Hgt. Residue	HTR 6	$.9396..*2^{-13}$	3.758455145m	
1614	Align Filter Initial Vector Y	VNO			
1615					
1616	Align Filter Initial Vector X	VEO			
1617					
1620	Align Filter Initial Vector Z	VZO			
1621					
1622					
1623	Current Estimate Of Tilt Y	THETAN			
1624	Heading Error for X Calibr.	XHE			
1625	Current Estimate Of Hdg.Err.	PHIO			
1626		PHI1			
1627		PHI2			
1630		PHI3			
1631	Current Estimate of Tilt X	THETAE			
1632	Frozen 0.6 sec. Velocity Y	VNAV			
1633					
1634	Frozen 0.6 sec. Velocity X	VEAV			
1635					

SECTOR 17 (15 DEC.)		INS-DATA STORAGE ALLOCATION CHART			
STORE ADDRESS	DATA QUANTITY	SYMBOL	LSB SCALING	OVERFLOW RANGE	COMMENTS
1700					
1701					
1702	LEVEL 3				
1703	Working Stores				
1704	For Synchro-Digital				
1705					
1706					
1707					
1710	Sine (Az)	SIGMASIN			
1711					
1712	Cosine (Az)	SIGMACOS			
1713					
1714	Counter for Coarse Az. Est.	SDCOUNT			
1715	W.S.	CHNADD			
1716	Azimuth Servo Output	AZDRIV			
1717	Fault Counter for S/D	FAULT CNT			
1720	CDP Output DSA Buffer	CDP A			
1721	CDP Output DSA Buffer	CDP B			
1722	CDP Output DSA Buffer	CDP C			
1723	CDP Output DSA Buffer	CDP D			
1724	CDP Output DSA Buffer	CDP E			
1725	CDP Output DSA Buffer	CDP F			
1726	CDP Output DSA Buffer	CDP G			
1727	CDP Output DSA Buffer	CDP H			
1730	CDP Input Data 1	CDPINA			
1731	CDP Input Data 2	CDPINB			
1732					
1733					
1734	Q saved during Level 2	Q50			
1735					

Appendix D. FILS MK_II Serially Dumped Data

The Mark II inertial surveying system presently outputs four distinct groups of data on a serial output to magnetic cartridges for post-processing and data storage purposes. These groups are:

A) Keyboard data entry information
B) Change of Mode Information (Offset information)
C) Update Information
d) Navigation data dumped at a specified time interval.

All the data dumped for these various groups are defined on two ROM chips in plug in sockets. If information other than what is currently being output is required, two new ROM chips can be fused to replace the existing ones. The four groups listed above are now described in more detail.

A) KEYBOARD DATA ENTRY INFORMATION

This dump consists of the following words:

1. Type Code = 01
2. Pointer
3. Sign
4. BCD word 3
5. BCD word 1
6. BCD word 2
7. Time
8. Status word
9. Check sum

The code 01 signifies that some data has been entered through the keyboard. The pointer shows what type of data. The sign and BCD words combine to form the new value which was entered. The time shows exactly when this entry was made. The status word can be inspected to ascertain what the system was doing at the time the entry was made. The check sum is used to varify a good data dump and read from the magnetic cartridge.

This output is not normally decoded or displayed to the operator during post processing. Its purpose is to be able to reconstruct what the operator did in the field if there is any problem with the data. This reconstruction of events may help in correcting the problem on a line or at least isolating where the problem occured.

B) CHANGE OF MODE INFORMATION

The change of mode information is the longest of the four data types output and consists of fifty separate words. This dump occurs whenever the system goes from one operational mode to another or when an update is initiated by entering station offset information.

The following information is dumped:

1) Type code = 31
2) Predicted Longitude
3) Predicted Latitude
4) Predicted Height
5) Time
6) Time Residue
7) Line Pass Designation
8) Station Designation
9) Uncorrected Longitude
10) Uncorrected Latitude Residue
11) Uncorrected Latitude
12) Uncorrected Longitude Residue
13) Uncorrected Height
14) Uncorrected Height Residue
15) Offset Range
16) Offset Angle
17) Offset Delta Height
18) Roll
19) Pitch
20) Azimuth
21) Radius Residual Term AM
22) Radius Residual Term BM
23) Radius Residual Term AT
24) Radius Residual Term BT
25) X Accelerometer Scale Factor
26) Y Accelerometer Scale Factor
27) Y Accelerometer Nonorthogonality
28) X Accelerometer Nonorthogonality
29) Z Accelerometer Nonorthogonality to North
30) Z Accelerometer Nonorthogonality to East
31) Free Air Plus Slab Correction
32) Gravity Residue
33) X Gyro Drift
34) Y Gyro Drift
35) Z Gyro Drift
36) Fixed Offset Delta Angle
37) Offset Center Delta X
38) Offset Center Delta Y
39) Offset Center Delta Z
40) Mirror Correction
41) EDM Measured Range
42) Vertical Angle Encoder Value
43) Horizontal Angle Encoder Value
44) Assembled EDM Vertical Angle
45) Status C
46) Rho in Decimal Degrees
47) Nu in Decimal Degrees
48) Sigma in Decimal Degrees
49) DB8 in Decimal Degrees
50) Checksum

All the information which would normally be required is given in this dump. It is from this dump that station numbers and offset information are applied to corresponding updates during post-processing.

C) **UPDATE INFORMATION**

The update information block is dumped once every 0.64 second during a twenty second updata period and consists of the following information:

1) Type Code = 44
2) East Velocity
3) North Velocity
4) Height Velocity
5) Time
6) Uncorrected Longitude
7) Uncorrected Longitude Residue
8) Uncorrected Latitude
9) Uncorrected Latitude Residue
10) Uncorrected Height Residue
11) Uncorrected Height
12) Check Sum

It is this data which is used for curve fitting to control and correct for system errors.

D) **TIME DUMP INFORMATION**

Time dump information occurs at a fixed interval specified on the fused chips which control dumping of the four modes of data. The base time unit is 1.2845456 seconds. By selecting one of the multipliers of 1, 2, 4, 8, or 16, a time of from 1.28 to 20.55 seconds can be chosen. The current time interval for the fils system is 10.28 seconds (for most applications).

A time dump has the following information:

1) Type Code = 44
2) East Velocity
3) North Velocity
4) Height Velocity
5) Time
6) Uncorrected Longitude
7) Uncorrected Longitude Residue
8) Uncorrected Latitude
9) Uncorrected Latitude Residue
10) Uncorrected Height Residue
11) Uncorrected Height
12) Predicted Longitude
13) Predicted Latitude
14) Predicted Height
15) Roll
16) Pitch
17) Azimuth
18) Check Sum

It can be seen that a time dump is similar to an update dump but it contains six (6) more words of data. The information from these timed dumps is used to calculate cross-product accelleration terms in post processing as well as to provide profile lines.

Appendix E. FILS MK_II Test Plug Pinouts

On the back of the FILS unit is a 155 pin test connector which contains the majority of important voltage levels and signals.

The pinout for this connector is given in the following table. These are considered to be correct, but if they are to be used to actually make a connection to a FILS unit, they should be confirmed with FERRANTI representative. This is especially true if the unit is a MK_III rather than a MK_II unit.

1.	0 V (5 V)	68.	Azimuth gyro pickoff output
2.	5 V	69.	Azimuth gyro caging current
3.	Power supply good	70.	Azimuth alignment error
4.	Rapid heat on	71.	Outer roll syncro S1
5.	Battery positive	72.	Outer roll syncro S3
6.	Output stages good	73.	X accelerometer pickoff output
7.	Spin motor supply good	74.	Y accelerometer pickoff output
8.	Spin motor runup	75.	Inertial platform D.C. level A
9.	Spin motor high power	76.	Inertial platform D.C. level B
10.	350 Hz	77.	Synchro digital error
11.	Inertial platforms temperature < 40° C	78.	-sin/S1 (buffered)
12.	Capture amplifiers good	79.	-cos/S3 (buffered)
13.	Series switch monitor	80.	Azimuth resolver (-sin n0)
14.	Inertial platform good	81.	Azimuth resolver (-cos n0)
15.	Power supply good	82.	Azimuth resolver (-sin 0)
16.	Auto switch off	83.	Azimuth resolver (-cos 0)
17.	Inhibit auto switch off	84.	Pitch syncro S1
18.	Gyros caged	85.	Pitch syncro S3
19.	Mode control good	86.	Angular error
20.	CS0	87.	
21.	CS1	88.	
22.	CS2	89.	
23.	Nav B	90.	
24.	Computer good	91.	
25.	CPA good	92.	
26.		93.	0 V (40)
27.		94.	+40 V
28.	Invertor good	95.	spin motor supply phase A
29.		96.	spin motor supply phase B
30.		97.	spin motor supply phase C
31.	0 V (16 & 22)	98.	0 V (40 V T.C.)
32.	+16 V	99.	
33.	-16 V	100.	
34.	+12 V	101.	Primary supply earth
35.	-12 V	102.	Primary supply (monitor)
36.	- 6 V	103.	Rapid heat relay
37.	-22 V	104.	Inhibit rapid heat
38.	+22 V	105.	
39.	Fault reference	106.	
40.	6V 15 KHz (sin)	107.	0 V 400 Hz monitor
41.	15 KHz square B	108.	Synchro supply (400 Hz)
42.	Inertial platform temperature	109.	
43.	5V A/D bite test reference	110.	
44.		111.	DC signal earth
45.	A.C. Signal earth 1	112.	+10 V reference
46.	0° SS	113.	-10 V reference
47.	270° SS	114.	"X" accelerometer force coil
48.	Azimuth motor drive	115.	"X" force coil screen
49.	Pitch motor drive	116.	"Y" accelerometer force coil
50.	Inner roll motor drive	117.	"Y" force coil screen
51.	Outer roll motor drive	118.	"X" gyro torque motor
52.	Outer roll motor drive "B"	119.	"Y" gyro torque motor
53.	Outer roll motor drive "A"	120.	"Z" gyro torque motor
54.	Azimuth error	121.	"X" accelerometer buffer amp
55.	Pitch error	122.	"Y" accelerometer buffer amp
56.	Inner roll error	123.	Can temperature monitor
57.	Outer roll error	124.	Heat pipe heater monitor
58.	"X" axis error	125.	Can heater monitor
59.	"Y" axis error	126.	External fan control monitor
60.	"X" error sin 0	127.	Inner roll syncro S1
61.	"Y" error sin 0	128.	Inner roll syncro S3
62.	"X" gyro pickoff output	129.	Outer roll tacho A
63.	"Y" gyro pickoff output	130.	Outer roll tacho B
64.	"X" gyro caging current	131.	38V positive (floating)
65.	"Y" gyro caging current	132.	38V negative (floating)
66.	"X" alignment error	133.	Positive switch line
67.	"Y" alignment error	134.	Negative switch line

Appendix F. External Computer Platform Alignment Printout

A sample of the data output during the simulation of an at sea alignment is presented in this appendix. The run was made on February 15-16, 1987 at the Nortech Calgary office.

The output has lebels on each line which reflect the type of data shown. The vector TILTCK(*) contains the absoulute test tilt values in arc seconds for the X, Y, and Z misalignments which, when exceeded, will caused the platform to be releveled. The external update rate can be seen to have been set at 180.0 seconds. The velocities are in terms of m/s and the time is in seconds. The third value shown on the "TIME,AZIMUTH (DEG) = " line is the normal gravity value in terms of m/s^2.

```
RELAX,TILTCK(*) =    .900     2.000     2.0000    45.000
 COARSE LEVELING WAIT TIME = 35.0000 SECONDS  (Wtime)
 REMOTE UPDATES TO BE DONE EVERY    180.000 SECONDS
INITIAL X,Y,Z DRIFTS AND GRES AS INTEGER VALUES:
       -71        20      -595            6
MODIFIED X,Y,Z DRIFTS AND GRES AS INTEGER VALUES:
       -71        20      -595            6
DEL TM,VN,VE,VH = 35.323904  -3.948623   5.006994   -.048469
TIME,AZIMUTH (DEG) =    41.1042   2.018737788   9.811719
************************************************************
X,Y,Z TILT G.RES = -2349.94  -2979.81  5123.74   -137.21
X,Y,Z RATES =    -10.00000   10.00000   15.00000
MODIFIED X,Y,Z DRIFTS AND GRES AS INTEGER VALUES:
    -13621      13570     19730         -33
DEL TM,VN,VE,VH = 35.323904  -3.355393   4.383988   -.031973
TIME,AZIMUTH (DEG) =   114.9633   2.158813471   9.811719
************************************************************
X,Y,Z TILT G.RES = -1996.89  -2609.04  4619.47    -90.51
X,Y,Z RATES =   -10.00000   10.00000   15.00000
MODIFIED X,Y,Z DRIFTS AND GRES AS INTEGER VALUES:
    -13621      13570     19730         -20
DEL TM,VN,VE,VH = 35.323904  -2.761894   3.764724   -.019669
TIME,AZIMUTH (DEG) =   188.8223   2.304382318   9.811719
************************************************************
X,Y,Z TILT G.RES = -1643.68  -2240.50  4095.42    -55.68
X,Y,Z RATES =   -10.00000   10.00000   15.00000
MODIFIED X,Y,Z DRIFTS AND GRES AS INTEGER VALUES:
    -13621      13570     19730         -10
DEL TM,VN,VE,VH = 35.323904  -2.167942   3.150965   -.009259
TIME,AZIMUTH (DEG) =   262.6814   2.449951166   9.811719
************************************************************
```

```
X,Y,Z TILT G.RES = -1290.21  -1875.23  3571.38    -26.21
X,Y,Z RATES =    -10.00000   10.00000    15.00000
MODIFIED X,Y,Z DRIFTS AND GRES AS INTEGER VALUES:
    -13621      13570     19730        -2
DEL TM,VN,VE,VH = 35.323904  -1.574694   2.542593    .000957
TIME,AZIMUTH (DEG) =    336.5405   2.595520013   9.811719
************************************************************
X,Y,Z TILT G.RES =  -937.15  -1513.17  3047.33      2.71
X,Y,Z RATES =    -10.00000   10.00000    15.00000
MODIFIED X,Y,Z DRIFTS AND GRES AS INTEGER VALUES:
    -13621      13570     19730        7
DEL TM,VN,VE,VH = 35.323904   -.980560   1.939510    .003393
TIME,AZIMUTH (DEG) =    410.3995   2.738342278   9.811719
************************************************************
X,Y,Z TILT G.RES =  -583.56  -1154.26  2533.17      9.61
X,Y,Z RATES =    -10.00000   10.00000    15.00000
MODIFIED X,Y,Z DRIFTS AND GRES AS INTEGER VALUES:
    -13621      13570     19730        9
DEL TM,VN,VE,VH = 35.323904   -.387098   1.341411    .006556
TIME,AZIMUTH (DEG) =    484.2586   2.903137200   9.811719
************************************************************
X,Y,Z TILT G.RES =  -230.37   -798.31  1939.91     18.56
X,Y,Z RATES =     -5.86957   10.00000    15.00000
MODIFIED X,Y,Z DRIFTS AND GRES AS INTEGER VALUES:
     -8024      13570     19730        11
DEL TM,VN,VE,VH = 35.323904   -.038346    .747417    .006908
TIME,AZIMUTH (DEG) =    558.1177   3.034973137   9.811719
************************************************************
X,Y,Z TILT G.RES =   -22.82   -444.81  1465.30     19.55
X,Y,Z RATES =      -.58144   10.00000    15.00000
MODIFIED X,Y,Z DRIFTS AND GRES AS INTEGER VALUES:
      -859      13570     19730        12
DEL TM,VN,VE,VH = 35.323904   -.001391    .155661    .001100
TIME,AZIMUTH (DEG) =    631.9768   3.186035148   9.811719
************************************************************
X,Y,Z TILT G.RES =     -.83    -92.64   921.47      3.11
X,Y,Z RATES =      -.02108    2.36029    15.00000
MODIFIED X,Y,Z DRIFTS AND GRES AS INTEGER VALUES:
      -100       3218     19730        7
DEL TM,VN,VE,VH = 35.323904    .000857    .015964   -.001202
TIME,AZIMUTH (DEG) =    705.8358   3.331603995   9.811719
************************************************************
X,Y,Z TILT G.RES =      .51     -9.50   397.43     -3.40
X,Y,Z RATES =       .01299     .24207    10.12581
MODIFIED X,Y,Z DRIFTS AND GRES AS INTEGER VALUES:
       -53        348     13126        5
DEL TM,VN,VE,VH = 35.323904   -.000202    .001835   -.000456
TIME,AZIMUTH (DEG) =    779.6949   3.427734366   9.811719
************************************************************
X,Y,Z TILT G.RES =     -.12     -1.09    51.36     -1.29
X,Y,Z RATES =      -.00306     .02783     1.30840
MODIFIED X,Y,Z DRIFTS AND GRES AS INTEGER VALUES:
       -75         58      1178        6
DEL TM,VN,VE,VH = 35.323904   -.002040    .000510   -.000339
TIME,AZIMUTH (DEG) =    853.5540   3.446960440   9.811719
************************************************************
X,Y,Z TILT G.RES =    -1.21      -.30   -17.86      -.96
X,Y,Z RATES =      -.03093     .00773     -.45498
```

Releveling (alignment) stopped at this point as all the X,Y,Z tilts (misalignments) were within the specified limits of 2.0, 2.0, and 45.0 arc seconds respectively.

Appendix G. Additional FILS Bench Run Plots

FILS 34.5 Hour Bench Run With Normal Updates

A second bench run lasting a period of 34.5 hours was made with the FILS unit using normal updates. On this run the height velocity did not reach the 5.85216 m/s fixed point arithmetic boundary problem until 26 hours into the run. The velocity profiles, and predicted height for this run were similar the the 18 hour run, and can be found in Appendix G.

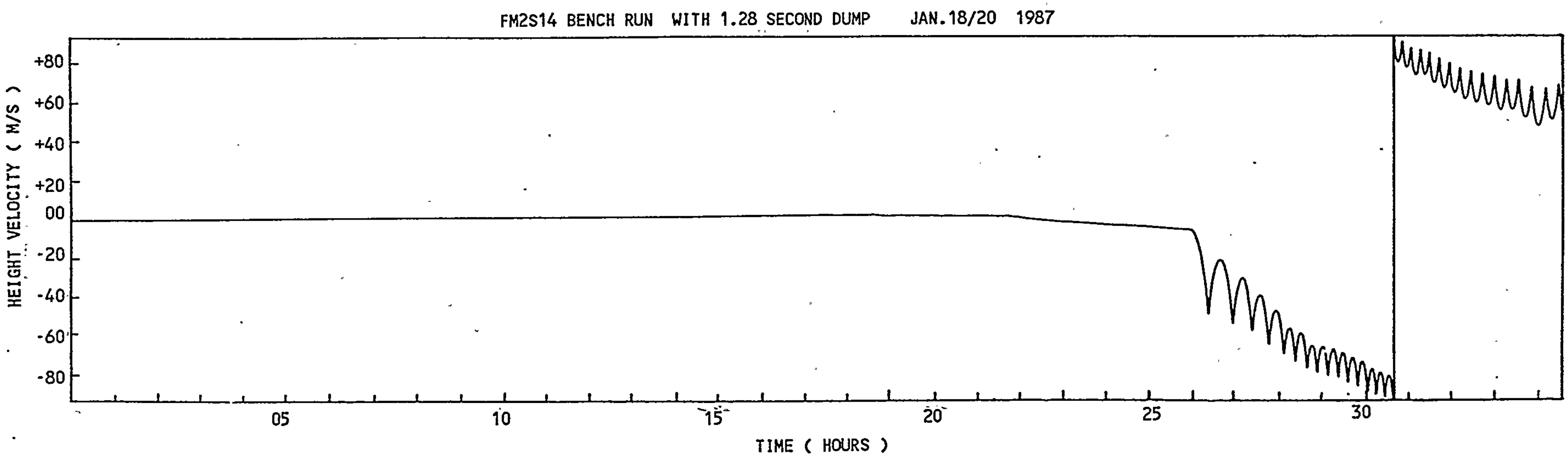

34.5 HR BENCH RUN Total Height Velocity Vs. Time

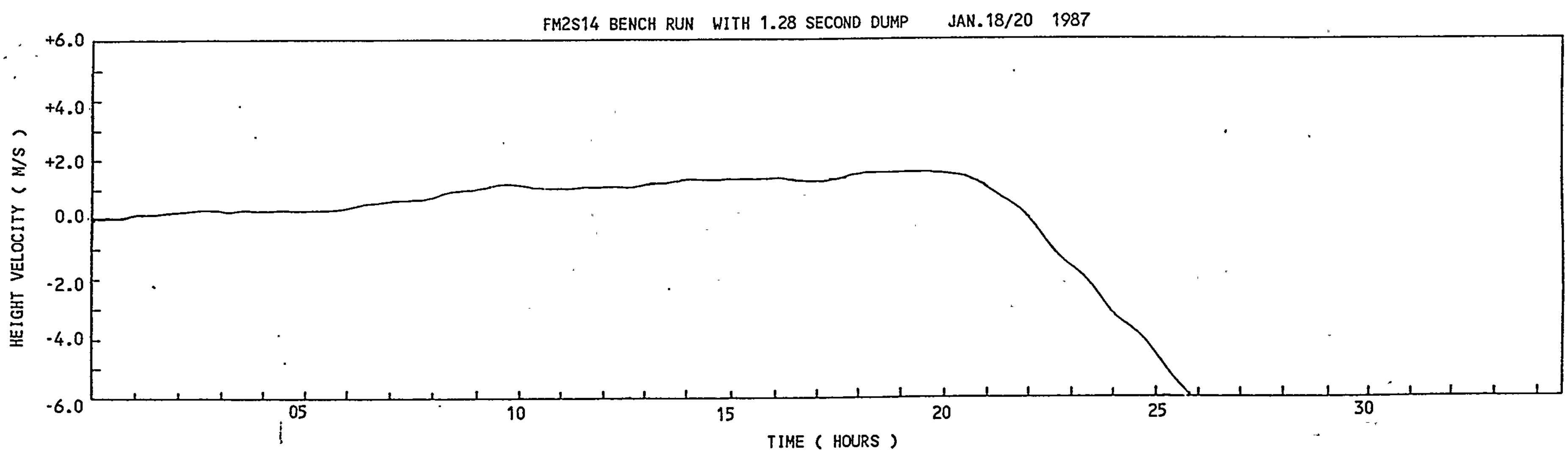

34.5 HR BENCH RUN ±6m/s Height Velocity Vs. Time

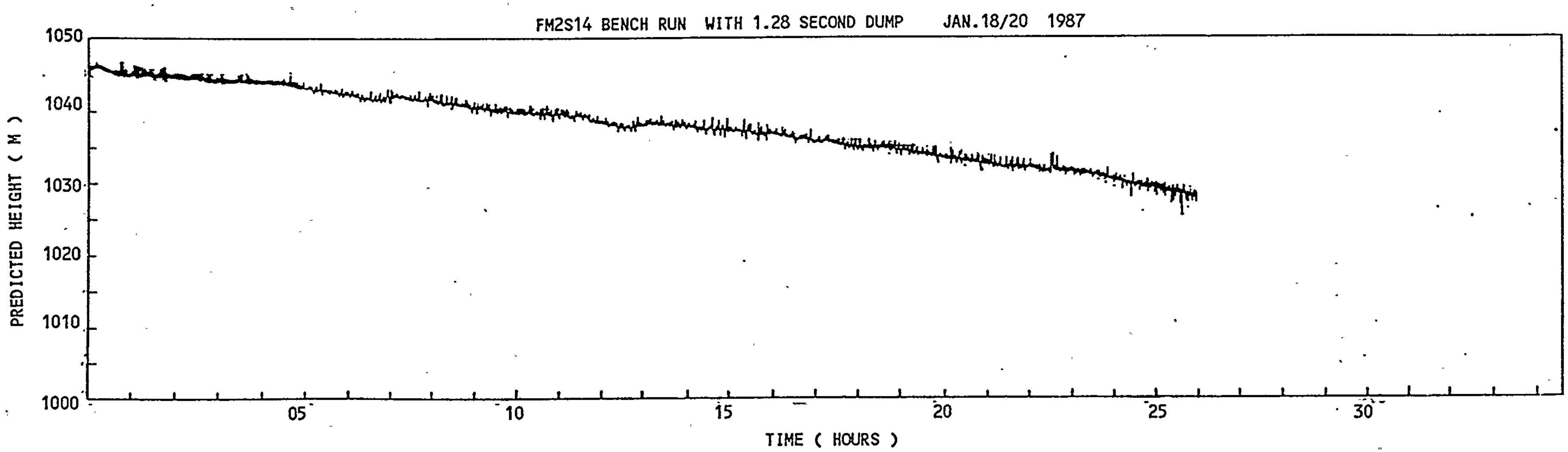

34.5 HR. BENCH RUN PREDICTED HEIGHT VS. TIME

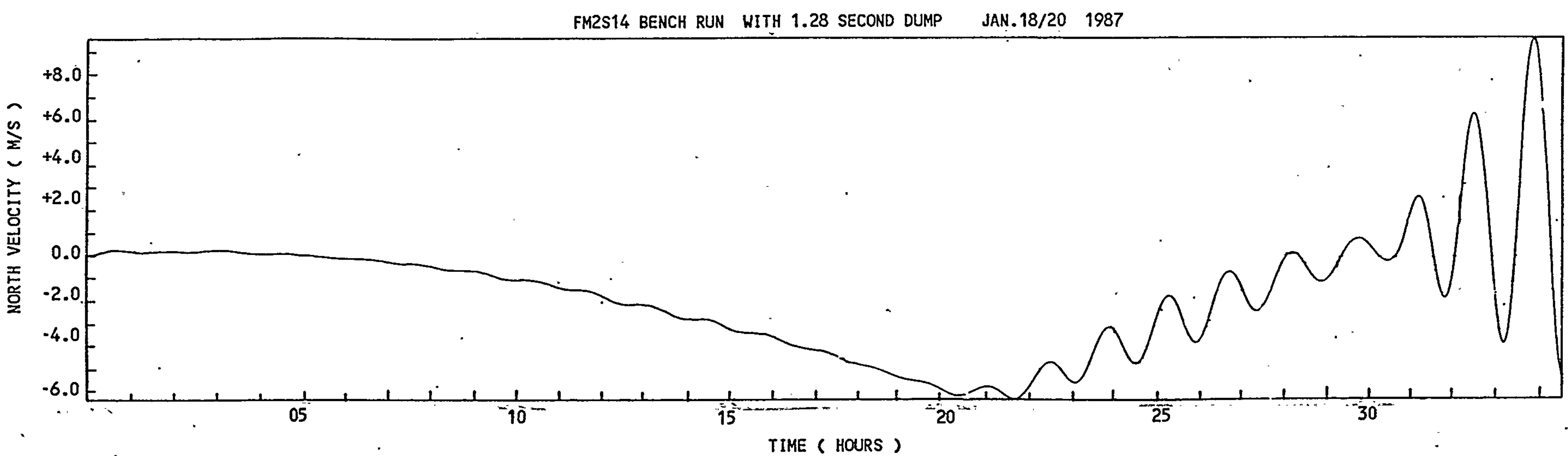

34.5 HR BENCH RUN Total North Velocity Vs. Time

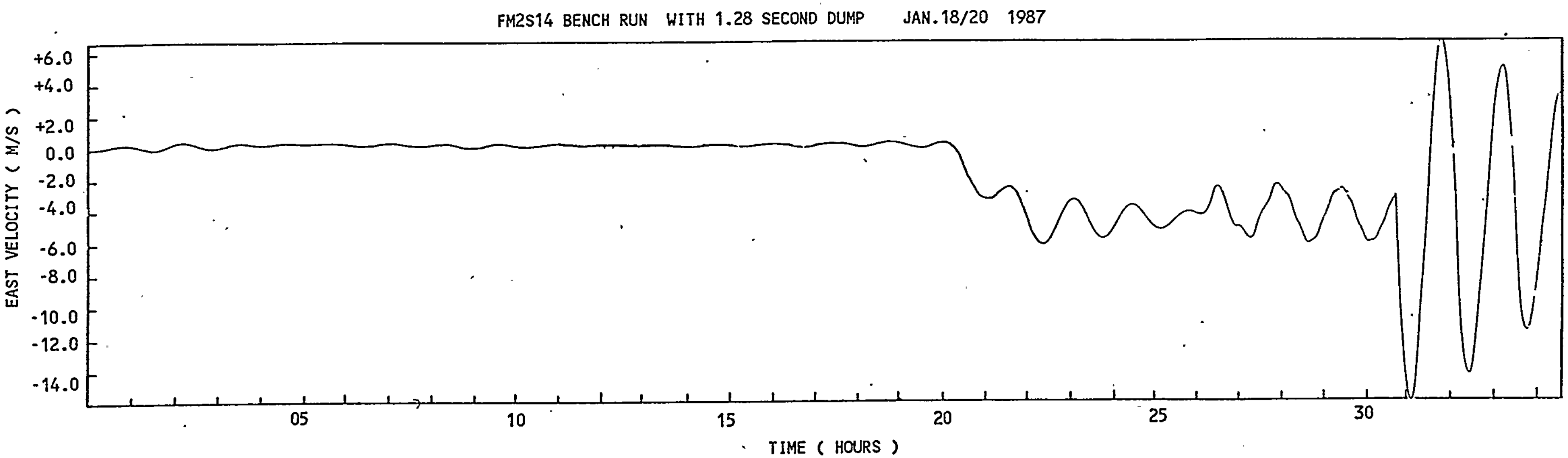

34.5 HR. BENCH RUN Total East Velocity VS. TIME